Order Number 1348516

Convective thermal model formulation of a three dimensional vascular system with simplified blood flow paths: Temperature distributions during hyperthermia

Huang, Huang-Wen, M.S.

The University of Arizona, 1992

U·M·I
300 N. Zeeb Rd.
Ann Arbor, MI 48106

Convective Thermal Model Formulation of A Three Dimensionl Vascular System with Simplified Blood Flow Paths: Temperature Distributions During Hyperthermia.

by

Huang-Wen Huang

A Thesis Submitted to the Faculty of the

DEPARTMENT OF AEROSPACE AND MECHANICAL ENGINEERING

In Partial Fulfillment of the Requirements
For the Degree of

MASTER OF SCIENCE
WITH A MAJOR IN AEROSPACE ENGINEERING

In the Graduate College

THE UNIVERSITY OF ARIZONA

1 9 9 2

STATEMENT BY AUTHOR

This thesis has been submitted in partial fulfillment of requirements for an advanced degree at The University of Arizona and is deposited in the University Library to be made available to borrowers under rules of the Library.

Brief quotations from this thesis are allowable without special permission, provided that accurate acknowledgement of source is made. Requests for permission for extended quotation from or reproduction of this manuscript in whole or in part may be granted by the head of the major department or the Dean of the Graduate College when in his or her judgment the proposed use of the material is in the interests of scholarship. In all other instances, however, permission must be obtained from the author.

SIGNED: Kuang-wen Kuang

APPROVAL BY THESIS DIRECTOR

This thesis has been approved on the date shown below:

Robt B Roemer — 4/10/92

ROBERT B. ROEMER
Professor of Aerospace and
Mechanical Engineering

DATE

ACKNOWLEDGEMENTS

The author would like to express his sincere thanks to Dr. R. Roemer for his constant advice, guidance and support during the research process. Special thanks go to Drs. Hal Tharp, Cholik Chan and Zong-Ping Chen who provided technical support and advice. The author would also like to thank Chihng-Tsung Liauh, Jong-Sheng Chen, Kyle Potocki and Angelo Toglia who provided friendship and advice. Sincere thanks go to Helen Perkins for her many contributions.

The author would like to express the greatest thanks to his family ,especially to his parents, Chi-Shung Huang and Yue-Chao Chiu Huang for their moral support, and to offer a special thank you to his friend Lin-Yu Yu for his encouragement.

This research has been supported by NCI grant CA 36428.

TABLE OF CONTENTS

TABLE OF CONTENTS--Continued

LIST OF ILLUSTRATIONS

LIST OF ILLUSTRATIONS--Continued

LIST OF ILLUSTRATIONS--Continued

LIST OF ILLUSTRATIONS--Continued

LIST OF ILLUSTRATIONS--Continued

LIST OF ILLUSTRATIONS--Continued

LIST OF ILLUSTRATIONS--Continued

LIST OF ILLUSTRATIONS--Continued

LIST OF TABLES

ABSTRACT

The development and verification of thermal models for use in hyperthermia treatment planning is essential for obtaining accurate predictions of temperature fields. This thesis presents a three-dimensional blood vessel network constructed from connected straight-line segments. The geometry of this convective thermal model is an (approximate) cube. The model contains seven levels of different size arterial vessels.

The calculations of the mean blood temperature inside the vessels are based on the convective energy balance equation for the bulk fluid temperature. The adjacent tissue temperature calculations are based on either pure conduction heat transfer or the bioheat transfer equation of Pennes [22]. The validity of the convective thermal model is checked by comparing it's predictions to those of an analytical solution for a single vessel, and by checking the energy balance calculations of the whole control volume.

The results show that the level-7 arteries still contribute a large percentage of the total heat transfer rate between the blood vessels and the surrounding tissues; and values of the Nusselt number being either 10% higher or 10% lower than 4 do not strongly affect the temperature field.

CHAPTER 1

INTRODUCTION

During the past few years there has been a growing interest in the use of hyperthermia for the treatment of tumors. In an effort to devise a model to quantitatively calculate the temperatures in living tissues, Pennes [22] performed a series of experiments which measured the temperature in the forearms of volunteers, and empirically derived a thermal energy conservation equation. The Pennes bioheat transfer equation (BHTE) is written as

$$\nabla \cdot k\nabla T + q_p + q_m - Wc_b(T - T_a) = \rho c_p \frac{\partial T}{\partial t} \qquad (1.1)$$

where $T(°C)$ is the local tissue temperature; T_a $(°C)$ is the arterial temperature; $c_b(J/kg/°C)$ is the blood specific heat; $c_p(J/kg/°C)$ is the tissue specific heat; $W(kg/m^3/s)$ is the local tissue blood perfusion rate; $k(W/m/°C)$ is the tissue thermal conductivity; $\rho(kg/m^3)$ is the tissue density; $q_p(W/m^3)$ is the energy deposition rate; and $q_m(W/m^3)$ is the metabolism, which is the metabolic conversion of chemical energy into thermal energy. This equation has the energy storage, power deposition and conduction terms just like a standard heat conduction equation, but also has two extra terms, q_m and $Wc_b(T-T_a)$. The term q_m is the metabolism, which is usually very small

compared to the external power deposition term q_p, and can often be neglected (Jain 1983 and Roemer 1989). On the other hand, the blood perfusion term $Wc_b(T-T_a)$ accounts for the energy removal resulting from the blood flow through the region. This blood perfusion term assumes that the blood enters the control volume at some arterial temperature T_a (generally assumed to be constant), and then reaches equilibrium with the tissue temperature. As the blood leaves the control volume, it carries away the energy, and hence acts as an isotropic energy sink.

Many researchers have chosen this BHTE formulation because it qualitatively describes the tissue temperature reasonably well, and is also a very simple equation to solve numerically as long as the adjustable parameter W_b is provided. Despite the BHTE's experimental success [9,13,14] in approximating temperature distributions, it has been argued that the BHTE lacks a theoretical basis.

Recent papers have postulated that the blood has a thermally significant effect upon the surrounding tissue only in large single or countercurrent vessels [1,3,9]. Several investigators have developed alternative formulations to predict the temperature field in living tissue. The first of those equations was derived by Chen and Holmes (1980), and has a very strong physical and physiological basis. The equation can be written as :

$$\rho c_p \frac{\partial T}{\partial t} = \nabla\bullet(k+k_p)\nabla T + q_m + q_p - Wc_b(T-T_a) - \rho_b c_b\, u\bullet\nabla T \quad (1.2)$$

Comparing the above equation with the traditional bioheat transfer equation, one notices that two extra terms have been added. The term $\nabla \cdot k_p \nabla T$ accounts for the enhanced tissue conductive heat transfer due to blood perfusion in the tissues ,where k_p is called the perfusion conductivity, which depends on blood perfusion rate. The other term $-\rho_b c_b \mathbf{u} \cdot \nabla T$ is the convective heat transfer term ,which accounts for the thermal interactions between the blood vessels and the tissues. The perfusion term $-Wc_b(T-T_a)$ also appears in Chen's equation to explain the effect of the capillary and small vessel structures whose individual dimensions are very small relative to the macroscopic phenomenon.

Despite its very solid physical derivation, the above equation has never been used in practice, or been successful in predicting the temperature field during hyperthermia. Because it requires detailed knowledge of the vascular anatomy and the flow pattern, it is very difficult to solve.

Another well-known alternative formulation of the BHTE was presented by Weinbaum and Jiji and their associates [15, 16, 17, 18, 19, 23] and has been studied for many years and reported in several papers. Their formulation is based on their observations from the vascular network of rabbit thighs that blood vessels that have significant effects on the heat transfer in tissue always occurred in countercurrent pairs (with diameters of about 50-500μ). Their formulation can be written in tensor notation as:

$$\rho c \frac{\partial \theta}{\partial t} - \frac{\partial}{\partial x_i}\left[(k_{ij})_{eff} \frac{\partial \theta}{\partial x_j} \right] = - \frac{\pi^2 n a^2 k_b^2}{4\sigma k} Pe^2 l_j \frac{\partial l_i}{\partial k_j} \frac{\partial \theta}{\partial x_j} + Q_m \qquad (1.3)$$

where θ is the local temperature, ρ, c are the volume average tissue density and the specific heat, a is the local blood vessel radius, σ is a shape factor for the thermal conduction resistance between adjacent countercurrent vessels, n is the number density of blood vessels of size a, k_b is the blood thermal conductivity, Pe is the local Peclet number ($=2\rho_b c_n a u/k_b$), u is the average blood flow velocity in the vessels, l_i is the direction cosine of the i^{th} pair of countercurrent vessels, and $(k_{ij})_{eff}$ is the effective conductivity tensor element, which is given by :

$$(k_{ij})_{eff} = k\left(\delta_{ij} + \frac{\pi^2}{4\sigma k^2} na^2 k_b{}^2 Pe^2 l_i l_j \right) \qquad (1.4)$$

where δ_{ij} is the Kronecker delta function, and k is the tissue thermal conductivity. Obviously this formulation represents a very complicated approximation to the bioheat transfer process formulation. This equation requires details of the size ,orientations ,and blood flow velocities in countercurrent pairs to predict the temperature. Because of this it is difficult to solve at present. Also, it was derived based on the superficial normal tissue anatomy and is not valid for general tissue-tumor macroscopic regions [20, 21].

Several theoretical studies on simplified models for the effect of isolated large blood vessels have been presented (e.g. Torell [12], Chato [13, 14], Lagendijk et al., Lagendijk and Mooibroek [24], Charny [5, 6] and Baish [7, 8]). These isolated vessel models complement the BHTE, the Chen-Holmes equation and the Weinbaum and Jiji equation which are field equations that describe the directionality of the blood flow in (50-500u) diameter countercurrent vessels.

Recently, Jaap Mooibroek and Jan J. W. Lagendijk [32] presented an algorithm for the calculation of convective heat transfer by large vessels in three-dimensional tissues. Three dimensional anatomical data of tissues and vessel structures are decomposed into elementary cubic nodes with vessels represented by connected strings of vessel nodes. G. S. Barozzi and A.Dumas [33] also presented a numerical study of convective heat transfer in the vessels of the circulatory system.

Basically, the vascular system in the human body consists of many large, medium and small vessels, and an extremely large number of very small vessels and capillaries which mostly do not have thermal significance with the surrounding tissue. The purpose of this study is to construct a simplified vessels model and to try to find a reasonable vascular numerical model and compare it's prediction with those of the traditional bioheat transfer equation.

The two main reasons this study was performed are 1.)to use the convective thermal model as a basic(reference) model to see if the BHTE can also predict the same results. 2.)to see what the effects are of adding vessels to the BHTE model. Therefore, a simplified blood flow circulation model is investigated here to see the differences between the convective and the BHTE thermal models. In this thesis, a model of the branching vessels which is a much more complicated model than the models of both (Baish [7]) and (Lagendijk [25]) was constructed with simplified blood flow paths. This present work extends the work of Williams [31] who used single and multiple straight vessels to investigate thermal models of living tissue in the extremities.

Chapter 2

METHOD

The convective thermal model presented here implements blood vessels in the model. Four descriptions are needed to characterize this model. These are the blood vessel geometry, the mass flows in those vessels, the temperature calculations, and the energy balance calculations.

Geometry

The geometry used for these studies consists of (Figure 2.1) a control volume which is an (approximate) cube of dimensions L = W =8cm and D = 8.2 cm, with the branching network as shown in Figure 2.2(a). Figure 2.2(b), shows one quarter of the entire flow path. For the other three quarters of flow paths, each has the same pattern flow as Figure 2.2(b). All vessels are straight line segments parallel to one of the three cartesian axes. The pattern of the arteries in this thesis consists of seven layers of branching arteries, beginning with the main artery which lies along the central (z) axis of the control volume. Table 2.1 describes the vessels' geometry. The diameters of blood vessels are determined by the ratio γ between successive levels where vessels divide (but not where they only change direction), e.g.

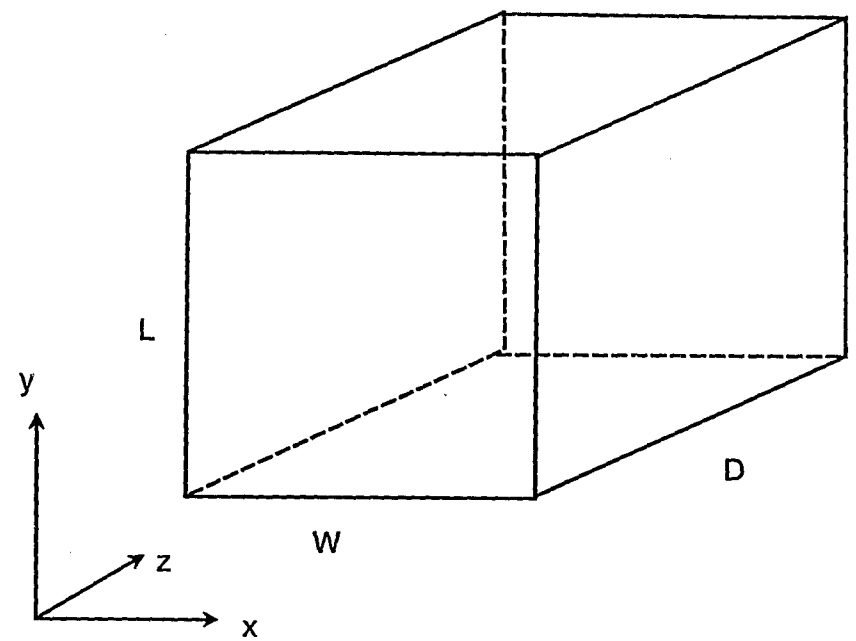

Figure 2.1 Schematic of control volume which contains the seven levels of blood vessels.

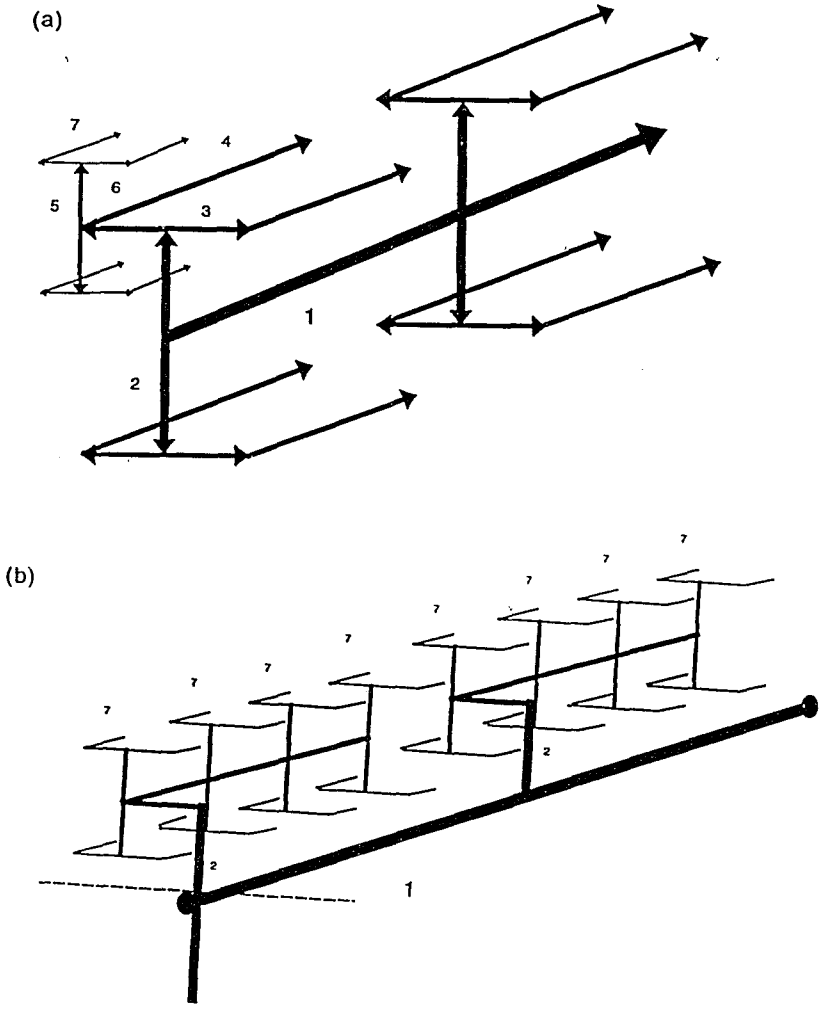

Figure 2.2 (a) A partial figure of the flow paths of the seven levels of vessels in the whole thermal model. Only one set of level 5-6-7 vessels is shown. A total of 32 such sets are used in the model. (b) One quarter of the entire blood flow path. This quadrant contains eight sets of the level five, six and seven vessels.

VESSEL LEVEL	NUMBER OF VESSELS	DIRECTION OF FLUID MOTION	X POSITION OF VESSEL CENTER	Y POSITION OF VESSEL CENTER	Z POSITION OF VESSEL CENTER
1	1	Z	21	21	1-41
2	4	Y	21	21-31 21-11	2,22
3	8	X	21-31 21-11	31,11	2,22
4	8	Z	11,31	31,11	2-17 22-37
5	64	Y	11,31	11-16 11-6 31-36 31-26	2, 22 7, 27 12, 32 17, 37
6	128	X	11-16 11-6 31-36 31-26	6,16,26 36	2, 22 7, 27 12, 32 17, 37
7	128	Z	6,16,26 36	6,16,26 36	2-6 22-26 7-11 27-31 12-16 32-36 17-21 37-41

Table 2.1 The geometry of the seven level vessels. For example, there is one level 1 vessel whose center is located at x=21 and y=21, and that runs from node z=1 to z=41. The spacing between nodes is 2mm.

levels 6 and 7 only change direction. The ratio γ is used in the following equation where Di is the diameter of the level i vessels:

$$\gamma = \frac{D2}{D1} = \frac{D3}{D2} = \frac{D4}{D3} = \frac{D5}{D4} = \frac{D6}{D5}, \quad D6=D7 \qquad (2.1)$$

The basic arterial model consists of a large central vessel (level one) running lengthwise (z) which has two pairs of symmetric vertical (y) feeder vessels (level two) branching from it; one pair at the beginning of the parallelepiped (z = 0) and one pair at its central plane (z = L/2). The mass flow rate in the main arterial vessel changes in a stepwise manner at both Z = 0 and at the central plane due to the blood removed from the main vessel by these branching second level vessels. Each of these second level vessels branch into two level three vessels which run crosswise (x). Each of the level three vessels changes direction and becomes a level four vessel extending one-half of the systems' length. Each of these level four vessels periodically has two vertical (y) level five vessels branching off. There are four such sets of branches on each level four segment, including those where vessel levels three, four and five meet. Each level five vessel branches into two level six vessels which run crosswise (x). Each level six vessel then changes direction and becomes a level seven vessel which runs lengthwise.

The "H" pattern of the vascular system which is seen in the z direction end view is presented in Figure 2.3 for one quarter of the paths and also can be seen in Figure 2.2. All vessels parallel to the

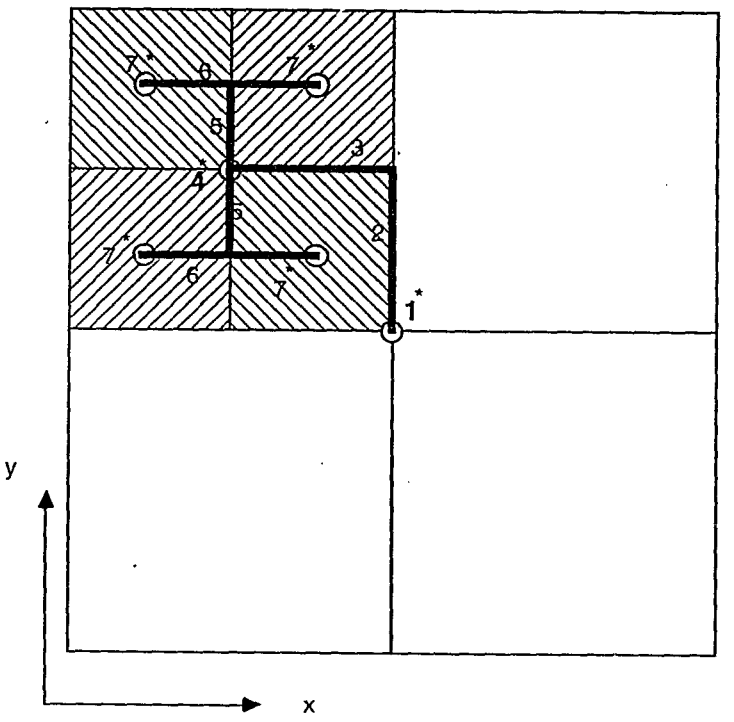

Figure 2.3 An end view of the control volume in the first branching plane (x-y plane). The open circles indicate vessels parallel to the z axis.

z direction (i.e. the level 1, 4 and 7 vessels) have been symmetrically located with respect to the x and y directions; i.e. the level 1 artery is in the center of the x and y plane , the level 4 vessels are located at the centers of the four x,y quadrants, and the level 7 vessels are located at the centers of the 16 squares that divide up any x, y plane. The vessels parallel to the x and y direction (levels 3, 6 and 2, 5 respectively) are uniformly spaced in the z direction. This basic pattern was chosen to provide a good overall representation of the vessel distribution in muscle tissue, and to yield a regular, equally spaced distribution of terminal vessels.

Straight lines are used to model all vessels in order to take advantage of easy numerical calculations of the effects of vessels. These simple equations require modifications at the turns or joints. All vessel turns are 90 degrees. There are several types of special geometries needed in order to construct the whole vascular system. These vascular connections are classified in Table 2.2. Different numerical formulations of the tissue and fluid equation are needed in these different cases.

For all vessels, we use a Nu number of 4 for calculating the heat transfer coefficients for the different diameters of the blood vessels in the vascular system. It should be noted here that in the Chapter 3 parametric studies, there are almost no differences in the temperature distributions obtained when using either a 10% higher or a 10% lower value than Nu=4.

CASE	Particular Vessel Geometry
a	a single vessel with constant flow rate and without any connections or turns. (e.g. the segments of the level one vessel)
b	a vessel having two perpendicular vessels branch from it at a single position. (e.g. level two branching from level 1).
c	a single vessel splitting into two vessels. (e.g. the level three vessels splitting from a level two vessel).
d	a single vessel splitting into three vessels. (e.g. the level four vessels and level five vessel splitting from level three vessel).
e	same as case a. but the mass flow rate is linearly decreasing. (e.g. the level 7 vessels)

Table 2.2 The types of vessel geometries that have different heat transfer formulations of the finite difference equations.

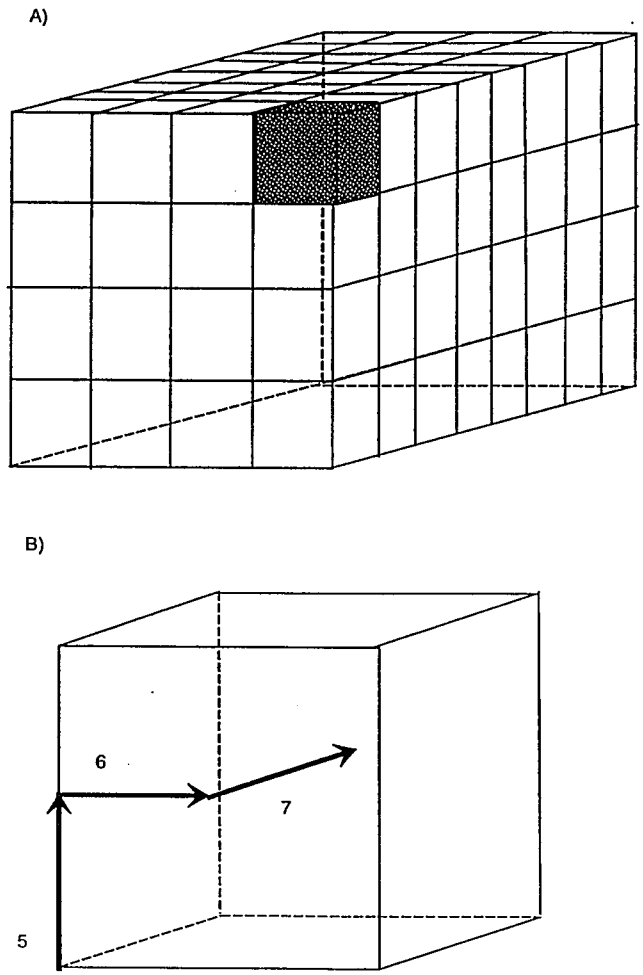

Figure 2.4 (a)The overall control volume is divided into the 128 terminal subvolumes shown here. One of these 128 terminal subvolumes is shown as shaded (b)An expanded view of the shaded subvolume showing the geometric arrangement of the vessels in the subvolume. All terminal subvolumes have the same basic vessel arrangement.

Figure 2.4, shows how the overall control volume is divided into the 128 terminal subvolumes, and one of these 128 terminal subvolumes is shown as shaded.

Mass flows

The mass flow rate carried into the whole control volume by the level one vessel is made up of two components: first, that mass flow rate that goes to perfuse the tissue, and second the mass flow which remains in vessel level 1 and merely transverses the complete control volume(M_{ta}). The total mass flow rate associated with the perfusion (M_p) is calculated by summing the mass flow rates going to each of the 128 terminal subvolumes. The mass flow rate to each of those subvolumes is calculated as the product of the volume of the terminal subvolume(V_{tsv}) times the perfusion assigned to that subvolume(P). In the present study P and V_{tsv} are the same for all terminal subvolumes. Conservation of mass is applied at all junctions of branching vessels.

Several assumptions have been made to simulate the branching vessels inside the control volume. First, the arteries carrying blood to the smallest vessels(level 7) are assumed to uniformly supply blood into the tissues(i.e., to all the unmodeled vessels down to the capillaries). So the mass flow rate along the smallest vessels(level 7) is assumed to linearly decrease from a maximum value at its inlet to zero at its terminus. This maximum flow rate is calculated using the assumed perfusion; $M=P*V_{tsv}$.

Temperature Calculation Procedures

The algorithm for calculating the temperature field is the successive overrelaxation method. The numerical procedures for calculating the temperature distributions of the vascular system and the tissue are shown in Appendix E. The blood temperatures and blood velocities are average or mean values. The Nusselt number is constant since the assumption is made of both thermally and hydrodynamic fully developed conditions. Since the diameter of the vessels is very small compared to the whole model geometry, the temperature distribution inside the vessels is represented by a mean temperature which is also a useful assumption.

To investigate the large vessels' effect on the tissue, implementation of the vessels in the simulation program is needed. Therefore, the combination of both the bioheat transfer equation (2.4) and the energy equation in vessels (2.2) will be used in the thermal reconstruction program. The arterial temperature in the perfusion loss term of the BHTE will depend on the temperature of the smallest arteries which drain the blood into tissues in the equal dimensional cross section area, if one is considering the perfusion effect($w \neq 0$) in the tissue. The combined equations will be used for simulation to give a more reasonable approximation during any hyperthermia process.

Theoretical Formulation

The convective thermal model describes the energy convected by the blood vessels, which is based on the conservation of energy equation for the blood in the vessels. The following equation is the one dimensional energy equation used everywhere in this thesis.

Conservation of Energy Equation in a Vessel

$$\rho c_b V_i A_i \frac{\partial T_b}{\partial S_i} = QA_i + A_{si} h(T_w - T_b) \qquad (2.2)$$

where

ρ	the density of blood
V_i	the velocity in the i^{th} vessel
A_i	the cross section area of the i^{th} cylindrical vessel
A_{si}	the perimeter of the cross section of the i^{th} cylindrical vessel
T_b	the blood temperature
T_w	the wall temperature of the vessel
S_i	the direction in either x, y or z

The term on the left-hand side is the convective energy term along the blood flow direction. The first term in the right-hand side is the deposited power into the vessel and the second term is the heat transfer through the vessel wall. Since it is assumed that in blood vessels Nu is generally 4 [13], the heat transfer coefficient depends on the diameter of the vessel and the conductivity of the blood. The fluid thermal conductivity used was 0.5. Hence, the diameter is the only factor that changes and affects the heat transfer coefficient.

Bioheat Transfer Equation

Pennes' simplified formulation of the bioheat transfer equation was an approximation used to model the temperature distribution in the tissue. This equation was generally used with W=0, thus representing a pure conductive media between vessels. In a few cases finite perfusion values($W \neq 0$) were used. That equation is:

$$\rho c_p \frac{\partial T}{\partial t} = \nabla \cdot (k \nabla T) - W_b c_b (T - T_a) + Q \qquad (2.3)$$

where

T	temperature of the tissue: $T=T(r,t)$ (°C)
T_a	arterial temperature (°C)
ρ	density of tissue (kg/m^3)
c_b, c_p	specific heat of blood and tissue, respectively(J/kg/°C)
k	thermal conductivity of tissue (W/m/°C)
W_b	mass perfusion rate of blood per unit volume of tissue ($kg/m^3/s$)
Q	total power generated per unit volume of tissue including the absorbed power and the generated power by metabolism (W/m^3)
∇	operator: $\nabla = i(\partial/\partial x)+j(\partial/\partial y)+k(\partial/\partial z)$

The term on the left-hand side of equation (2.3) represents the rate of energy accumulated. The first term of the right-hand side describes the amount of energy transferred due to conduction. The second term $-W_b c_b (T-T_a)$ approximates the amount of energy lost due to

the blood perfusion with the assumption that the blood enters the control volume at the temperature T_a and is in thermal equilibrium with the tissue when it leaves the volume. The last term Q represents the energy source which is the sum of the absorbed power and the power generated by the metabolism.

For this study, the energy source (Q) was assumed to be a known function which was uniform over the volume and independent of time. In addition, ρ(density), c_p, k(isotropic property of conductivity) and c_b were uniform and constant throughout the entire volume. Based on these assumptions, the BHTE equation can be rewritten as the following for steady state :

$$k\nabla^2 T - W_b c_b (T-T_a) + Q = 0. \qquad (2.4)$$

Numerical Formulation

To calculate the temperature distribution in this study, the temperature fields can be numerically solved if the thermophysical properties shown in equations (2.2) and (2.4) are known. In other words, if ρ, c_p, c_b, k, w_b and T_{art} are given, the steady-state temperature field (as a function of applied power) can be easily calculated by solving simultaneously equations (2.2) and (2.4).

The numerical algorithm developed by former Ph.d student Zong-Ping Chen[4] was used for the temperature calculations. This is a very general successive overrelaxation method (SOR) algorithm for solving the Bioheat Transfer Equation when vessels are present. The numerical algorithm used for calculating the blood temperature inside the vessels is an the upwind method. Thus, to solve for the entire

temperature field including the blood temperature within the vessels, it is necessary to combine two algorithms. The following is a general equation for calculating the temperatures both in the vessels and in the tissue.

$$T^{n+1}_{i,j,k} = (1-w)\ T^{n}_{i,j,k} + \frac{w}{\Phi}\ (\ \Psi^{n+1} + Q\ ) \qquad (2.5)$$

where

n	iteration number
i,j,k	position of a node in space
w	overrelaxation factor, $1 < w < 2$

$$Q = \dot{q} + \dot{W}c_b T_{art} \qquad (2.6)$$

$$\Phi = F_{i+1/2} + F_{i-1/2} + F_{j+1/2} + F_{j-1/2} + F_{k+1/2} + F_{k-1/2} + \dot{W}c_b \qquad (2.7)$$

$$\Psi^{n+1} = F_{i+1/2}\ T^{n}_{i+1} + F_{i-1/2}\ T^{n+1}_{i-1} + F_{j+1/2}\ T^{n}_{j+1} + F_{j-1/2}\ T^{n+1}_{j-1} + F_{k+1/2}\ T^{n}_{k+1} + F_{k-1/2}\ T^{n+1}_{k-1} \qquad (2.8)$$

For the tissue nodes that are adjacent only to other tissue nodes, and are not adjacent to any vessel nodes the factor coefficients for thermal conduction are represented as following:

$$F_{i+1/2} = \frac{k_{i+1/2}}{\Delta x_i \Delta x_i}$$

$$F_{i-1/2} = \frac{k_{i-1/2}}{\Delta x_i \Delta x_i}$$

$$F_{j+1/2} = \frac{k_{j+1/2}}{\Delta y_j \Delta y_j}$$

$$F_{j-1/2} = \frac{k_{j-1/2}}{\Delta y_j \Delta y_j}$$

$$F_{k+1/2} = \frac{k_{k+1/2}}{\Delta z_k \Delta z_k}$$

$$F_{k-1/2} = \frac{k_{k-1/2}}{\Delta z_k \Delta z_k}$$

When calculating the mean blood temperature along straight vessel segments(case a in Table 2.2), the factor coefficients are: (in this example the flow direction is along the x-direction, D is diameter, dx is gridsize(dx=dy=dz) and V is velocity))

$$F_{i+1/2} = 0.$$

$$F_{i-1/2} = (\rho c_b V \pi D^2)/(4*dx*dy*dz)$$

$$F_{j+1/2} = \frac{h\pi kD}{(2hD*\log(2dy/D)+4k)*dx*dz} \quad \text{where } h = \frac{Nu*k_f}{D}$$

$$F_{j-1/2} = F_{j+1/2}$$

$$F_{k+1/2} = F_{j+1/2}$$

$$F_{k-1/2} = F_{j+1/2}$$

When there is a vessel having two perpendicular vessels branch from it at a single position(e.g. case b in Table 2.2), the factors for calculating the temperature at the turn point are represented as:

$$F_{i+1/2} = \frac{h\pi kD}{(2hD*\log(2dy/D)+4k)*dx*dz} \quad \text{where } h = \frac{Nu*k_f}{D}$$

$$F_{i-1/2} = \frac{h\pi kD}{(2hD*\log(2dy/D)+4k)*dx*dz} \quad \text{where } h = \frac{Nu*k_f}{D}$$

$$F_{j+1/2} = 0.$$

$$F_{j-1/2} = F_{j+1/2}$$

$$F_{k+1/2} = 0.$$

$$F_{k-1/2} = (\rho c_b V \pi D^2)/(4*dx*dy*dz)$$

When there is a turn as case c in Table 2.2, the factors for calculating the temperature at the turn point are represented as following:

$$F_{i+1/2} = 0.$$

$$F_{i-1/2} = 0.$$

$$F_{j+1/2} = \frac{h\pi kD}{(2hD*\log(2dy/D)+4k)*dx*dz} \quad \text{where } h = \frac{Nu*k_f}{D}$$

$$F_{j-1/2} = (\rho c_b V \pi D^2)/(4*dx*dy*dz)$$

$$F_{k+1/2} = \frac{h\pi kD}{(2hD*\log(2dy/D)+4k)*dx*dz} \quad \text{where } h = \frac{Nu*k_f}{D}$$

$$F_{k-1/2} = \frac{h\pi kD}{(2hD*\log(2dy/D)+4k)*dx*dz} \quad \text{where } h = \frac{Nu*k_f}{D}$$

When there is a turn like case d in Table 2.2), the factors for calculating the temperature at the turn point are represented as following:

$$F_{i+1/2} = (\rho c_b V_i \pi D^2)/(4*dx*dy*dz)$$

$$F_{i-1/2} = \frac{h\pi kD}{(2hD*\log(2dy/D)+4k)*dx*dz} \quad \text{where } h = \frac{Nu*k_f}{D}$$

$$F_{j+1/2} = 0.$$

$$F_{j-1/2} = F_{j+1/2}$$

$$F_{k+1/2} = 0.$$

$$F_{k-1/2} = \frac{h\pi kD}{(2hD*\log(2dy/D)+4k)*dx*dz} \quad \text{where } h = \frac{Nu*k_f}{D}$$

The equation for case 'e' in Table 2.2 is of the same form as indicated in case 'a' except that the velocity is decreasing linearly along the vessel. (V is the entering velocity of the level 7 vessels, N is the number of nodes along the level 7 vessels, i is the node number along the level 7 vessel-- i goes from 1 to N). Therefore, the velocity along the vessel will be:

$$V_i = V-(V/N)*i \qquad (2.8.a)$$

The value of the overrelaxation constant w used in most simulations was 1.02. A final steady-state temperature was numerically calculated when the root of the mean square error was smaller than

10^{-6} °C between consecutive iterations of the temperature fields. The definition of ERMS was:

$$Erms = \sqrt{\frac{\sum_{i=1}^{NX}\sum_{j=1}^{NY}\sum_{k=1}^{NZ}\left(T_{i,j,k}^{I+1} - T_{i,j,k}^{I}\right)^2}{NX*NY*NZ}} \qquad (2.9)$$

where

NX,NY,NZ — total number of nodes in x, y,and z directions, respectively.

I — the I^{th} iteration

Two conditions for the arterial temperature in the BHTE have been used. In the first case T_{art} is kept at a constant value, 37°C. For the other case T_{art} is no longer kept at 37°C. Instead, it is set equal to the blood temperature(T_a=T_b) of the vessel which drains the blood into the tissue temperature. That is, each z plane of every subvolume uses the value of $T_b(z)$ in it's seventh level vessel as the value of T_{art} in the BHTE for that plane. A 2mm spacing was used in all calculations presented here.

Several calibration tests were run to check the program. These include checks of: the linearity between the increment of the uniform power and the increment of the temperature at some specific location; symmetric temperature fields for the y-z plane(nx=21) and the x-z plane(ny=21); linearity between the heat loss through the six surfaces and the increment of the uniform power; the same location for the

highest temperature after increasing the uniform power; and comparison of the heat loss from the opposite surfaces of the whole parallelepiped including the top and bottom and right and left surfaces. Test results from these checks are given in Appendix D.

ENERGY BALANCE CALCULATIONS

In order to continually check the numerical results from the simulations, an energy balance method is used. The following is how the energy balance has been calculated for the overall control volume with 37°c boundary surfaces temperature:

1. Energy Convected in by the Main Artery: ($Q_{conv.in}$)

$$Q_{conv.in} = \rho c_b V_i A_i T_i \qquad (2.10)$$

i: inlet
A_i: πr_i^2
T_i: 37°C at node K=1

2. Energy Convected out by the Main Artery: ($Q_{conv.out}$)

$$Q_{conv.out} = \rho c_b V_o A_o T_o \qquad (2.11)$$

o: outlet
A_o: πr_o^2
T_o: temperature at node K=nz-1

3. Absorbed power : ($Q_{e.p.}$)

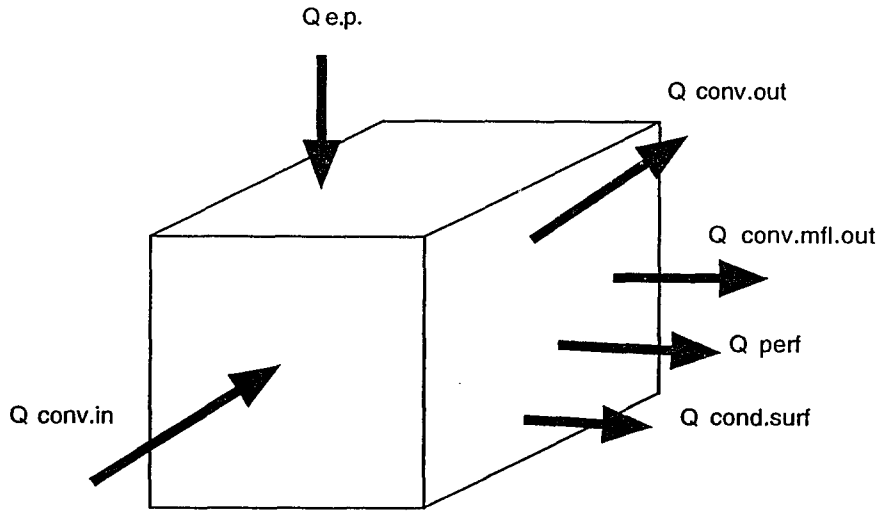

Figure 2.5 Energy balance terms for the complete control volume.

$$Q_{e.p} = \sum_{\text{all nodes}} Q\Delta x\Delta y\Delta z \qquad (2.12)$$

where $\dot{Q}$ is the applied power in W/m^3

4. Energy Loss by Surface Conduction: ($Q_{cond\cdot surf.}$)

$$Q_{cond\cdot surf} = \sum_{\text{surface 1}} kA\frac{dT}{ds} + \sum_{\text{surface 2}} kA\frac{dT}{ds} + \ldots\ldots\ldots + \sum_{\text{surface 6}} kA\frac{dT}{ds} \qquad (2.13)$$

surface 1: at nodes k=2, i=2 - nx-1, j=2 - ny-1

surface 2: at nodes k=nz-1, i=2 - nx-1, j=2 - ny-1

surface 3: at nodes i=2, j=2 - ny-1, k=2 - nz-1

surface 4: at nodes i=nx-1, j=2 - ny-1, k=2 - nz-1

surface 5: at nodes j=2, i=2 - ny-1, k=2 - nz-1

surface 6: at nodes j=ny-1, i=2 - nx-1, k=2 - nz-1

5. Energy Loss due to Perfusion Term in (BHTE): ($Q_{perf.}$)

$$Q_{perf} = \sum_{V_{tsv}\ 1} \dot{w}c_b(T-T_a)\Delta x\Delta y\Delta z + \sum_{V_{tsv}\ 2} \dot{w}c_b(T-T_a)\Delta x\Delta y\Delta z + \ldots + \sum_{V_{tsv}\ 128} \dot{w}c_b(T-T_a)\Delta x\Delta y\Delta z \qquad (2.14)$$

6. Energy Loss by Terminal Vessels(level 7) Whose Mass Flow Rates Decrease Linearly: ($Q_{conv\cdot mfl\cdot out}$)

$$Q_{conv\cdot mfl\cdot out} = \sum_{\text{vessel 1}} \Delta\dot{m}T_l + \sum_{\text{vessel 2}} \Delta\dot{m}T_l + \ldots\ldots\ldots + \sum_{\text{vessel 128}} \Delta\dot{m}T_l \qquad (2.15)$$

where

$$\Sigma = \sum_{i=1}^{N}$$

N: vln/dz+1(number of nodes along vessel)
vln: the length of the smallest vessels.
dz: gridsize along z-dir

T_i is the blood temperature

at the i_{th} point along the vessel

There are 128 smallest level 7 vessels draining into the entire control volume.

The energy conservation equation check of Figure 2.7 is:

$$Q_{conv\cdot in} + Q_{e\cdot p\cdot} = Q_{conv\cdot out} + Q_{cond\cdot surf} + Q_{perf\cdot} + Q_{conv\cdot mfl\cdot out} \qquad (2.16)$$

CHAPTER 3

PARAMETRIC STUDIES

The Temperature Distributions in The 7-level Vessel Model

Because of the complexity of the temperature distributions resulting from the many blood vessels interwoven in the tissue, in order to develop an understanding of the general results it is better to first look at temperature profiles from selected cross sections of the entire thermal model. Several plane-cuts of the iso-thermal lines of the thermal model show how the temperature field is impacted by the vessels (Figure 3.1). Results from the different iso-thermal planes shown in Figure 3.1 are given in Figure 3.2 - 3.8 for the case of uniform power Q=30000 $w/m^3/s$, tissue conductivity k=0.5 w/m/°C, specific heat c_b=4000 kj/kg/°C, W=0, P=1 and boundary conditions of surface temperatures of 37°C. The diameter of the level 1 vessel is 1mm and the diameter branching ratio is 1. Unless indicated otherwise, these values are used in all studies presented in this thesis.

In Figure 3.2, the two big cold streams carrying the blood in the second level branches are seen. In plane 2 of the x-z plane the level 1 vessel(main artery) runs directly through and there are no branches in this plane(Figure 3.3). The highest temperature is located

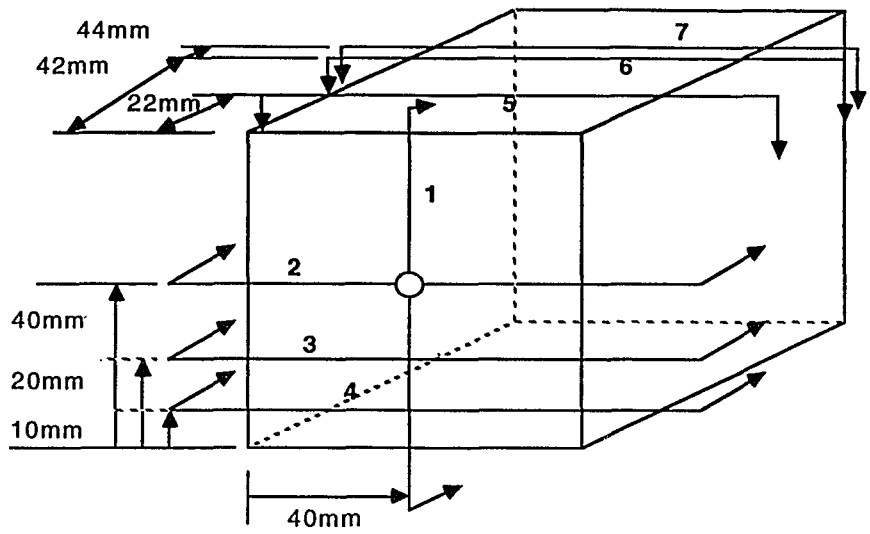

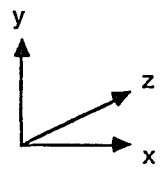

plane 1: y-z plane

plane 2,3,4: x-z plane

plane 5,6,7: x-y plane

Figure 3.1 The seven iso-thermal plane-cuts.

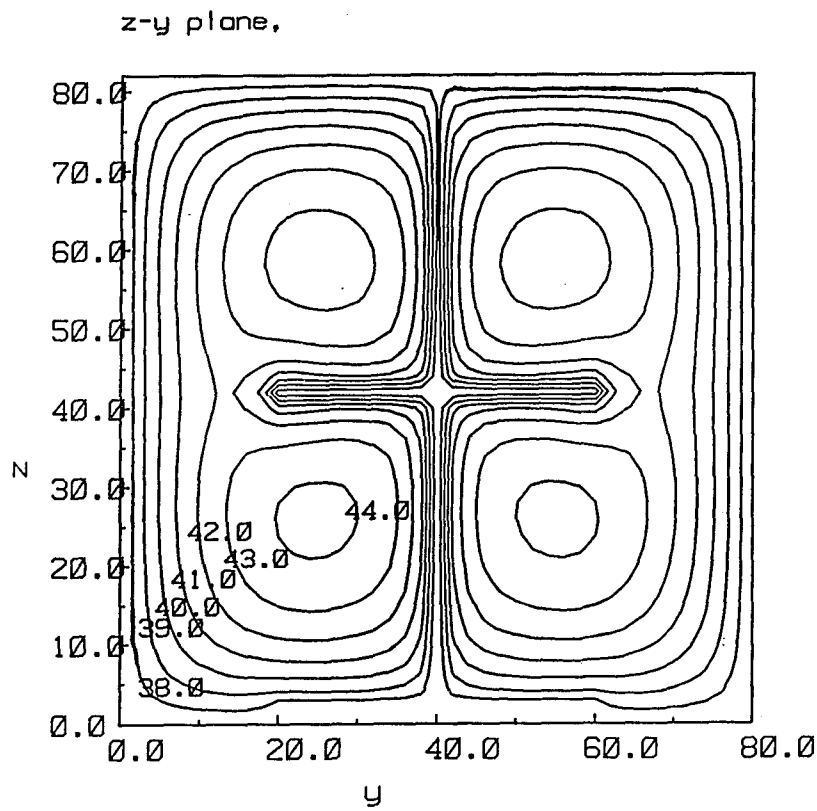

Figure 3.2 The iso-thermal plane-cut number 1 in a y-z plane.

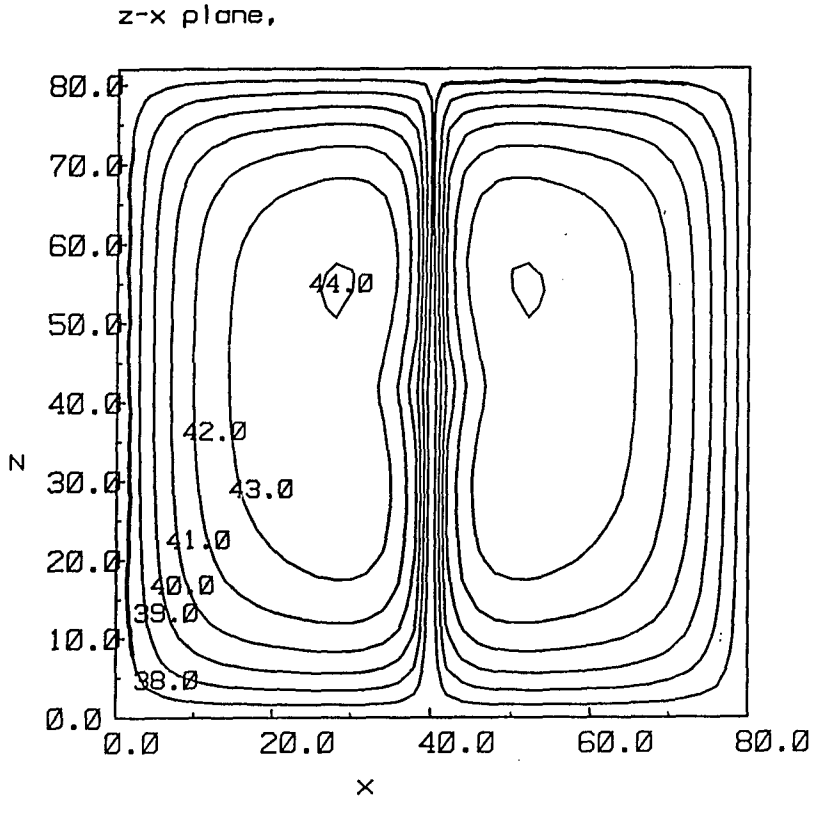

Figure 3.3 The iso-thermal plane-cut number 2 in a x-z plane.

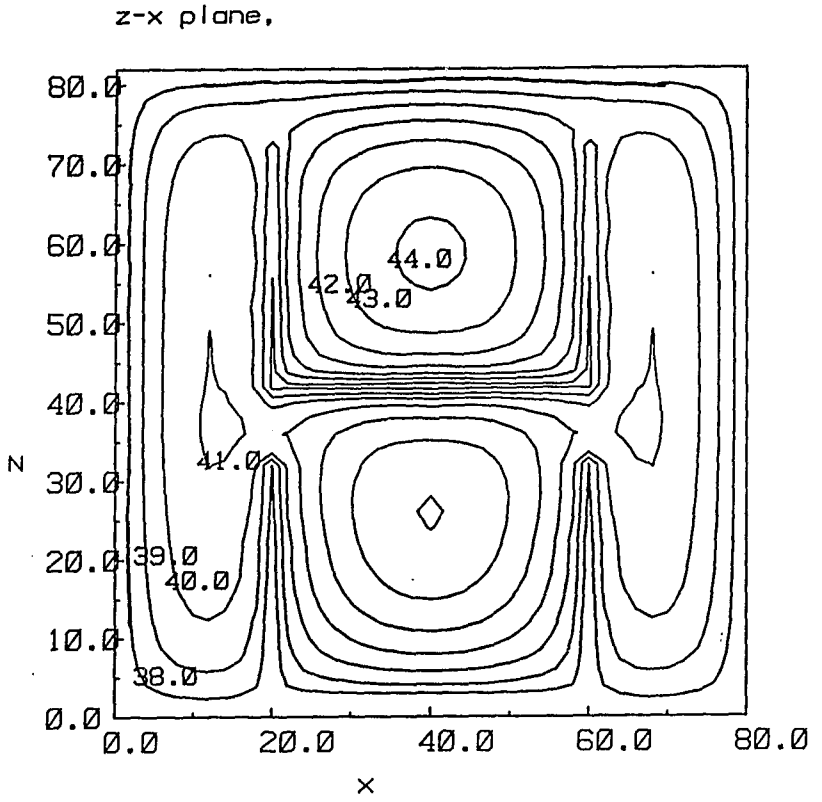

Figure 3.4 The iso-thermal plane-cut number 3 in a x-z plane.

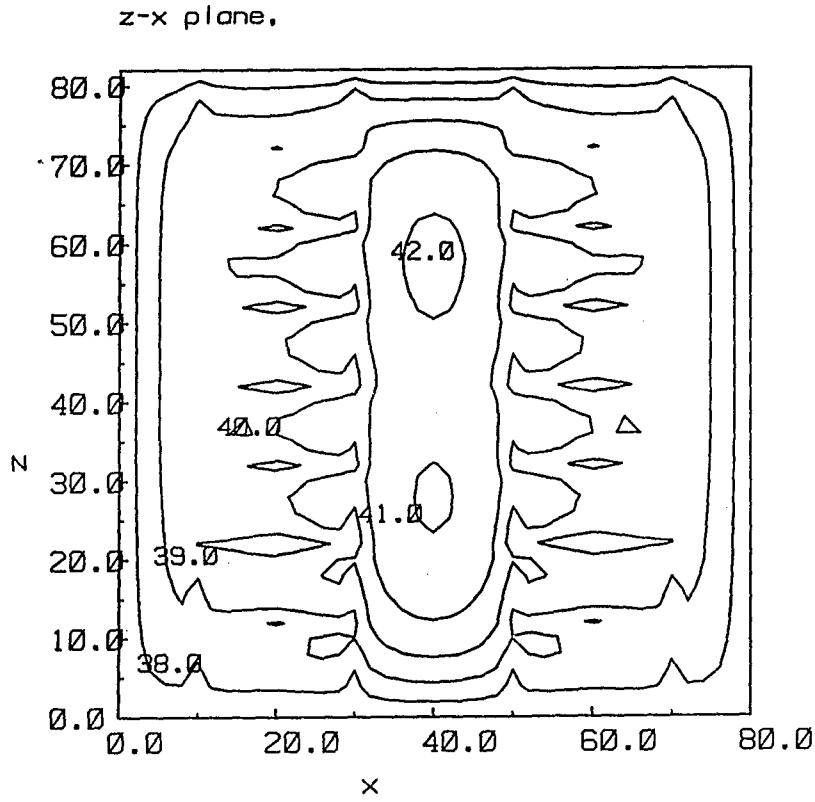

Figure 3.5 The iso-thermal plane-cut number 4 in a x-z plane.

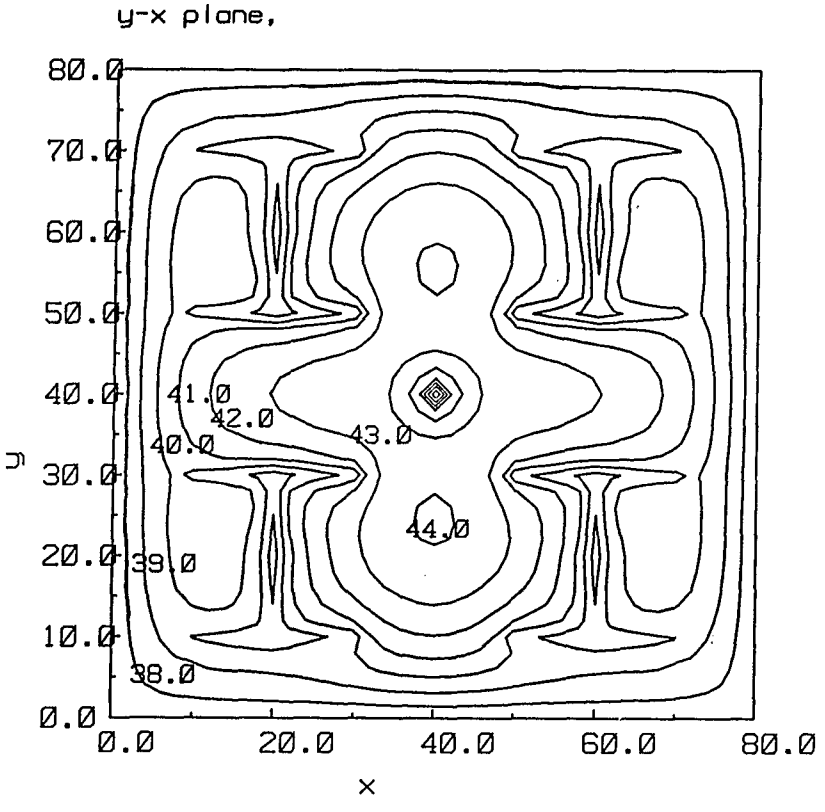

Figure 3.6 The iso-thermal plane-cut number 5 in a x-y plane.

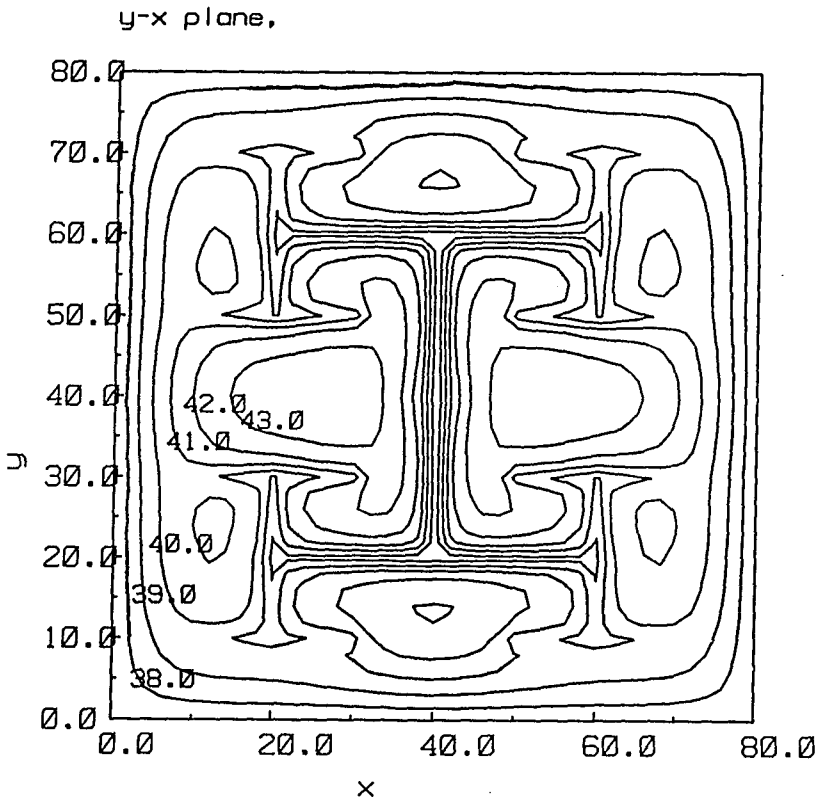

Figure 3.7 The iso-thermal plane-cut number 6 in a x-y plane.

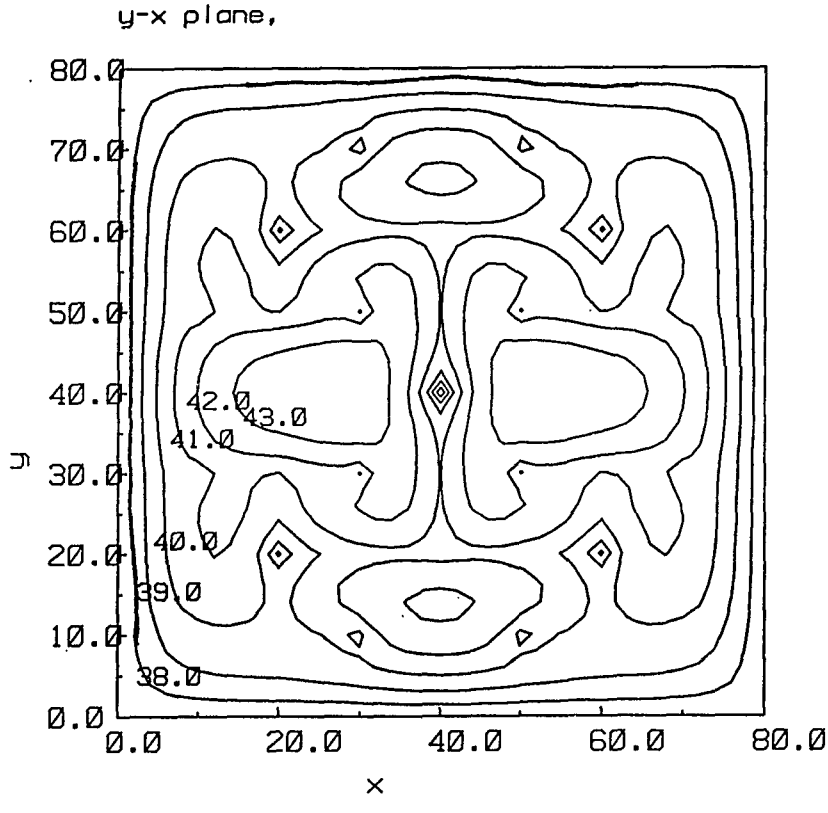

Figure 3.8 The iso-thermal plane-cut number 7 in a x-y plane.

slightly over half way along the z plane as we can see in plane 2. In plane 3 of the x-z plane two pairs of level 4 vessels show different temperatures along the level 4 vessels. The upper pair has higher temperatures than the lower pair. Plane 4 of the x-z plane covers 32 of the smallest vessels (level 7). Since the temperature difference of the iso-thermal lines is 1°C, it is hard to see any trends for the level 7 vessels. A big difference between plane 5 and plane 6 is that in plane 6 one can see the level two and three vessels. In plane 7 of the x-y plane some cold spots appear in the same way caused by small arteries.

The Effect of P value(perfusion rate)

One of the major parameters which will influence the temperature field of the convective thermal model is the magnitude of the mass flow rate. As one knows, W(the BHTE perfusion rate coefficient) in the traditional BHTE supposedly represents the blood perfusion in the tissues. Here, in the convective thermal model without the BHTE term(i.e., W=0; only conduction in tissues) the blood cooling effect is only determined by the vessels. For this latter case, the larger the P value(the blood perfusion rate) is, the larger the velocity is in the blood vessels model.

The second factor which affect the velocity field is the diameter branching ratio γ. In this section the results of studies varying P and γ will be presented. The question of how W and P can be related is discussed later.

Vessel Level	Vessel Diameters			
	Diameter Branching Ratio 1.0	Diameter Branching Ratio 0.9	Diameter Branching Ratio 0.8	Diameter Branching Ratio 0.5
1	1 mm	1 mm	1 mm	1 mm
2	1 mm	900 um	800 um	500 um
3	1 mm	810 um	640 um	250 um
4	1 mm	730 um	510 um	125 um
5	1 mm	660 um	410 um	62.5 um
6	1 mm	590 um	330 um	31.25 um
7	1 mm	590 um	330 um	31.25 um

Table 3.1 The diameters of the vessels in different levels due to different diameter branching ratios(γ).

Vessel Level	Velocity (m/s)		
	Diameter Branching Ratio 1.0	Diameter Branching Ratio 0.9	Diameter Branching Ratio 0.8
1-1	0.426	0.426	0.426
1-2	0.100	0.100	0.100
2	0.163	0.201	0.255
3	0.081	0.124	0.199
4-1	0.061	0.115	0.233
4-2	0.040	0.076	0.155
4-3	0.020	0.038	0.077
5	0.010	0.024	0.061
6	0.005	0.015	0.047
7	*	*	*

Table 3.2 Velocity(m/s) in each level of vessels for P=1.(* in the level seven vessels the velocity decreases linearly from the value in the level six vessels to zero).

Vessel Level	Velocity (m/s)		
	Diameter Branching Ratio 1.0	Diameter Branching Ratio 0.9	Diameter Branching Ratio 0.8
1-1	0.752	0.752	0.752
1-2	0.100	0.100	0.100
2	0.326	0.402	0.509
3	0.163	0.248	0.398
4-1	0.122	0.230	0.466
4-2	0.080	0.153	0.311
4-3	0.040	0.076	0.155
5	0.020	0.047	0.121
6	0.010	0.029	0.095
7	*	*	*

Table 3.3 Velocity in each level of vessels for P=2.(* in the level seven vessels the velocity decreases linearly from the value in the level six vessels to zero).

Vessel Level	Velocity (m/s)		
	Diameter Branching Ratio 1.0	Diameter Branching Ratio 0.9	Diameter Branching Ratio 0.8
1-1	1.730	1.730	1.730
1-2	0.100	0.100	0.100
2	0.815	1.006	1.273
3	0.407	0.621	0.995
4-1	0.306	0.575	1.166
4-2	0.200	0.383	0.777
4-3	0.100	0.192	0.388
5	0.051	0.118	0.304
6	0.025	0.073	0.237
7	*	*	*

Table 3.4 Velocity in each level of vessels for P=5.(* in the level seven vessels the velocity decreases linearly from the value in the level six vessels to zero).

Vessel Level	Velocity (m/s)		
	Diameter Branching Ratio 1.0	Diameter Branching Ratio 0.9	Diameter Branching Ratio 0.8
1-1	3.359	3.359	3.359
1-2	0.100	0.100	0.100
2	1.630	2.012	2.546
3	0.815	1.242	1.989
4-1	0.611	1.150	2.332
4-2	0.400	0.766	1.554
4-3	0.200	0.383	0.777
5	0.102	0.237	0.607
6	0.051	0.146	0.474
7	*	*	*

Table 3.5 Velocity in each level of vessels for P=10.(* in the level seven vessels the velocity decreases linearly from the value in the level six vessels to zero).

Table 3.1 shows the diameters in different levels as a function of the branching ratio. Table 3.2 ,Table 3.3 ,Table 3.4 and Table 3.5 show the velocity magnitudes in the vessels for perfusion P values of W=1 ,W=2 ,W=5, W=10, and for different branching ratios.

Figures 3-9 and 3-10 show the results of studies using these P and γ values in terms of two important criteria, the maximum temperature, which indicates the highest value in the whole model and the average tissue temperature. Results are shown in these graphs for both the seven level vessel model at the various perfusion(P) values used to calculate the velocities in Tables 3.2 to 3.5, and for the Pennes BHTE when a uniform BHTE perfusion parameter(W) is present. W and P both have the same units, and both are related to perfusion in some manner. That is, W is the "perfusion" parameter in the BHTE, and P is the "perfusion" value used to determine the velocities of the blood in the terminal level vessels.

The reason for the big differences between the predictions of the BHTE model and the seven level vessel model at high P and W values is that the cooling effect of the vessel model is weaker than the cooling effect of the perfusion term in the BHTE model. In other words, the cooling effect in the vessels model is due to the limited location of vessels without any heat sink in the tissue, but in the BHTE model the perfusion is uniform throughout the tissue volume and the blood enters at a constant arterial temperature of 37°C. See Roemer, et.al(1992) for a further discussion of this.

For the lower BHTE perfusion and the lower velocity field

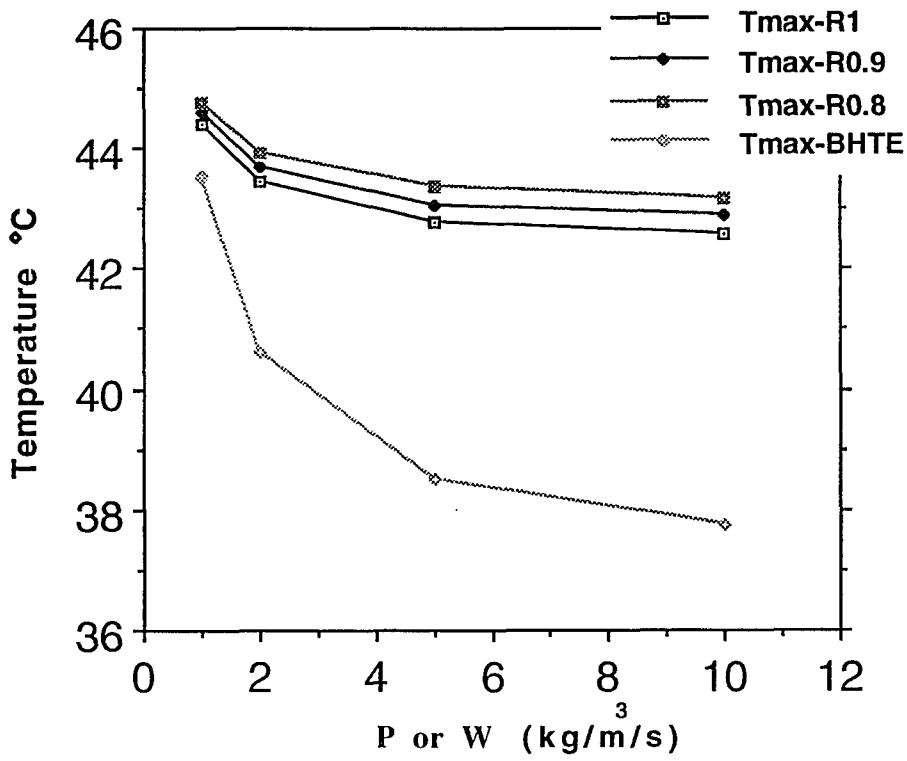

Figure 3.9 The maximum tissue temperatures predicted by the BHTE model(no vessels) at several W values and the 7-level vessels model for different perfusion P values and diameter ratios.

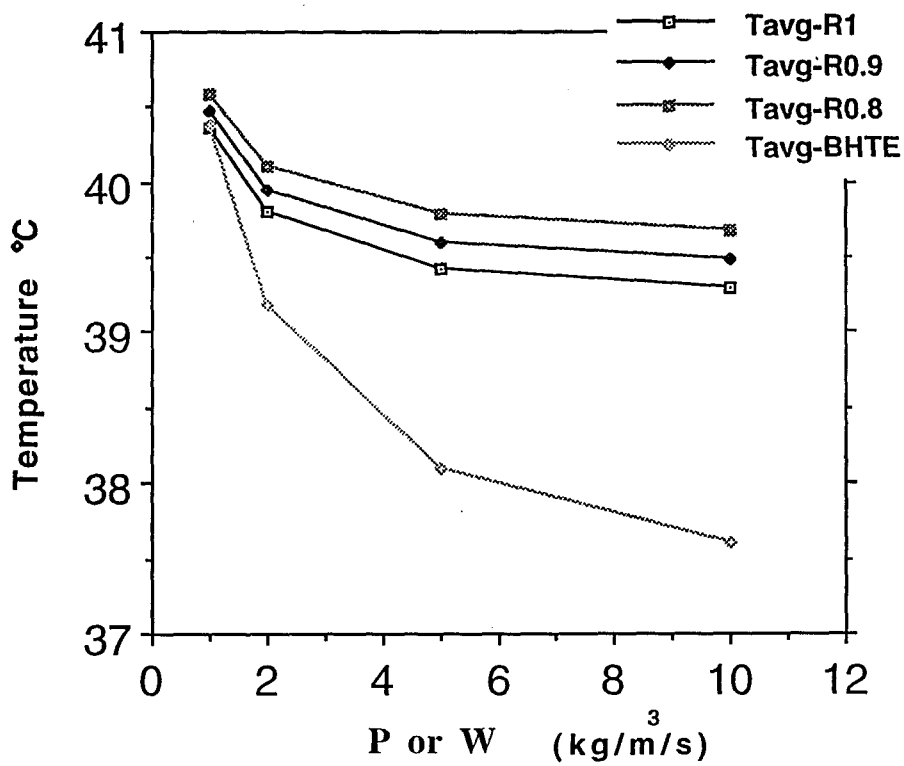

Figure 3.10 The average tissue temperatures predicted by the BHTE model(no vessels) at several W values and the 7-level vessels model for different perfusion P values and diameter ratios.

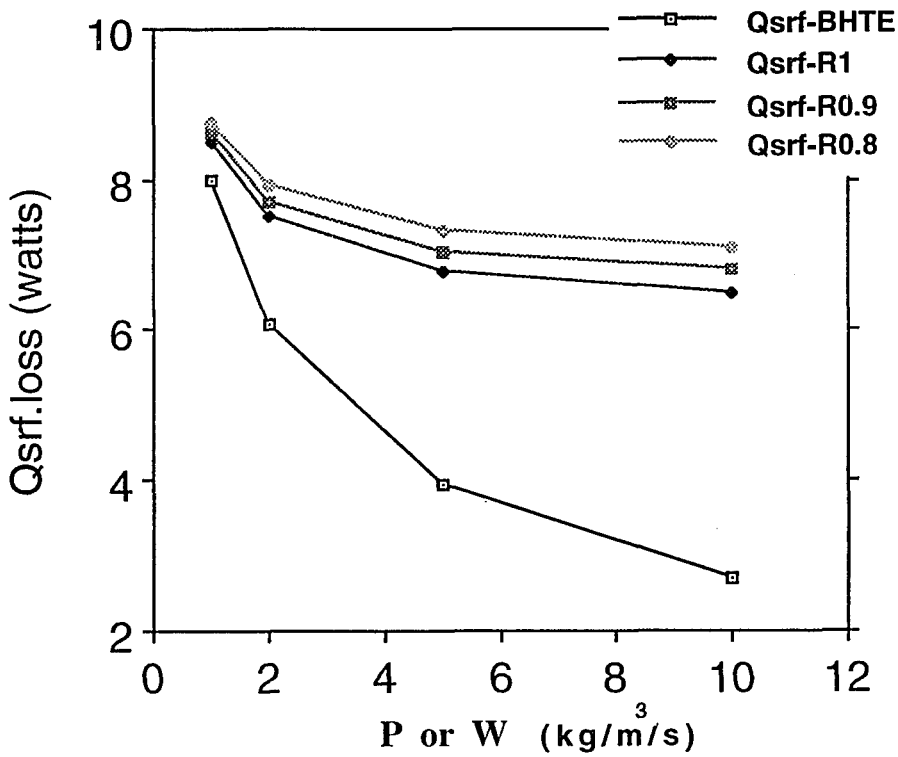

Figure 3.11 The surface heat loss predicted by the BHTE model(no vessels) at several W values and the 7-level vessels model for different perfusion P values and diameter ratios.

cases, good agreement exists between the two models for the two temperature criteria shown. The explanation of this result is that the energy loss caused by blood cooling is relatively small and conduction effects are more important. The heat loss from the surfaces of the entire geometry for the two models is shown in Figure 3.11. As we can see, for higher P or W values the surface heat loss stayed almost the same for the vessels model, but lowered considerably in the BHTE.

The Effect of Nu Number

Another parameter studied is the Nusselt number used in the seven level vessel model. The Nusselt number has been varied from 3.6 to 4.4. Figure(3.12) shows that the maximum temperature changes very little when the Nu number increases from 3.6 to 4.4. Based on Figure(3.12) and the total average tissue temperature in Figure(3.13) it can be seen that a 10% higher or lower value than Nu 4 will not dramatically change the temperature distribution. Therefore, the following results are based on a Nu number of 4.

The Effect of the Diameter Branching Ratio(γ):

The diameter branching ratio was defined previously in Equation 2.1. As this ratio gets smaller, the diameters of vessels become smaller. Table 3.1 shows the diameters of different levels of vessels for different ratio magnitudes. For a ratio of 0.8, we can get minimum

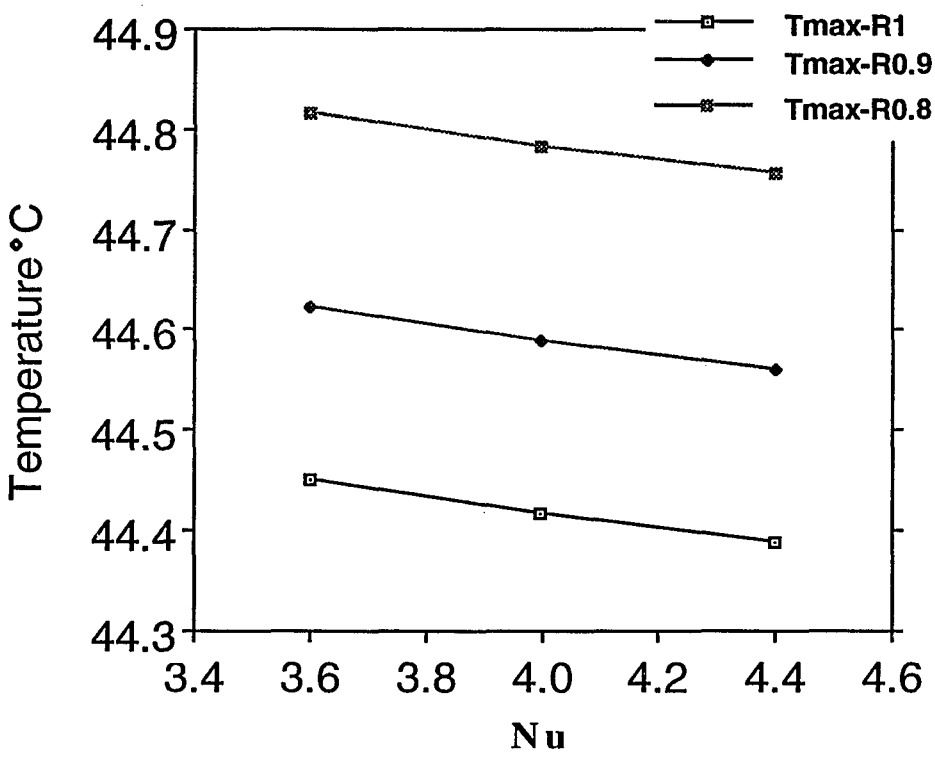

Figure 3.12 The maximum tissue temperature vs Nu for the 7-level vessels model with different diameter ratios.

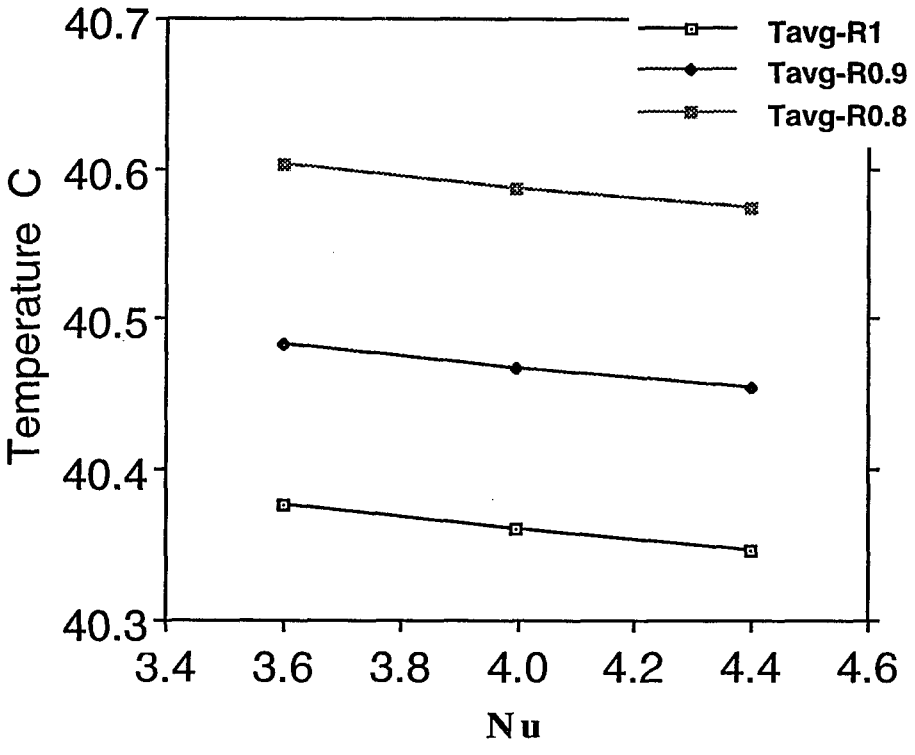

Figure 3.13 The average tissue temperature vs Nu for the 7-level vessel model with different diameter branching ratios.

diameters of about 300 um. From Figure (3.9) and Figure (3.10) the smaller the ratio the higher the maximum temperature and the higher the average tissue temperature.

The effect of the ratio changes can be discussed by rewriting Equation (2.2) as:

$$\frac{\partial T_b}{\partial x_l} = \frac{QA_{cl}}{\rho C_b V_l A_{cl}} + \frac{1}{\rho C_b V_l A_{cl}} \left(\frac{1}{h\pi D} + \frac{\ln(r_2/r_1)}{2\pi k} \right)^{-1} (T - T_b) \qquad (3.1)$$

where T_b is the blood temperature, x_l is the direction (either x, y or z), Q is the applied power per volume, T is the tissue temperature of vessel, Nu is the average Nusselt number, k is the conductivity in tissue, V_l is the velocity of vessel, r_1 is the radius of vessel, r_2 is the distance(radius) in conductive media between the node in the center of vessel and its four surrounding tissue nodes, and A_{cl} is the cross section area of the vessel.

As γ gets smaller, the diameter of the vessel gets smaller. Two factors influence both the blood and the tissue temperature due to this diameter decrease. One: Less power is deposited in the vessel volume and more power is deposited in the tissue. This makes it more difficult for the energy to move(e.g. by advection) out of the control volume than if the vessel were of a larger diameter; and two: There is a higher thermal conduction resistance between the blood flow node and the adjacent tissue node. This makes it more difficult for energy deposited in the tissue to be transported to the fluid to be advected away. The consequences of these effects are higher Tmax and Tavg values in the tissues and lower T_b in the vessel.

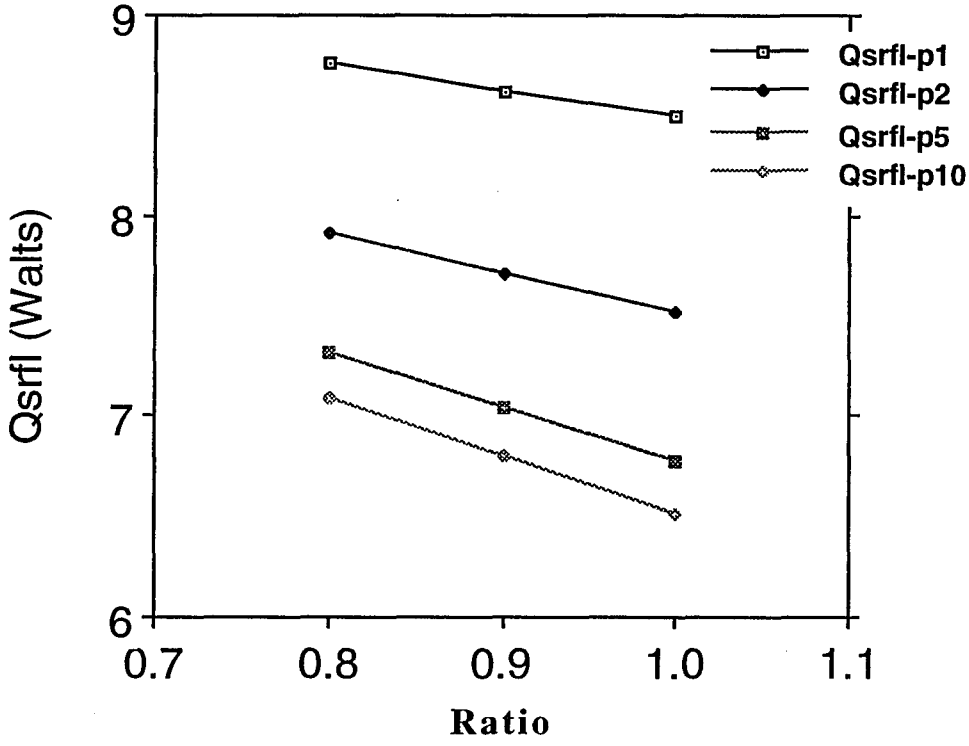

Figure 3.14 The equation 2.13 vs diameter branching ratio for the 7-level vessels model with different velocity fields as obtained by using P values of 1, 2, 5 and 10 ($kg/m^3/s$).

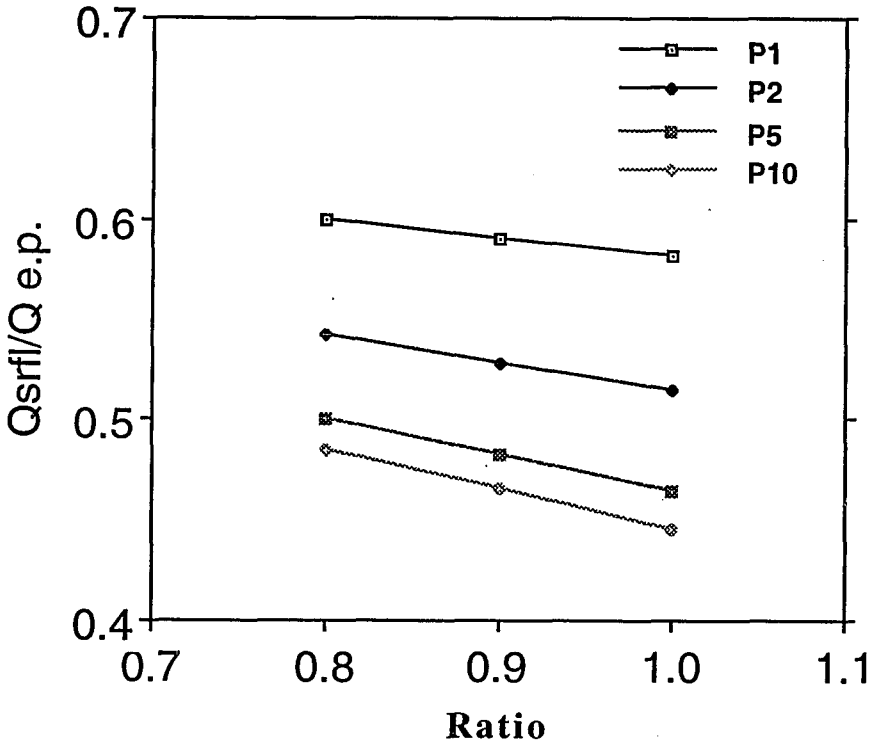

Figure 3.15 The ratio of equation 2.13 and equation 2.12 vs diameter ratio for the 7-level vessels model with different velocity fields.

as γ decreasing. Figures (3.14) and (3.15), show the energy loss through surface conduction, which indicates that the smaller ratio has more energy loss at the surfaces than the bigger ratio. That also indicates another point of higher tissue temperature in a smaller ratio. For those cases, the energy loss at the surface removed about 50% of the power applied (input uniform power) to the model.

The effect of the BHTE

The perfusion parameter(W) in the BHTE plays an important role as an adjustable parameter, just as the P value does in the convective thermal model. Hence, it is necessary to have an idea about the effect of this perfusion parameter in the BHTE predictions. In the calculation used to obtain the results in Figure (3.16) the geometry, the applied power Q and the properties of tissue are all the same as were used in obtaining the convective thermal model results. In the BHTE model, there are only two energy removal mechanisms from the control volume. One is the surface energy loss from the six surfaces of the control volume. The other is the perfusion heat loss by the BHTE model. The percentage of the total energy removed by these two loss term is shown in Figure 3.16 for various perfusion values. For perfusion values from 2 to 10 the perfusion energy loss is always above 50% of total input energy. This is a dominant term.

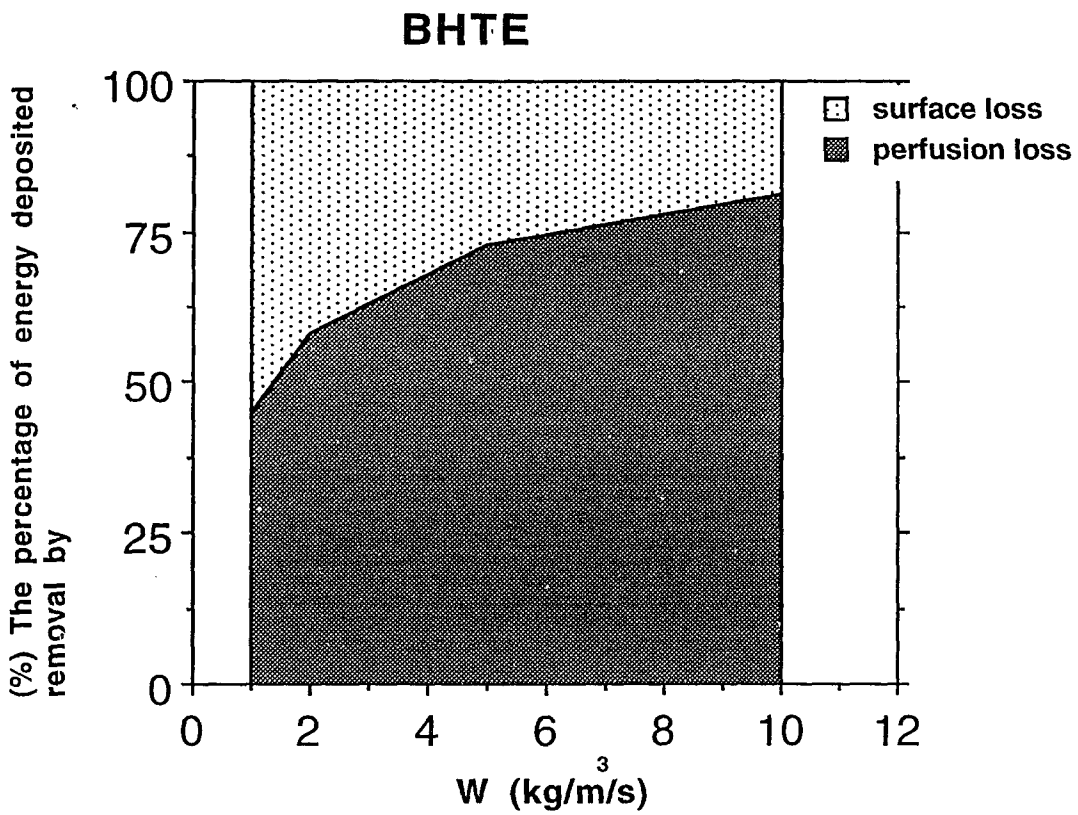

Figure 3.16 The percentage of the total energy deposited($Q_{e \cdot p}$) removed by either boundary surface conduction loss($Q_{cond \cdot surf}$) or perfusion loss in BHTE(Q_{perf}) for calculation with no blood vessels present.

CHAPTER 4

DISCUSSION

The convective thermal model consists of many distributed blood vessels which simulate the blood cooling effects. In this model, seven levels of vessels are used. The second model used the bio-heat transfer equation presented by Pennes, and is an approximation for predicting the over all temperature field using a heat sink term, $WC_b(T-T_b)$, to simulate the blood cooling effects. The following compares the convective thermal model predictions to those of the BHTE. For the seven level model, the following factors are looked at; the heat transfer between the tissue and the blood vessels, the surface area, and the volume and the velocity distribution in every level of the vessels model.

Figure 4-1, shows the percentage of the total surface area of blood vessels, the percentage of the total blood vessels' volume, the blood velocity and the percentage of total heat transfer between the tissue and the blood vessels for each level of the seven level model. This graph shows that about 15% of the total heat transfer between the tissue and blood vessels occurs in the level 7 vessels. Thus, a large heat transfer interaction still exists at level 7. Since one goal of

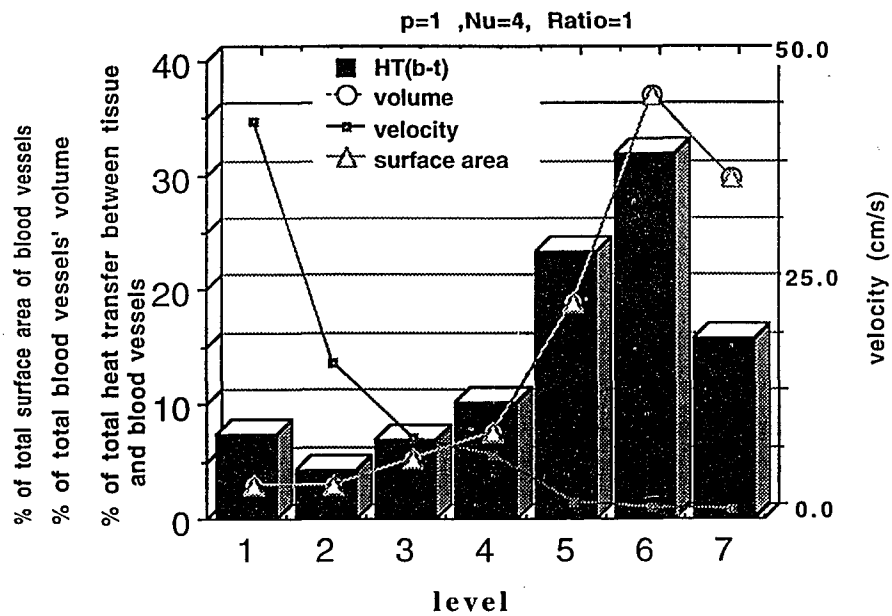

Figure 4.1 The comparison of the percentage of the total heat transfer between the tissue and blood vessels, percentage of total blood vessels' volume, percentage of blood vessels' surface area and the velocity magnitude in each level of the 7-level vessels model for a diameter branching ratio of 1(For levels 1 and 4 the velocity graphed is the value in the first section of that level).

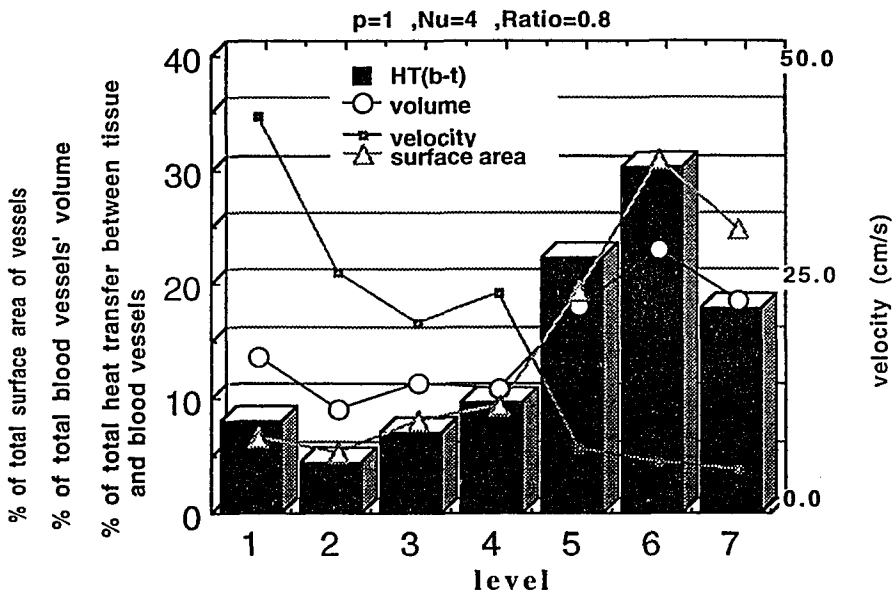

Figure 4.2 The comparison of the percentage of the total heat transfer between the tissue and blood vessels, percentage of total blood vessels' volume, percentage of blood vessels' surface area and the velocity magnitude in each level of the 7-level vessels model for a diameter branching ratio of 0.8(For levels 1 and 4 the velocity graphed is the value in the first section of that level).

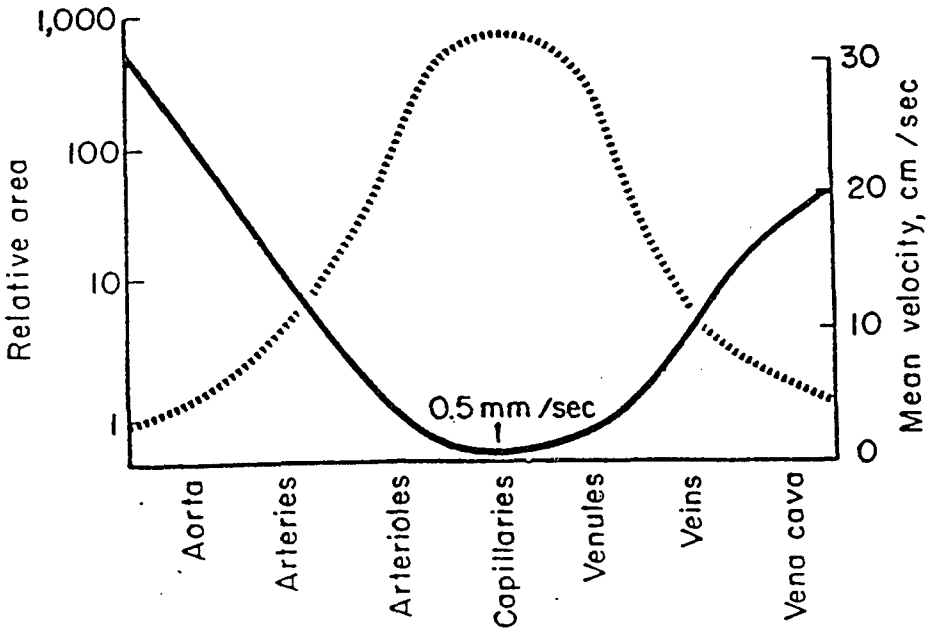

Figure 4.3 Schematic graph showing:broken line, the changes in relative total cross-sectional area(on a logarithmic scale) of the vascular bed; solid line, the mean velocity in the different categories of vessel.(From Alan C. Burton, Ph.D, Physiology and Biophysics of the Circulation, p64, 1984)

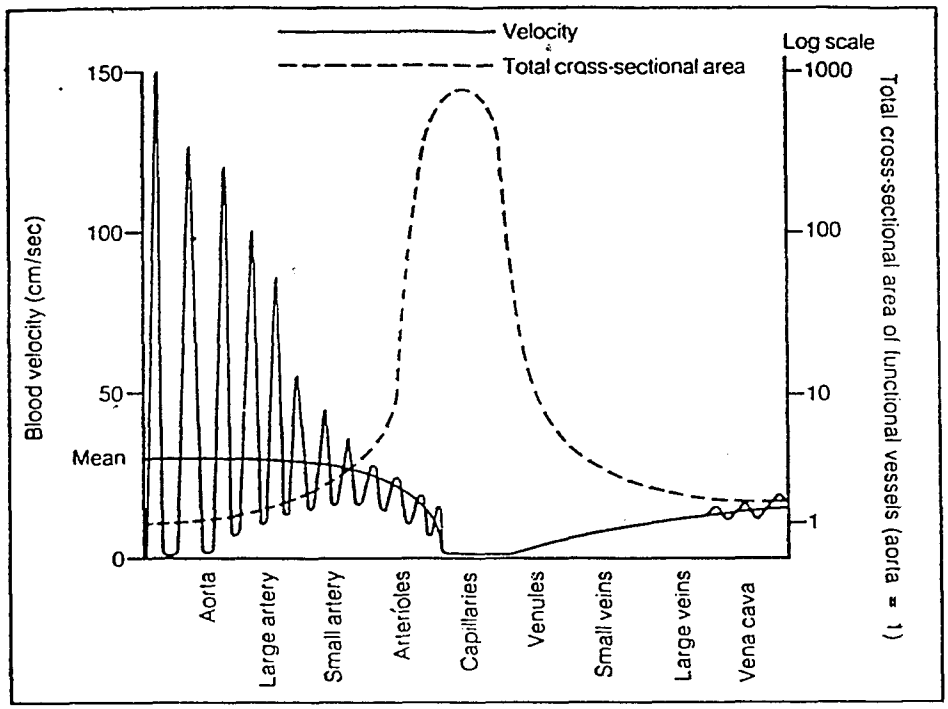

Figure 4.4 Blood velocity in different parts of the systemic vascular circuit(total blood flow being the same).(From Henry S. Badeer & Omaha, Nebr., Cardiovascular Physiology, p141, 1984).

this study was to determine at what level there was no significant thermal exchange, this question can be answered. Therefore, modification of the model is necessary to add further levels in order to reach a level which contributes negligible heat transfer between the tissue and the blood vessels. We also can see this in the diameter branching ratio 0.8 case in Figure 4.2. In Figure 4.3, the schematic graphs show the relative cross-sectional area and velocity of the systemic vascular circuit. The trends in the seven level model are the same as those shown in the Figures 4.3, 4.4.

If there are only 6 instead of 7, levels of vessels in the entire model, then the level six vessels become the terminates. The leakage of the mass flow rate is now from the end of the terminates vessels(level 6). The average temperature of the overall tissue is higher than that of the 7-level vessels model because less energy is removed by the blood vessels. Figure 4.5 compares the average temperature for the 7-level vessels ,the 6-level vessels and the BHTE models.

The seven level vessel model(7LM) and the BHTE model have their basic differences as mentioned previously. In the 7LM, the P value is an index of the total mass flow rate entering the cubic model in all the vessels if it is divided by the total volume(i.e. P=M/V; M is the total mass flow rate entering the tissue volume; V is the volume of the cubic model). Then it can be considered as equivalent to an average perfusion for the 7LM, and thus it can be compared to the perfusion parameter W in the BHTE. Figure 4.6 shows the W values corresponding to the variable P using the following two common

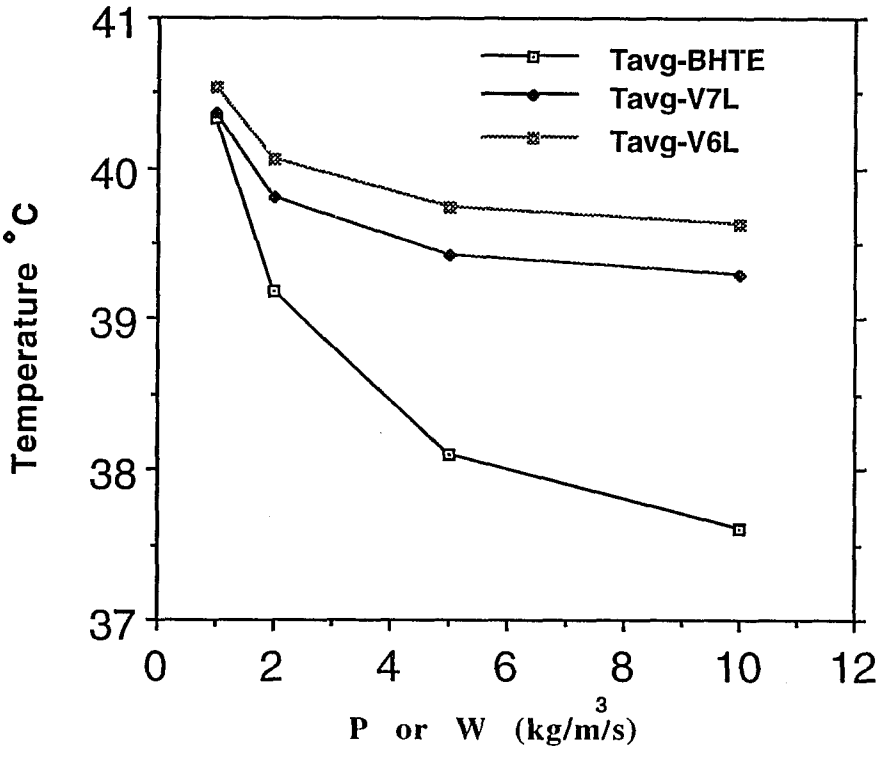

Figure 4.5 The comparison of the average tissue temperature for the BHTE model, the 7-level vessels model and the 6-level vessels model.

features. 1)The average tissue temperature(ATT) is the same for both models and 2)the amount of power removed by the blood flow term is the same for both models. Equations 4.1 and 4.2 are the blood flow terms of two models(the BHTE model and the 7LM).

$$Q_{blood\cdot BHTE} = Wc_b(T_{avg}-T_a)\cdot VOL \qquad 4.1$$

$$Q_{blood\cdot 7LM} = \sum_{i=1}^{7}\sum_{j=1}^{n} h_i A_i (T_{sj}-T_{bj}) \qquad 4.2$$

where T_{sj} is the wall temperature of the vessel at j node.

T_{bj} is the mean blood temperature of vessel at j node.

T_{avg} is the average tissue temperature in the tissue region.

VOL is the volume of cubic model.

n is the node number in i vessel.

A_i is the unit surface area of i^{th} blood vessel

The procedure used to calculate the W values shown in Figure 4.6 is to run a 7LM to determine both the RHS of Equation 4.2, and the average tissue temperature. Then, the uniform perfusion, W in the BHTE model, can be obtained by (a) equating Equations 4.1 and 4.2 and (b) using the T_{avg} value from the 7LM.

In Figure 4.6 when P = 5, W ≃ 1.7, giving a P/W ratio of about 2.7. This means that to produce the same ATT in the BHTE model (with the arterial temperature T_a = 37°C everywhere) a small W value can be used to simulate the vessel model with the same boundary conditions, and properties.

During the actual treatments or experiments we know that the local arterial temperature will not equal 37°C all the time(normally it will be greater than 37°C). In that case a higher value for W needs to be used to approximate the temperature field if the average temperatures are to be the same between the BHTE and 7LM. Provided, of course, that the 7LM is similar tissue.

Figure 4.7 shows a comparison of the average tissue temperature between the two models with respect to P and W. The W values shown in Figure 4.6 were used in Figure 4.7. From Figure 4.7, lower P and W values(less than 2) have a good approximation in the ATT. For P or W $>$ 2, ATT became smaller in the BHTE model than in the 7-level model. This means that the BHTE model is providing the better cooling effect than the 7LM.

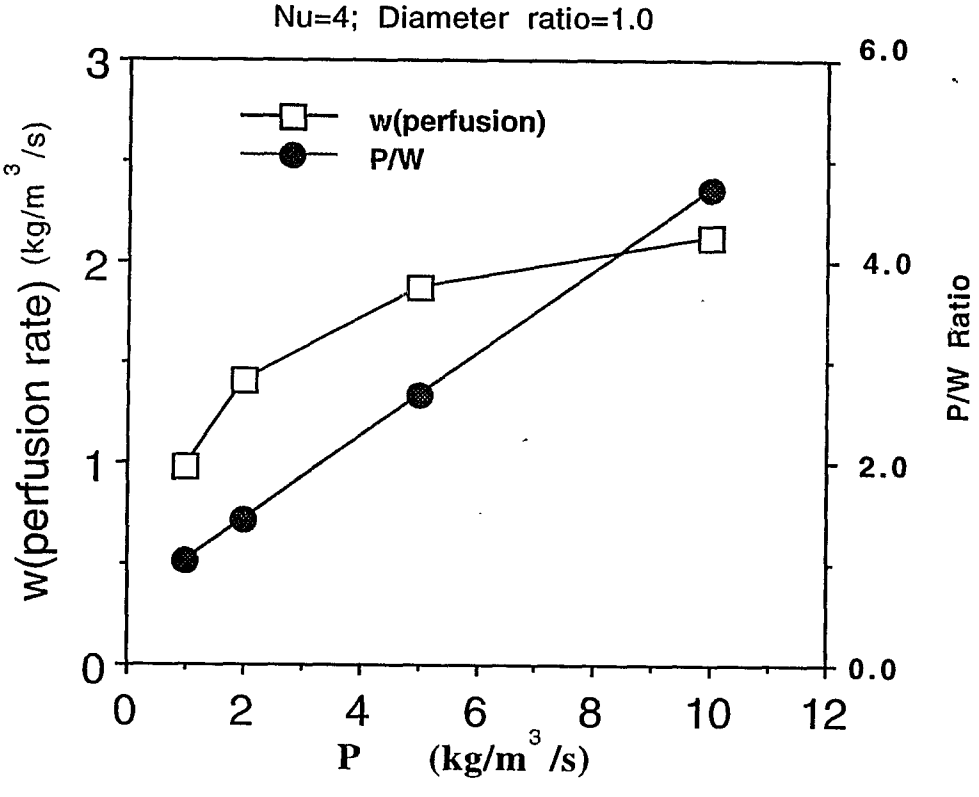

Figure 4.6 The value of the uniform perfusion(W) in the BHTE model that would be needed if (a) the BHTE heat sink term $Wc_b(T-T_a)$ is to be equal to the convection loss by all the blood vessels in the 7-level vessels model, and (b) The overall average tissue temperature is the same in both models, and is calculated from the 7-level vessels model.

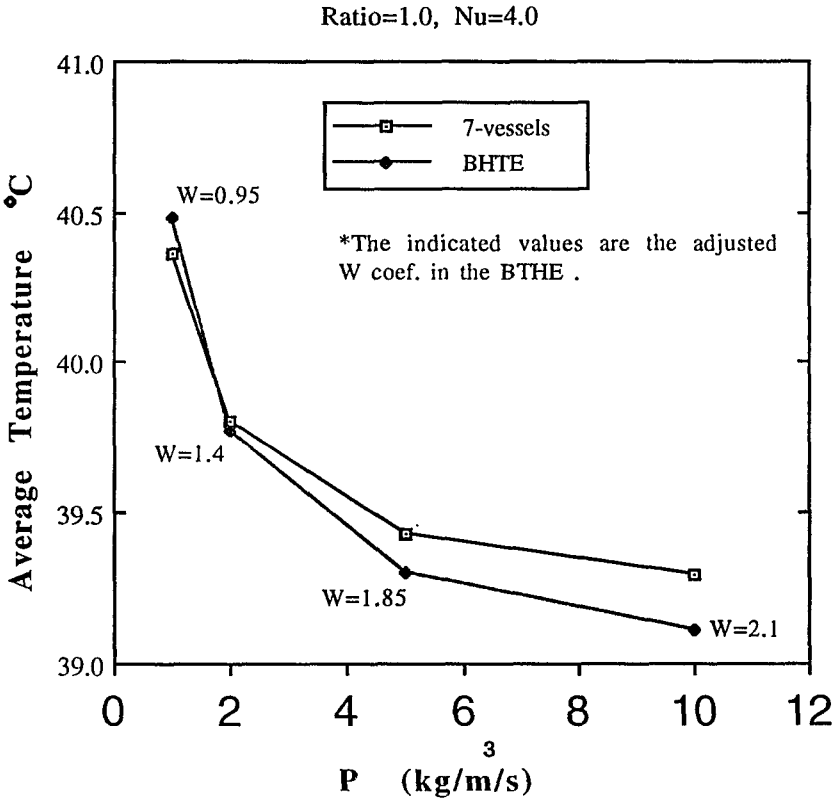

Figure 4.7 The comparison of the average temperature of whole control volume for both the 7-level vessel model and the BHTE for several P values. (W values in the BHTE are calculated based on Figure 4.6)

CHAPTER 5

CONCLUSIONS AND RECOMMENDATIONS

In this thesis, a simplified model to establish a vascular branching vessel model using the finite difference method to solve numerically for the temperature field has been successfully developed and tested. Although the model does not accurately reproduce all details of the vascular system in the human body, this thesis describes a tissue heat transfer model which is not a field equation approximation, and which retains the presence of the blood vessels and the basic physics of the blood vessel/tissue heat transfer processes. The basic approach used in this model can be extended and used as an alternative to the field equation approaches; or, since it retains the basic physics involved in the heat transfer processes, it can be used as a more fundamental basis against which such approximations can be compared. The 7-level blood vessel convective thermal model presented here, indicates that the level 7 vessels still contribute a large fraction of the thermal interaction between blood vessels and surrounding tissues.

In the future, the simplified and fixed branching pattern needs to be modified to allow for more flexible blood vessel patterns in which the blood vessels are not straight lines and can be traced by

machine. For example, we need to determine how many vessels are in one zone (or group) ,what is the spacing between vessels, how are the arteries and veins paired, how far can the levels go before reaching a small percentage of the heat transfer between the tissue and the vessels, and how do we develop the new simplified blood vessels' model etc. Consequently, for a good approximation and a reasonable thermal model formulation of the vascular system in the human body ,small grid sizes and large computer program (memory size) will be essential to improve upon the algorithm currently being used.

APPENDIX A

ANALYTICAL SOLUTIONS OF DIFFERENT SINGLE LARGE VESSEL CASES

Analytical solutions for a single large blood vessel surrounded by purely conductive tissues for both a constant arterial blood temperature and for a variable arterial blood temperature cases are derived below neglecting the conduction in the z direction. The cross section of the geometry is shown in Figure A.1.

The governing equation of Pennes bio-heat transfer equation is used:

$$\frac{1}{r}\frac{d}{dr}\left(kr\frac{dT}{dr}\right) + Wc_b(T - T_a(z)) = q \qquad (A.1)$$

with the boundary conditions of

$$T(R_1,z) = T_w(z) \qquad (A.2)$$

$$T(R_2,z) = T_0 \qquad (A.3)$$

$$T(r,0) = T_0 \quad r>R_1 \qquad (A.4)$$

$$T(r,L) = T_0 \quad r>R_1 \qquad (A.5)$$

The governing equation for the average temperature of the blood in the vessel is:

From top view of cylindrical vessel:

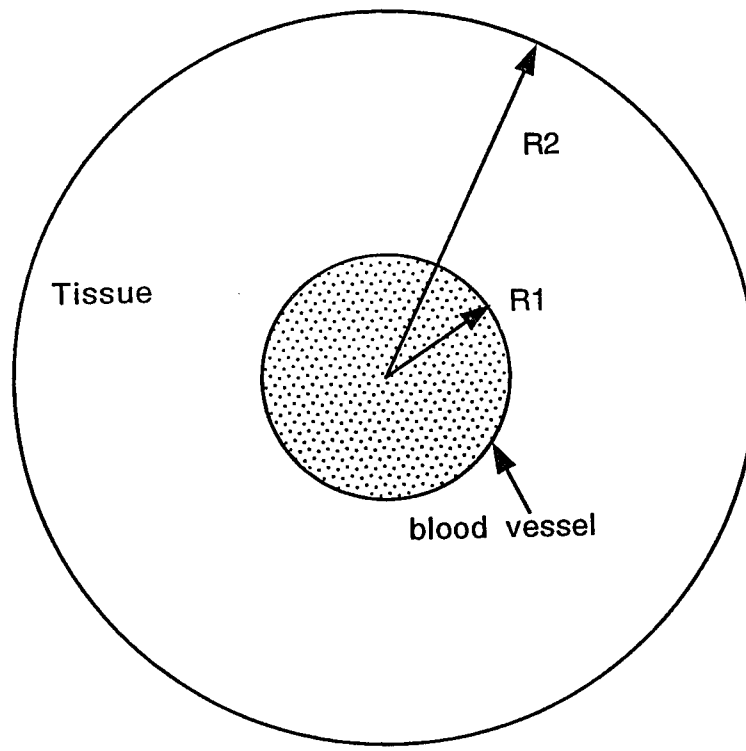

Figure A.1 The end view of the single large blood vessel model.

$$\rho c_b V A_c \frac{dT_b}{dz} = qA_c + hA_s(T_w - T_b) \qquad (A.6)$$

with the entrance condition of

$$T_b(0) = T_e \qquad (A.7)$$

and the heat transfer coefficient determined from

$$Nu = hD/K_b = 4.0 \qquad (A.8)$$

At the vessel wall the matching condition is

$$- k\frac{dT}{dr}\Big|_{r=R_1} = h(T_w - T_b) \qquad (A.9)$$

The solutions for the average blood temperature for the two cases are in non-dimensional form:

$$\theta(z) = \frac{T_b(z) - T_{b.i}}{T_{b.\infty} - T_{b.i}} = 1 - e^{-(z/z_{eq})} \qquad (A.10)$$

with

$$Z_{eq} = \frac{\gamma D_1}{4St} \qquad (A.11)$$

for the variable arterial blood temperature

and

$$Z_{eq} = \frac{\beta D_1}{4St} \qquad (A.12)$$

for the constant arterial blood temperature

where:

$T_b(z)$ is the blood temperature along z direction.

$T_{b.i}$ is the initial blood temperature

$T_{b.\infty}$ is the equilibrium blood temperature.

T_w is the wall temperature of the blood vessel.

$$St(\text{Stanton number}) = \frac{Nu}{RePr} = \frac{h}{\rho V c_p} \qquad (A.13)$$

$$X_p(\text{Penetration depth}) = (\sqrt{Wc_b/k}\,)^1 = (A)^{-0.5} \qquad (A.14)$$

$$Bi = \frac{hX_p}{K_s} \qquad (A.15)$$

$$C = \frac{K_1(r_1/X_p) + BiK_0(r_1/X_p)}{I_1(r1/X_p) - BiI_0(r1/X_p)} \qquad (A.16)$$

$$c1 = \frac{K_0(r_1/X_p)*(T_0 - B/A) - K_0(r_2/X_p)*(T_w - B/A)}{K_0(r_1/X_p)*I_0(r_2/X_p) - K_0(r_2/X_p)*I_0(r_1/X_p)} \qquad (A.17)$$

$$\beta = \frac{K_0(r2/X_p) + CI_0(r2/X_p)}{K_0(r2/X_p) + CI_0(r2/X_p) - \{K_0(r1/X_p)I_0(r2/X_p) - K_0(r2/X_p)I_0(r1/X_p)\}h/c1} \qquad (A.18)$$

$$\gamma = \frac{K_0(r2/X_p) + CI_0(r2/X_p)}{K_0(r1/X_p) + CI_0(r1/X_p)} \tag{A.19}$$

$$\delta = \frac{K_0(r2/X_p) + CI_0(r2/X_p)}{K_0(r2/X_p)+CI_0(r2/X_p)-\{K_0(r1/X_p)I_0(r2/X_p)-K_0(r2/X_p)I_0(r1/X_p)\}h/c1} \tag{A.20}$$

The equilibrium blood temperatures are:

$$T_{b.\infty} = T_0 + q\frac{X_p^2}{K}(1/\delta - 1) + qD_1/(4h)\gamma \tag{A.21}$$

for the arterial case. And

$$T_{b.\infty} = T_{art}(1 - \delta) + T_0\delta + q\frac{X_p^2}{K}(1 - \delta) + qD_1/(4h)\beta \tag{A.22}$$

for the constant case.

The non-dimensional solution for the tissue temperature and the wall temperature of the blood vessels are:

$$T_w(z) = Tb(z) + 1/\gamma\ (T_0 - B/A) - 1/\beta\ (T_b(z) - B/A) \tag{A.23}$$

$$\Phi = \frac{T_t - T_w}{T_0 - T_w} = C_{11}I_0(r/X_p) + C_{22}K_0(r/X_p) + \frac{T_w - B/A}{T_w - T_0} \tag{A.24}$$

where :

$$C_{11} = \frac{\left(\frac{T_0 - B/A}{T_0 - T_w}\right) K_0(r1/X_p) + \left(\frac{T_w - B/A}{T_w - T_0}\right) K_0(r2/X_p)}{K_0(r1/X_p) I_0(r2/X_p) - K_0(r2/X_p) I_0(r1/X_p)} \quad (A.25)$$

$$C_{22} = \frac{-\left[\left(\frac{T_0 - B/A}{T_0 - T_w}\right) I_0(r1/X_p) + \left(\frac{T_w - B/A}{T_w - T_0}\right) I_0(r2/X_p)\right]}{K_0(r1/X_p) I_0(r2/X_p) - K_0(r2/X_p) I_0(r1/X_p)} \quad (A.26)$$

$$\frac{B}{A} = T_{art} + q\frac{X_p^2}{K} \quad (A.27)$$

And:

T_{art} = const

for the constant arterial blood temperature case, and

$T_{art} = T_b(z)$

for the variable arterial blood temperature case.

APPENDIX B

PROGRAM VERIFICATION FOR A SINGLE LARGE BLOOD VESSEL WITH DIFFERENT CASES: COMPARISON BETWEEN ANALYTICAL AND NUMERICAL SOLUTIONS

The following results from the numerical simulation are compared with analytical solutions as the verifications of the computer program. Those cases are neglecting the conduction in the z direction. Three major comparisons of analytical solutions are:

CASE
1) for constant arterial blood temperature.
2) for variable arterial blood temperature.
3) for 2-d case, the same test case as Chato's results for no power, no perfusion, higher entrance temperature.

The model used for the three cases is the same as that used in Appendix A, a cylinder geometry, with length 10 cm and diameter 5 cm. The following symbols are described as follows. 1)In the legend, "new modified" means the numerical result with current blood vessel model which is formulated by former Ph.d student Z. P. Chen. 2)In the legend, "ana, for d50" means the analytical result with 50mm width in diameter. 3)The top line in the figures, "cylin" means the cylinder geometry, "Q" means the magnitude of the applied uniform power and "v" is the velocity of the blood in the vessel. 4)The bottom line of the

figures, "v.d" means the diameter of the vessel, "g.s" means the gridsize of numerical simulation, and "w" means the perfusion value.

There are 28 verifications with different input conditions. The constant arterial blood temperature case has 19 verifications, the variable arterial blood temperature case has 7 verifications and the comparison with Chato's solution has 2 verifications. The conditions applied for these verifications can be categorized into five subjects. These subjects are 1)power(both high and low) 2)perfusion rate(both high and low) 3)velocity(both fast and slow) 4)diameter(both large and small) and 5)gridsize(both large and small). The details of the conditions for each verification is shown in the figure text, and the author will not repeat it again.

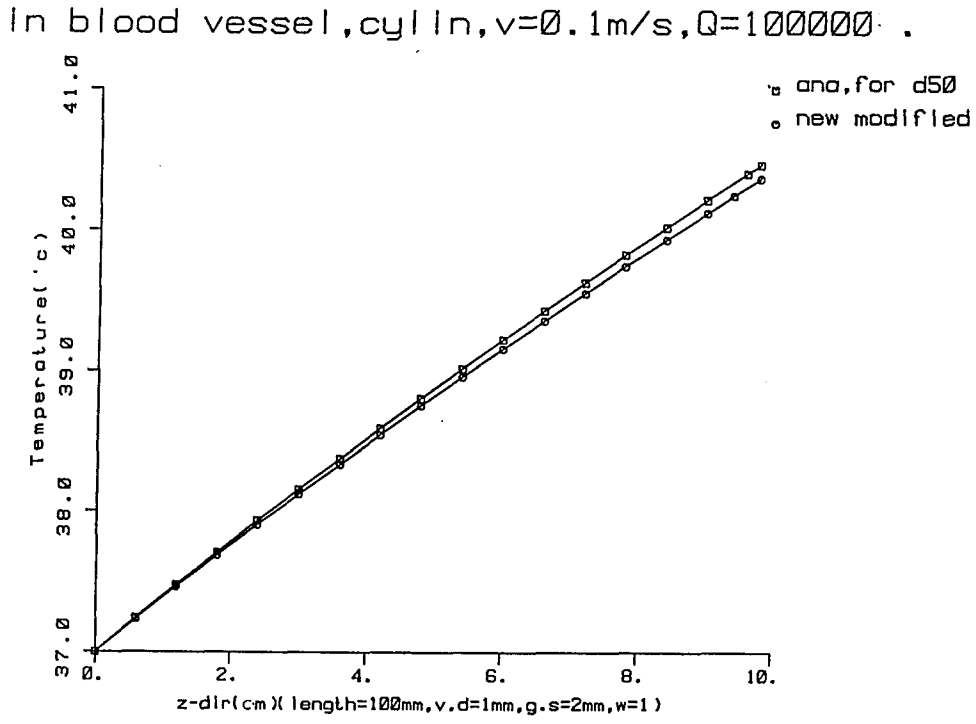

Figure B.1 Verification of the temperature distribution along the single large blood vessel for Q=100000 w/m^3 (uniform power), perfusion w=1 kg/m^3•C, velocity v=0.1 m/s, diameter d=1mm ,gridsize dz=2mm for the constant arterial case.

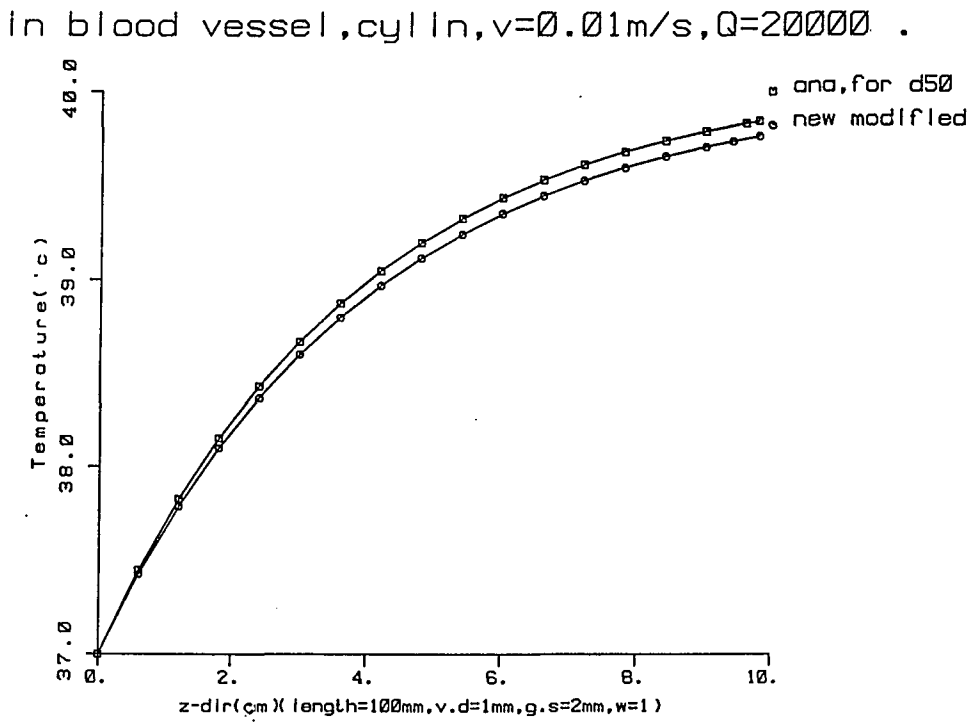

Figure B.2 Verification of the temperature distribution along the single large blood vessel for Q=20000 w/m^3 (uniform power), perfusion w=1 $kg/m^3 \cdot C$, velocity v=0.01 m/s, diameter d=1mm ,gridsize dz=2mm for the constant arterial case.

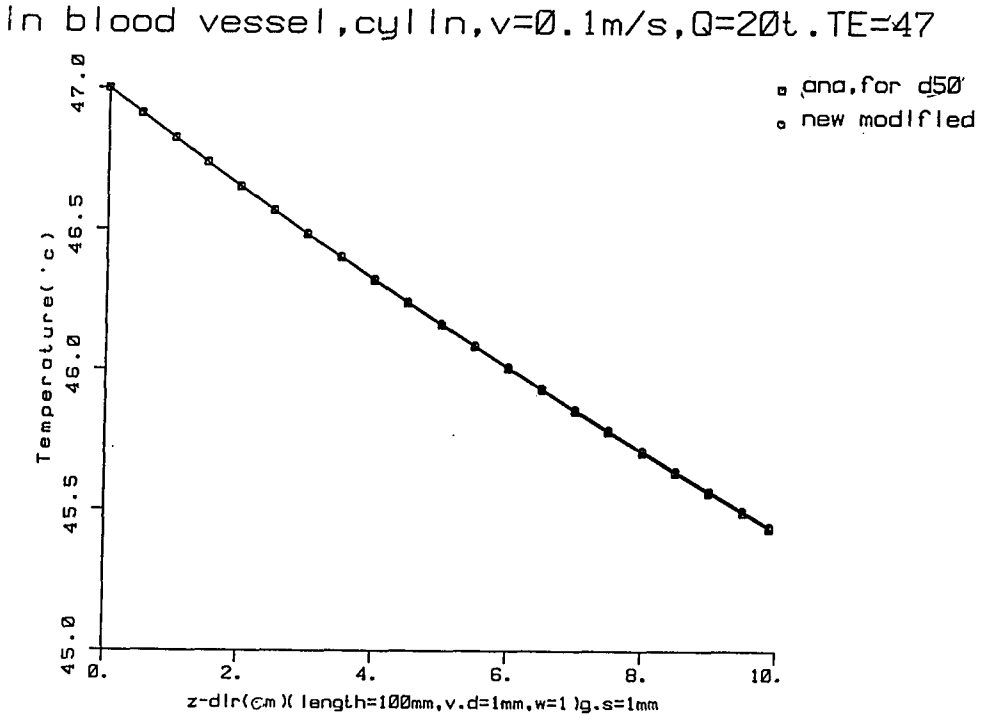

Figure B.3 Verification of the temperature distribution along the single large blood vessel for Q=20000 w/m^3 (uniform power), perfusion w=1 kg/m^3•C, velocity v=0.1 m/s, diameter d=1mm ,gridsize dz=1mm for the constant arterial case.

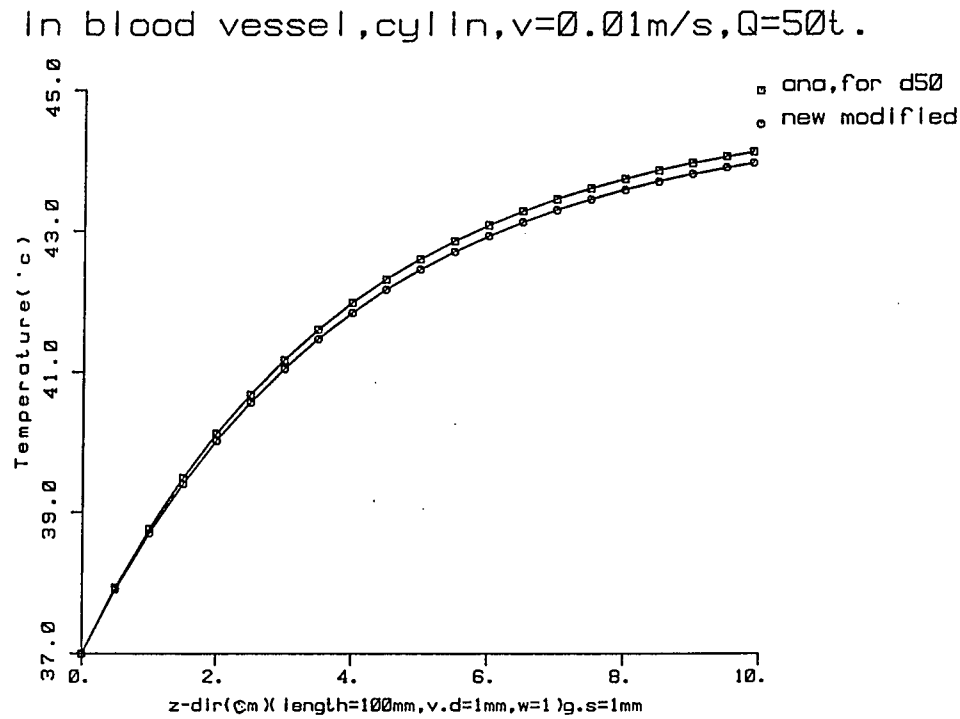

Figure B.4 Verification of the temperature distribution along the single large blood vessel for Q=50000 w/m^3 (uniform power), perfusion w=1 $kg/m^3 \cdot C$, velocity v=0.01 m/s, diameter d=1mm ,gridsize dz=1mm for the constant arterial case.

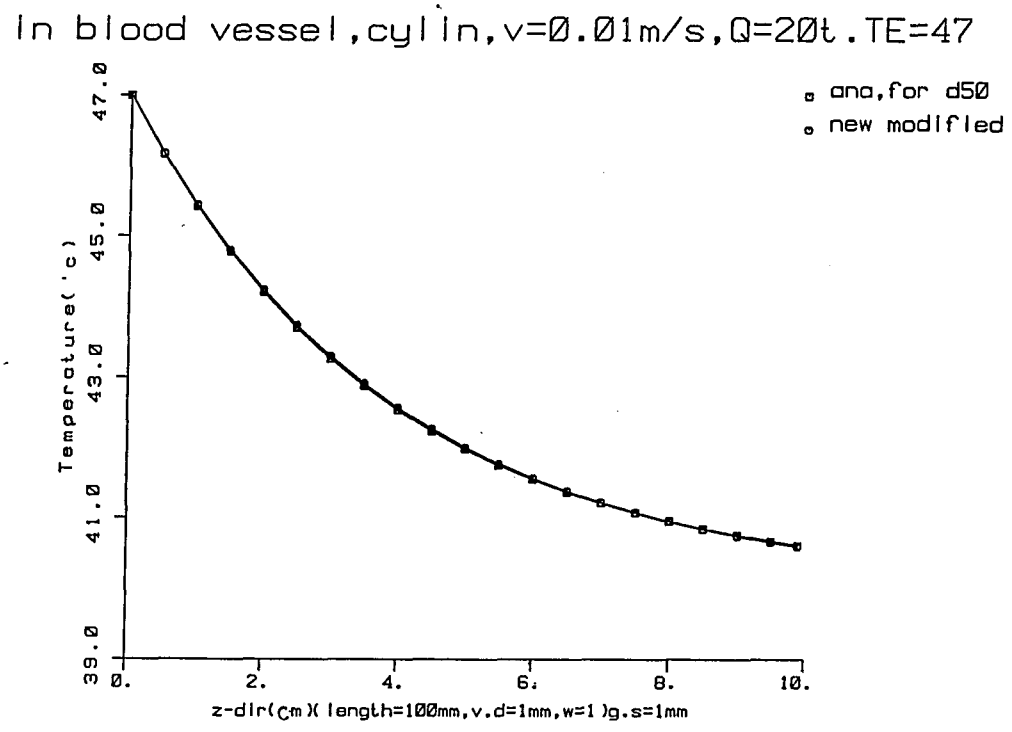

Figure B.5 Verification of the temperature distribution along the single large blood vessel for Q=20000 w/m^3 (uniform power), perfusion w=1 kg/m^3°C, velocity v=0.01 m/s, diameter d=1mm ,gridsize dz=1mm ,entrance temperature Te=47°c for the constant arterial case.

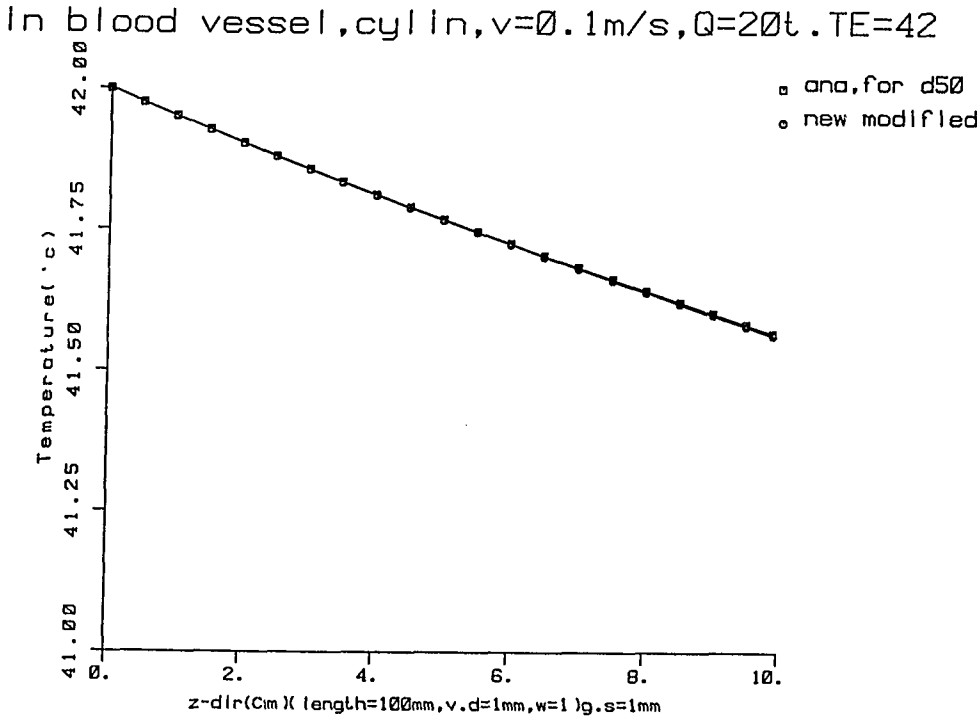

Figure B.6 Verification of the temperature distribution along the single large blood vessel for Q=20000 w/m^3 (uniform power), perfusion w=1 $kg/m^3°C$, velocity v=0.1 m/s, diameter d=1mm ,gridsize dz=1mm ,entrance temperature Te=42°c for the constant arterial case.

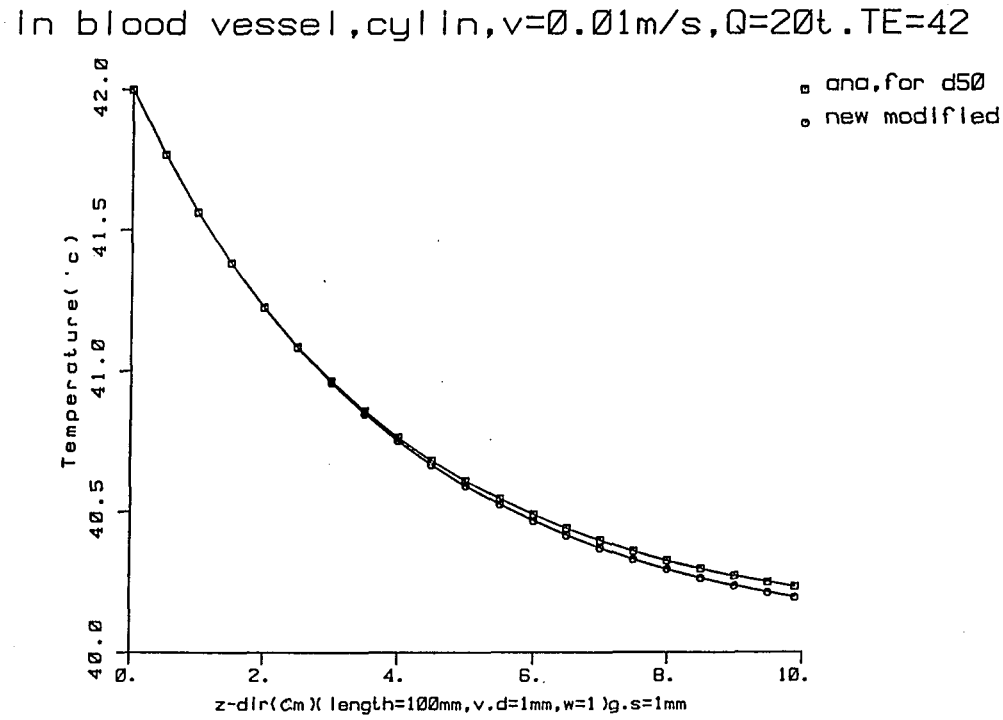

Figure B.7 Verification of the temperature distribution along the single large blood vessel for Q=20000 w/m^3 (uniform power), perfusion w=1 kg/m^3°C, velocity v=0.01 m/s, diameter d=1mm ,gridsize dz=1mm ,entrance temperature Te=42°c for the constant arterial case.

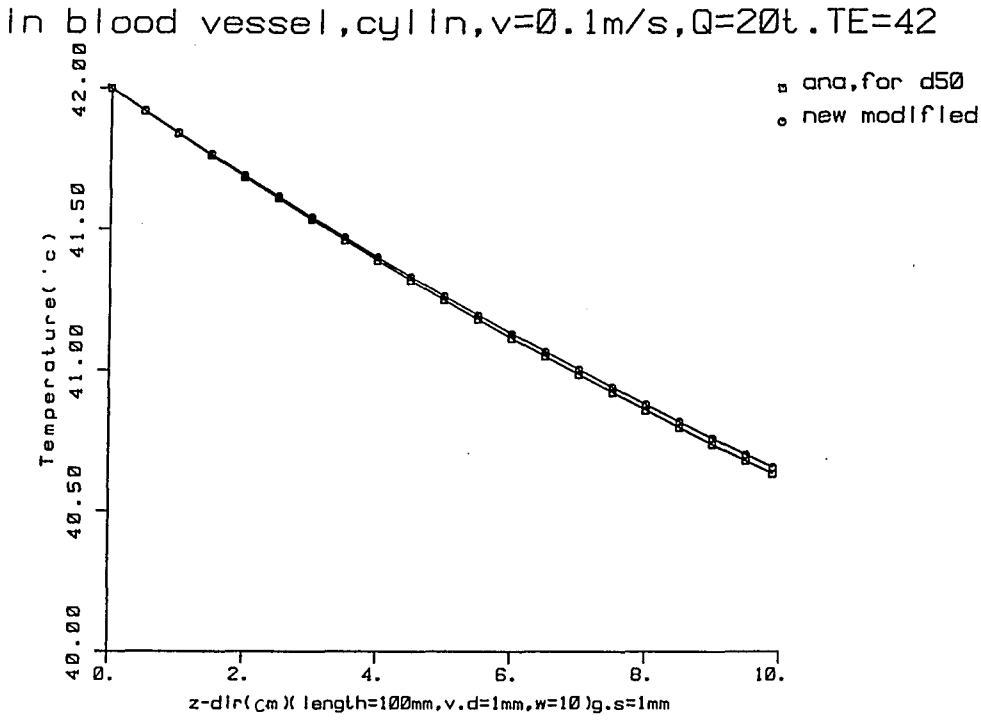

Figure B.8 Verification of the temperature distribution along the single large blood vessel for Q=20000 w/m^3 (uniform power), perfusion w=10 $kg/m^3 \cdot C$, velocity v=0.1 m/s, diameter d=1mm ,gridsize dz=1mm ,entrance temperature Te=42°c for the constant arterial case.

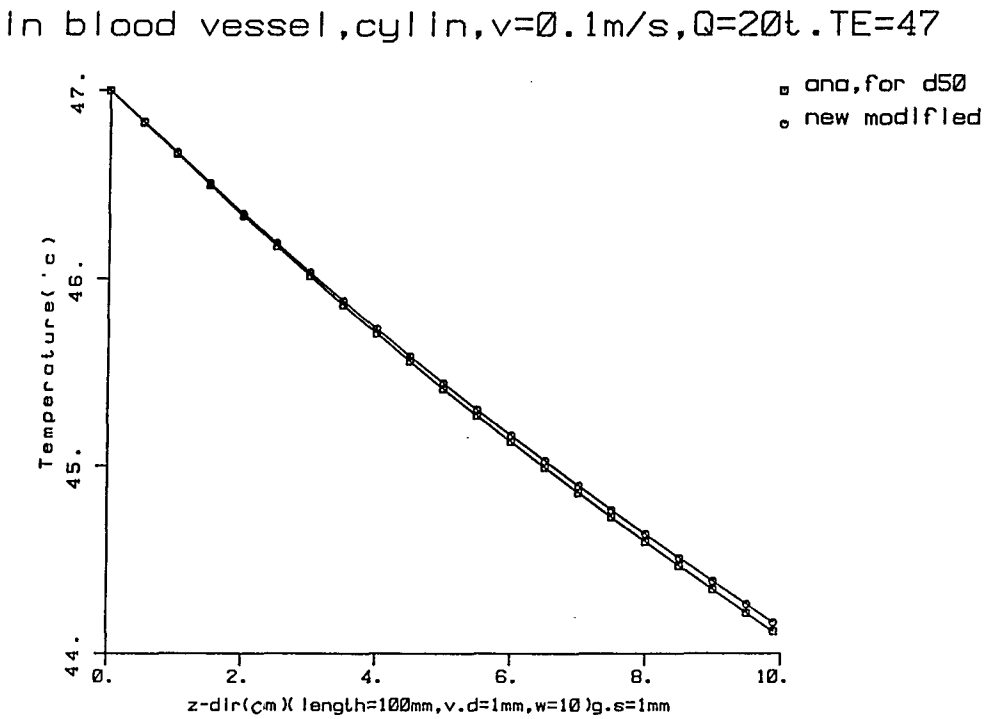

Figure B.9 Verification of the temperature distribution along the single large blood vessel for Q=20000 w/m^3 (uniform power), perfusion w=10 kg/m^3°C, velocity v=0.1 m/s, diameter d=1mm ,gridsize dz=1mm ,entrance temperature Te=47°c for the constant arterial case.

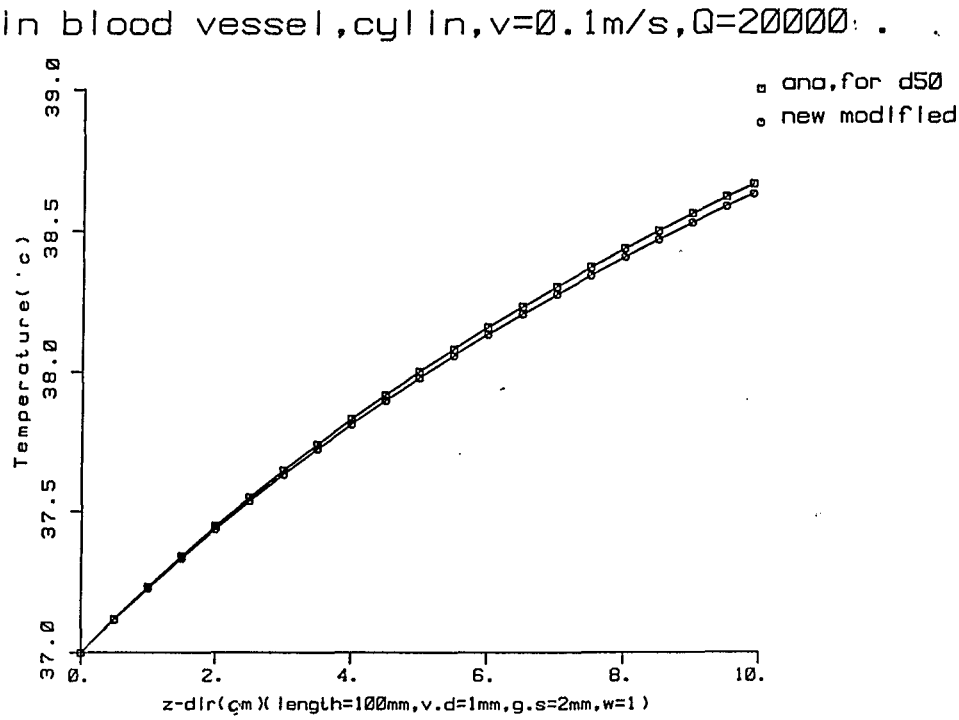

Figure B.10 Verification of the temperature distribution along the single large blood vessel for Q=20000 w/m^3 (uniform power), perfusion w=1 $kg/m^3 \cdot C$, velocity v=0.1 m/s, diameter d=1mm ,gridsize dz=2mm for the constant arterial case.

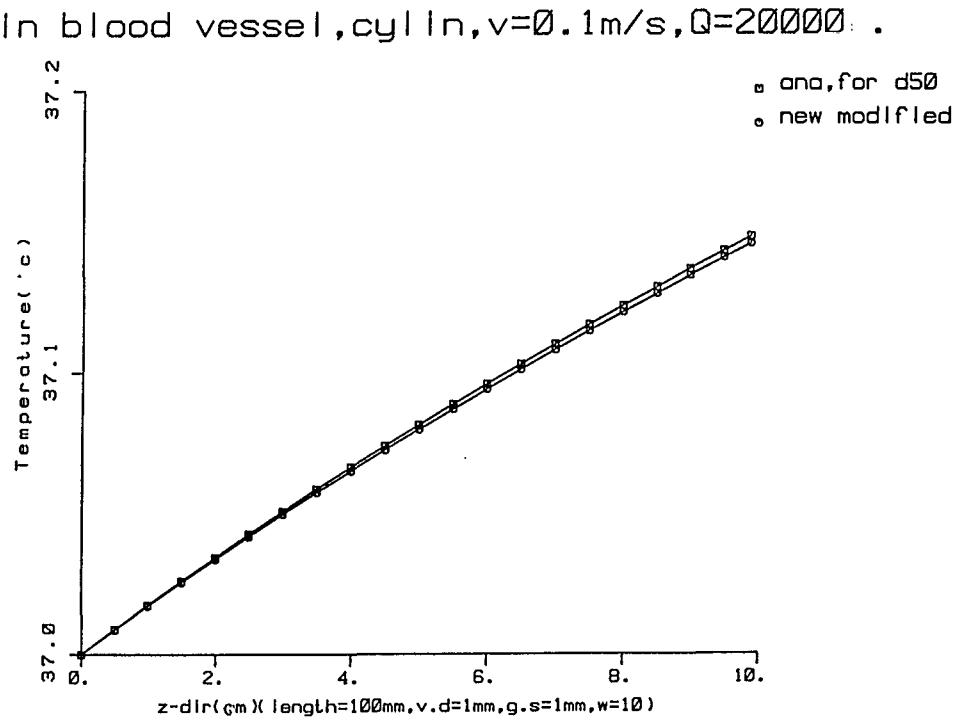

Figure B.11 Verification of the temperature distribution along the single large blood vessel for Q=20000 w/m^3 (uniform power), perfusion w=10 kg/m^3°C, velocity v=0.1 m/s, diameter d=1mm ,gridsize dz=2mm for the constant arterial case.

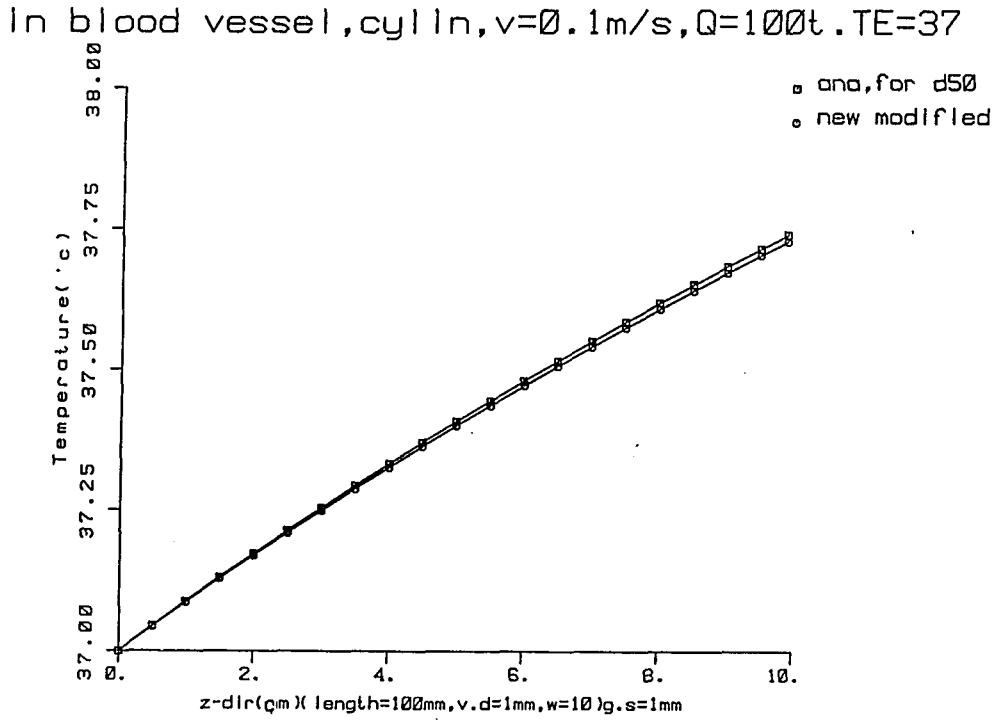

Figure B.12 Verification of the temperature distribution along the single large blood vessel for Q=100000 w/m^3 (uniform power), perfusion w=10 kg/m^3*C, velocity v=0.1 m/s, diameter d=1mm ,gridsize dz=1mm for the constant arterial case.

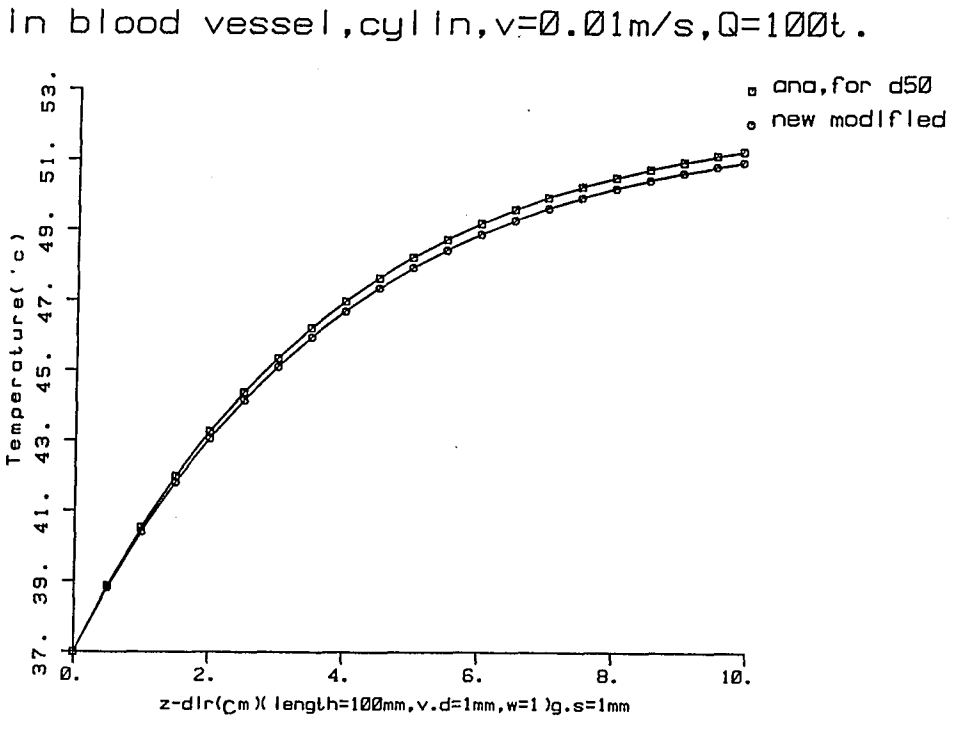

Figure B.13 Verification of the temperature distribution along the single large blood vessel for Q=100000 w/m^3 (uniform power), perfusion w=1 kg/m^3*C, velocity v=0.01 m/s, diameter d=1mm ,gridsize dz=1mm for the constant arterial case.

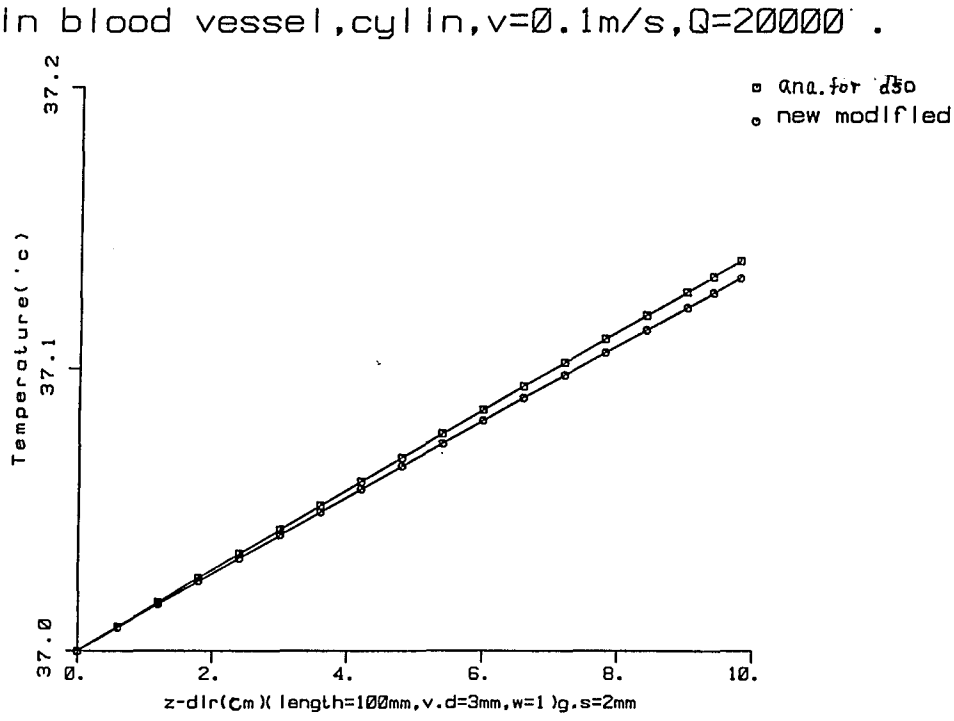

Figure B.14 Verification of the temperature distribution along the single large blood vessel for Q=20000 w/m^3 (uniform power), perfusion w=1 $kg/m^3 \cdot C$, velocity v=0.1 m/s, diameter d=3mm ,gridsize dz=2mm for the constant arterial case.

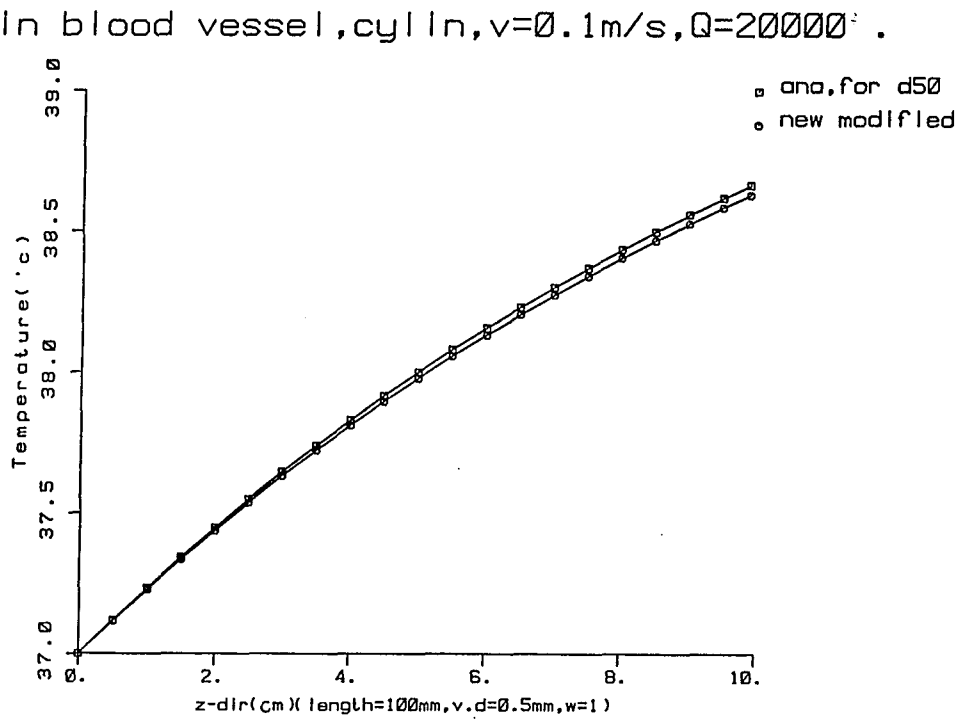

Figure B.15 Verification of the temperature distribution along the single large blood vessel for Q=20000 w/m^3 (uniform power), perfusion w=1 kg/m^3°C, velocity v=0.1 m/s, diameter d=0.5mm ,gridsize dz=2mm for the constant arterial case.

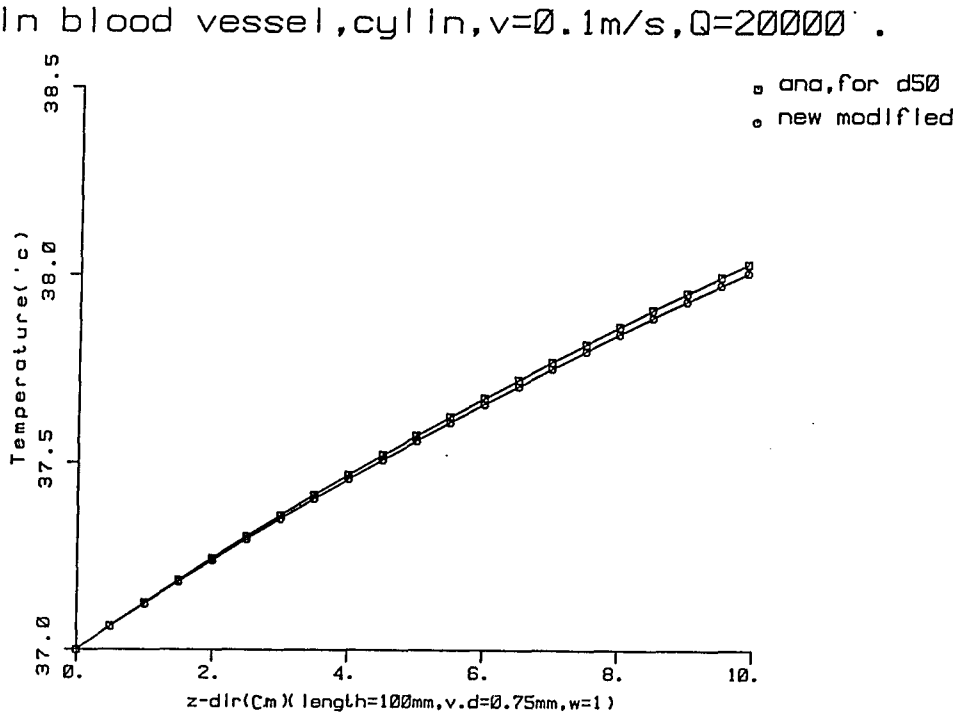

Figure B.16 Verification of the temperature distribution along the single large blood vessel for Q=20000 w/m^3 (uniform power), perfusion w=1 $kg/m^3 \cdot C$, velocity v=0.1 m/s, diameter d=0.75mm ,gridsize dz=2mm for the constant arterial case.

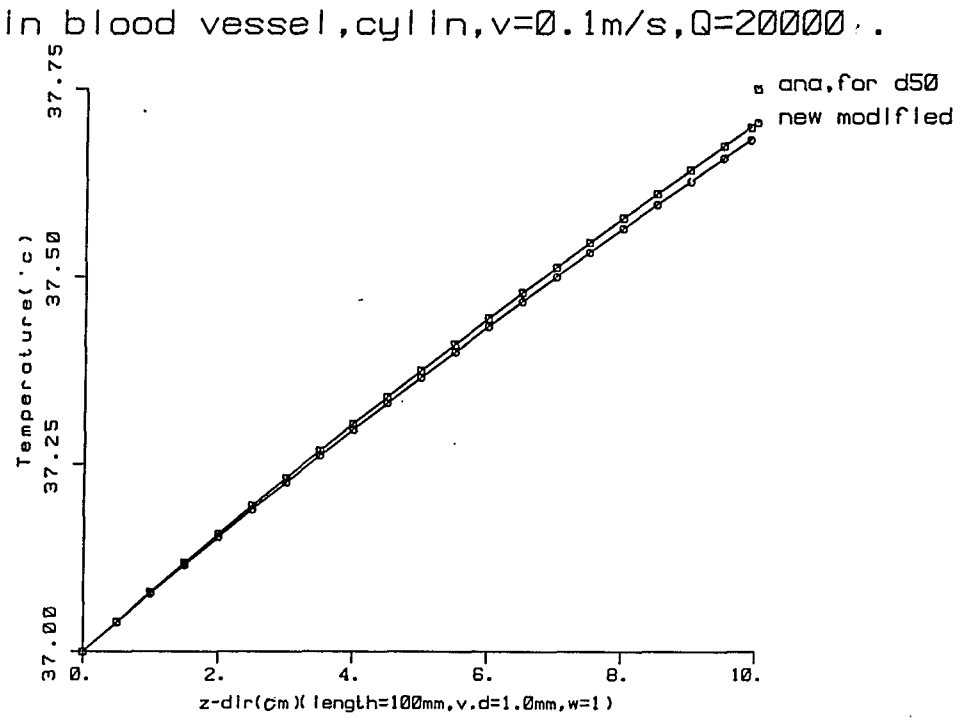

Figure B.17 Verification of the temperature distribution along the single large blood vessel for Q=20000 w/m^3 (uniform power), perfusion w=1 $kg/m^3 \cdot C$, velocity v=0.1 m/s, diameter d=1mm ,gridsize dz=2mm for the constant arterial case.

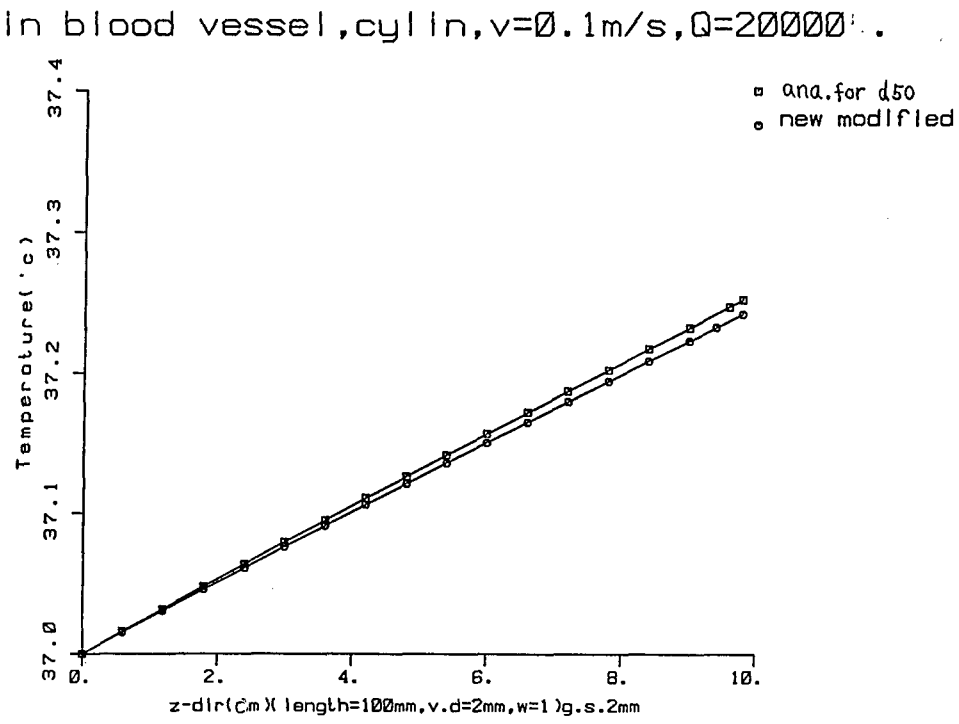

Figure B.18 Verification of the temperature distribution along the single large blood vessel for Q=20000 w/m^3 (uniform power), perfusion w=1 $kg/m^3 \cdot C$, velocity v=0.1 m/s, diameter d=2mm ,gridsize dz=2mm for the constant arterial case.

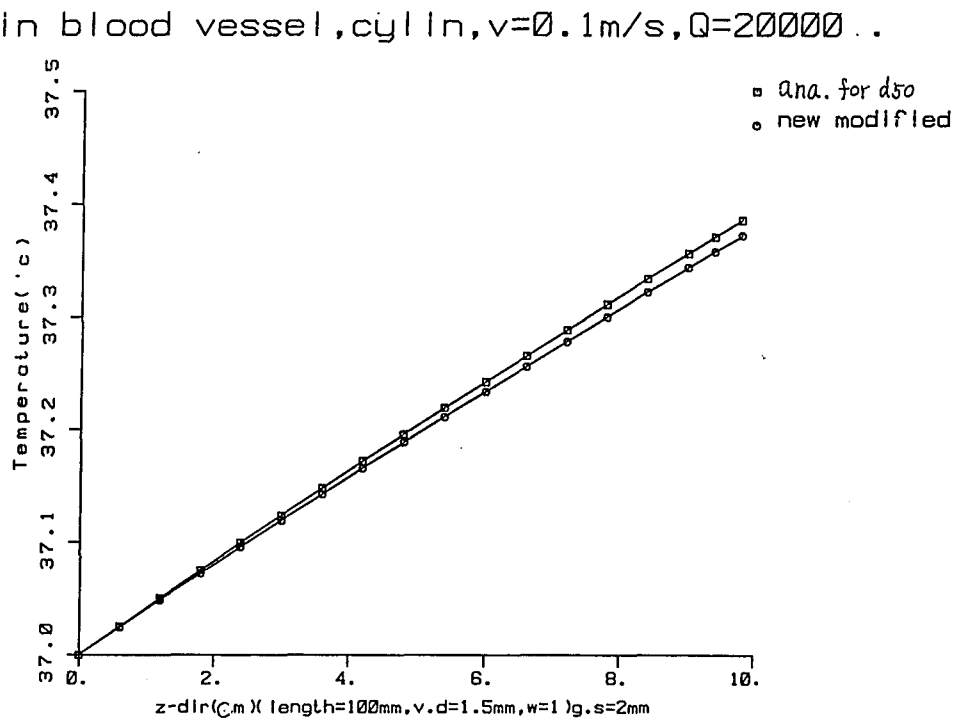

Figure B.19 Verification of the temperature distribution along the single large blood vessel for Q=20000 w/m^3 (uniform power), perfusion w=1 $kg/m^3 \cdot C$, velocity v=0.1 m/s, diameter d=1.5mm ,gridsize dz=2mm for the constant arterial case.

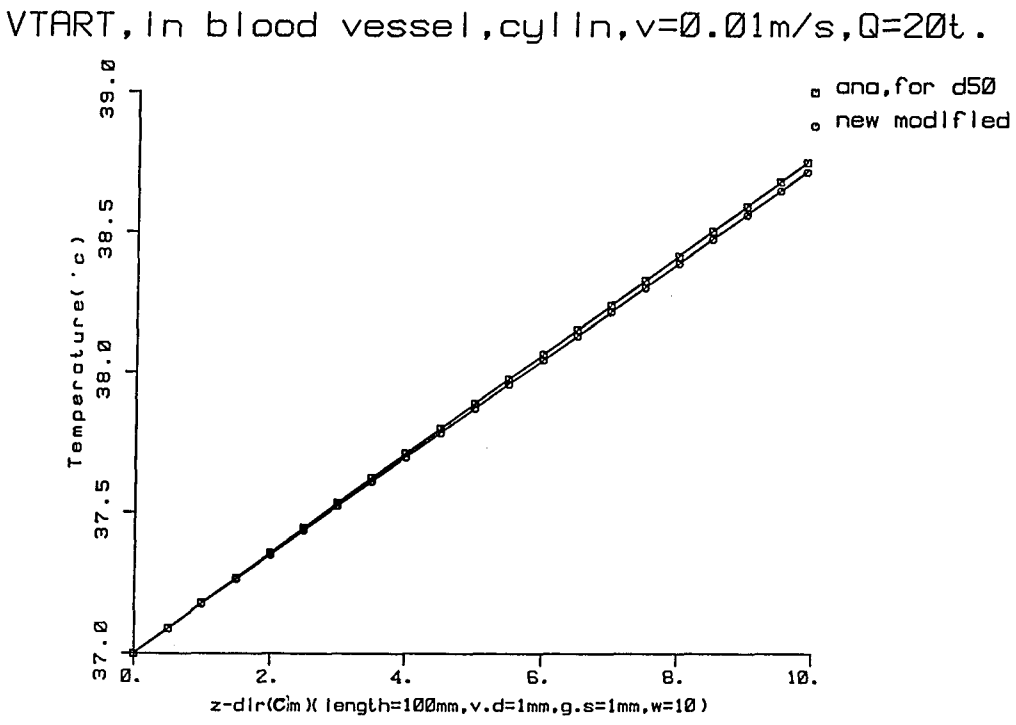

Figure B.20 Verification of the temperature distribution along the single large blood vessel for Q=20000 w/m^3 (uniform power), perfusion w=10 $kg/m^3 \cdot C$, velocity v=0.01 m/s, diameter d=1mm ,gridsize dz=1mm for the variable arterial case.

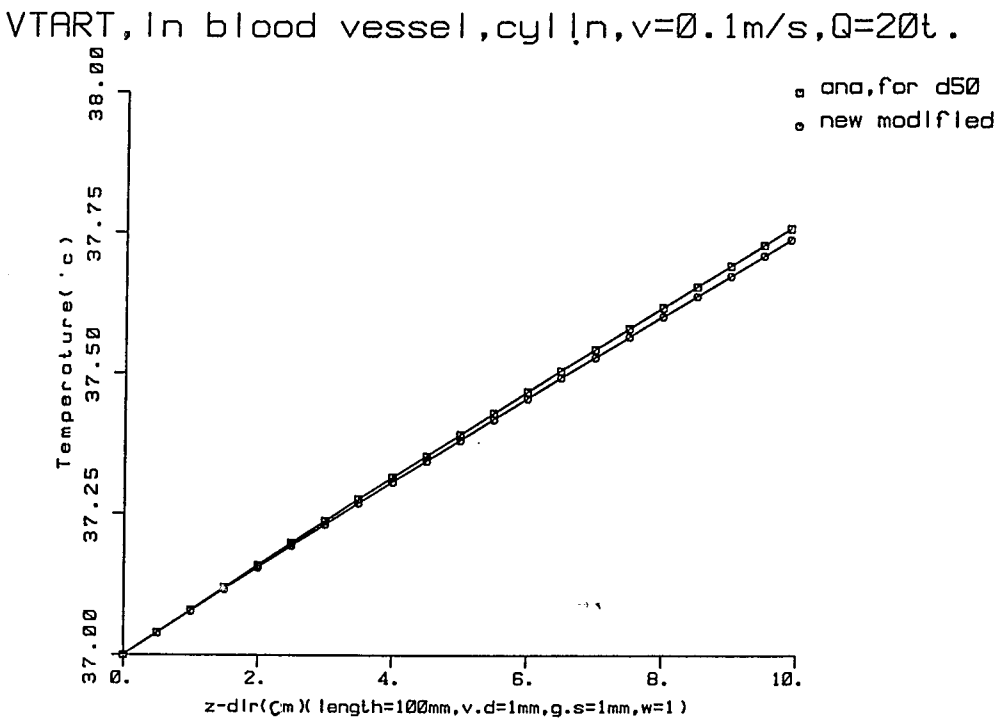

Figure B.21 Verification of the temperature distribution along the single large blood vessel for Q=20000 w/m^3 (uniform power), perfusion w=1 kg/m^3°C, velocity v=0.1 m/s, diameter d=1mm ,gridsize dz=1mm for the variable arterial case.

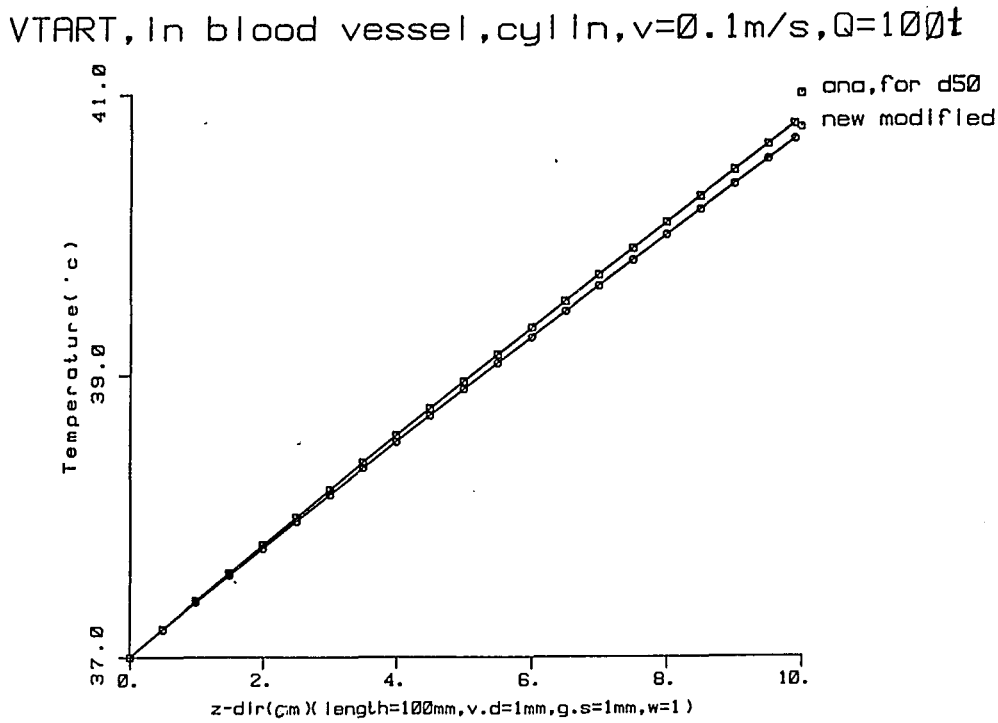

Figure B.22 Verification of the temperature distribution along the single large blood vessel for Q=100000 w/m^3 (uniform power), perfusion w=1 $kg/m^3 \cdot C$, velocity v=0.1 m/s, diameter d=1mm ,gridsize dz=1mm for the variable arterial case.

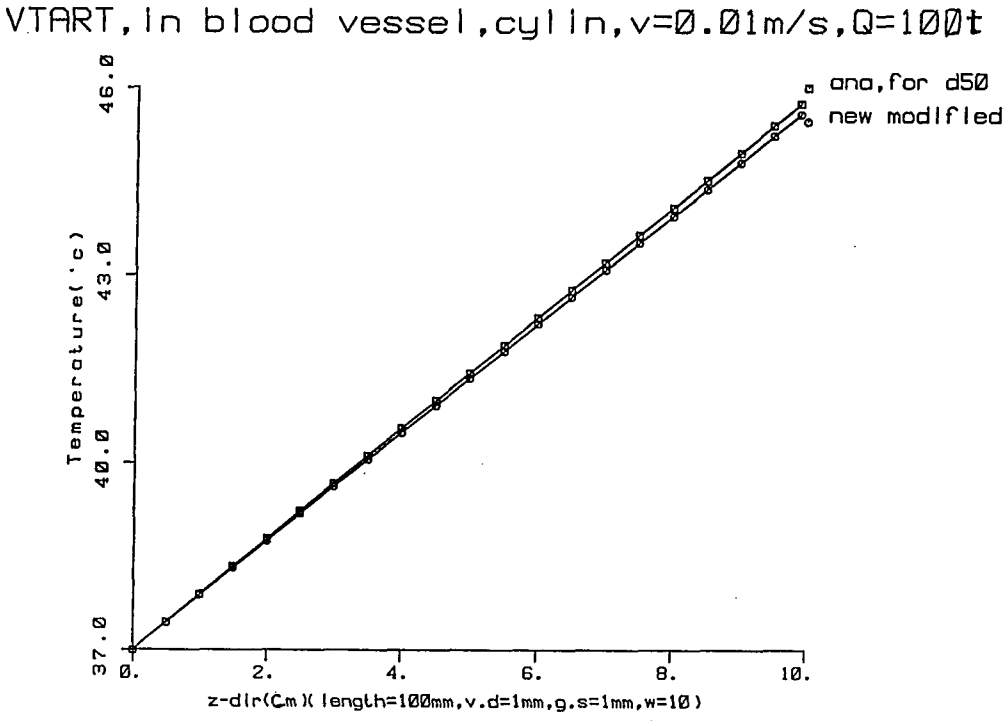

Figure B.23 Verification of the temperature distribution along the single large blood vessel for Q=100000 w/m^3 (uniform power), perfusion w=10 kg/m^3°C, velocity v=0.01 m/s, diameter d=1mm ,gridsize dz=1mm for the variable arterial case.

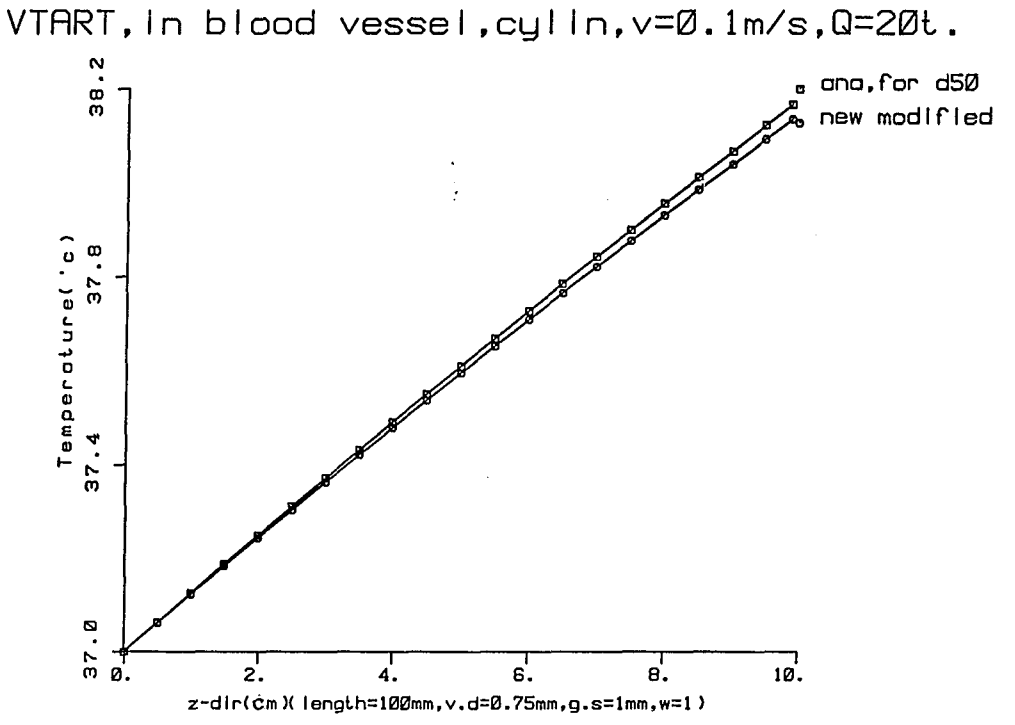

Figure B.24 Verification of the temperature distribution along the single large blood vessel for Q=20000 w/m^3 (uniform power), perfusion w=1 $kg/m^3 \cdot C$, velocity v=0.1 m/s, diameter d=0.75mm ,gridsize dz=1mm for the variable arterial case.

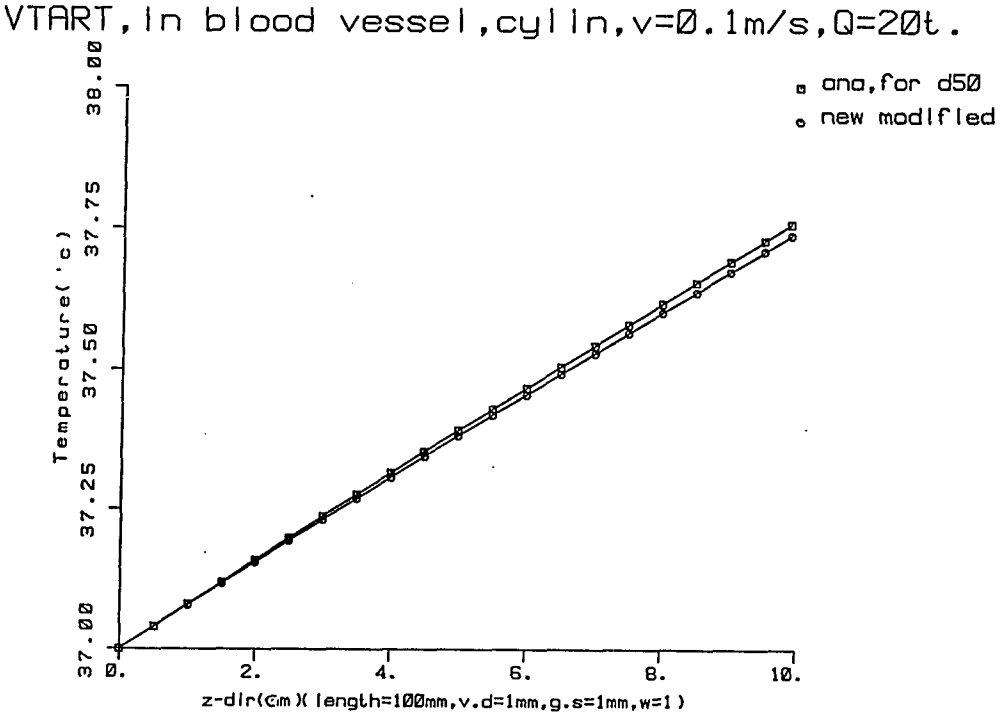

Figure B.25 Verification of temperature ditribution along the single large blood vessel for Q=20000 w/m^3 (uniform power), perfusion w=1 kg/m^3*C, velocity v=0.1 m/s, diameter d=1mm ,gridsize dz=1mm for variable arterial case.

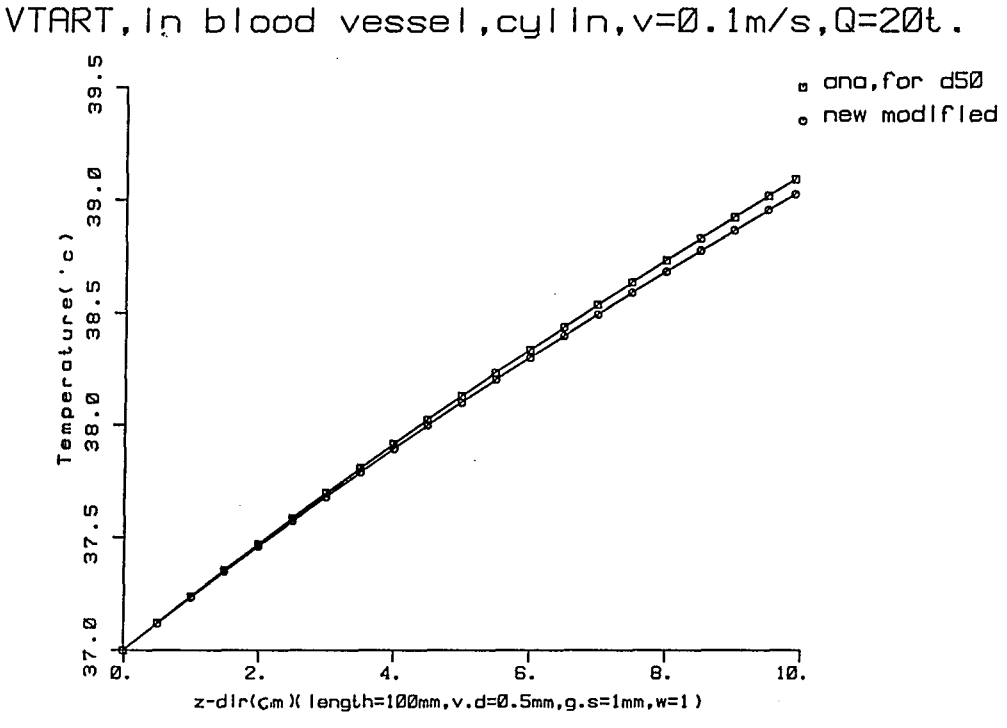

Figure B.26 Verification of the temperature distribution along the single large blood vessel for Q=20000 w/m^3 (uniform power), perfusion w=1 kg/m^3°C, velocity v=0.1 m/s, diameter d=0.5mm ,gridsize dz=1mm for the variable arterial case.

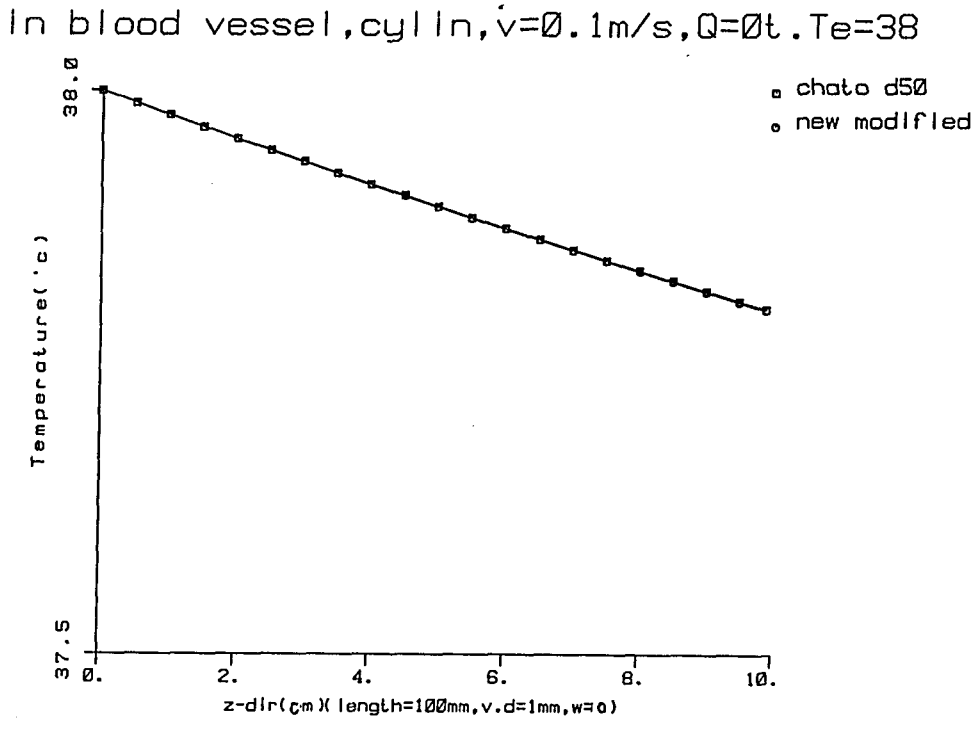

Figure B.27 Verification of the temperature distribution along the single large blood vessel for Q=0 w/m^3 (uniform power), perfusion w=0 $kg/m^3°C$, velocity v=0.1 m/s, diameter d=1mm, gridsize dz=2mm, entrance temperature Te=38°C for Chato's case.

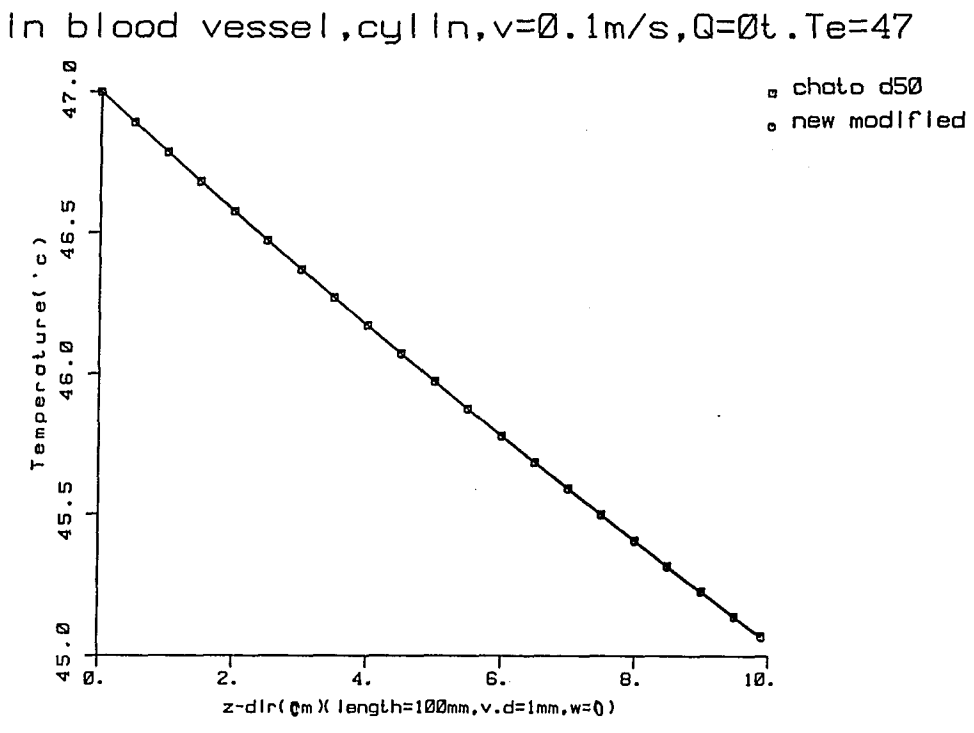

Figure B.28 Verification of the temperature distribution along the single large blood vessel for Q=0 w/m^3 (uniform power), perfusion w=0 $kg/m^3°C$, velocity v=0.1 m/s, diameter d=1mm, gridsize dz=2mm, entrance temperature Te=47°C for Chato's case.

APPENDIX C

DOCUMENTATION AND VERIFICATION OF BRANCHING PROGRAM

This program was especially written for a square cylinder (parallelepiped). The 16 parallelepiped regions have these dimensions: WIDTH/4 (WIDTH is the width of square) in width and subdivided into segments of length; L2-1(actually L2) which are perfused. Each segment (L2) consists of many subdivided segments of smallest regions (L2). Suppose the total length is LENGTH carried by one largest vessel; the length of each segment is L1 and each subdivided segment is L2. Then N1=LENGTH/L1 AND N2=L1/L2. N1 is the number of segments in the entire length, and N2 is the number of subdivided segments in each segment.

The velocities for each of the smallest parallelepipeds depend on the perfusion in that region. Then velocity and accumulated mass flow rates of vessels are calculated step by step back to the original largest vessel.

This branch pattern looks like a big stream (called the first level) flowing out into the four big streams (called the second level). Each of the four second level streams continues flowing in the same manner as the first level, to the second level, to the third level (the final stream) which is the smallest vessel.

There are some restrictions in this program. The first is that the geometry should be a parallelepiped. The second is that the total

dimension of geometry must correspond to the gridsize in each direction in order to exactly match nodes with the distance you want. For example: from the cross section area, if you choose the width to be 80mm then the gridsize (dx) should be divided as either 1mm or 2mm. Why not choose 4mm or 8mm? Those numbers also can divide into 80. Good thinking, but the point is that the structure of this program, the cross section area, is divided into 16 smallest areas (units). Each side of the square has 4 segments (total would be 16 areas), and for every single region there is an arterial vessel going down the center of the square. The distance between the vessel point (entering point) and the boundary of the area which belongs to the vessel (the perfusion region) will be half of the segment. So, if you have to choose a width, first it should be divided by 8, then divided by the gridsize(dx). If it is divisible, then the program can handle the location of the vessels exactly; otherwise, it fails. Finally, be careful of CPU time and do not pick small grid spacing.

HOW TO DETERMINE VELOCITIES:

As mentioned above, the velocities are determined by the perfusion of the contour volume, and in this program the file BLOOD.DAT has the values of perfusion which are read into the program node by node. At this moment, I should mention that the boundary nodes of the BLOOD.DAT are set to 100.00 that is for calculating the temperature distribution program, but here the data read in by this program transforms those boundary nodes into actual perfusion values

(which means the perfusion of the boundary nodes should be assigned the same perfusion as the margin region of part of 16 regions).

After the data has been read and transformed, in order to get all velocities, the program begins to search and assign all boundary and interface nodes, because the method of calculating the mass flow rate starts in the smallest region (parallelepiped). During the assignment, the nodes on the corner of the boundary nodes will have 0.25*perfusion (which means the value of perfusion will be accumulated to mass flow rate just one time). The nodes on the boundary not on the corner nor on the interface of the two regions will be 0.5*perfusion not only will the perfusion be accumulated just one time but also these nodes represent more area than the corner). The nodes right on the interface of the boundary will have 0.25*perfusion (those nodes have the same area as previous nodes but will be accumulated twice). The nodes on the interface of two regions inside the boundary will have 0.5*perfusion (those nodes will be accumulated twice so the perfusion is divided by two). Finally, the nodes on the interface of four regions inside the boundary will be 0.25*perfusion (those nodes will be accumulated four times, so the perfusion is divided by four). Now the program can calculate the velocities in each of the smallest parallelepiped regions.

The velocities of the connecting vessels are calculated according to the addition of the mass flow rate and by assuming no perfusion happened except in the smallest vessels in the z-direction. All of the vessels are specified at their location; then the

velocities can be calculated step by step and exactly assigned right on the location.

HOW TO DETERMINE THE DIAMETER OF VESSELS:

Six different diameters of vessels are used in the BRANCH PROGRAM. The parameter RATIO will set the other five diameters after the largest vessel diameter (dia1) is chosen. The second vessel diameter will be dia1*RATIO, the third will be dia1*RATIO*RATIO and so on.

HOW TO DETERMINE THE DIRECTION OF THE VESSELS:

In order to determine the direction of the vessels, index values are used. The directions of vessels are all in either the x ,y or z directions and straight lines are used between each connection. Those values are 1, 2, 3, -1, -2, -3, with positive numbers meaning flow either right or up in the x-y plane or up(increasing z-plane numbers) in the z-direction, and negative numbers meaning flow either left or down in the x-y plane or down(decreasing in the z-plane numbers) in the z-direction. Therefore, all vessels can be set in the branch system, and turns will be 90 degrees. That means the vessels will be perpendicular to each other or parallel to each other.

HOW TO DETERMINE THE LENGTH OF VESSELS:

The length indicated in the program represents how many nodes need to be added to reach the end point of a vessel. These numbers are

automatically calculated given the value of the gridsize because the branch pattern is fixed.

COMPUTER CALIBRATION:

Four cases have been calibrated (figure C.1) in order to check the program. The dimensions of the model are as follows: 80mmx80mmx102mm, the largest diameter equals 1mm, ratio=1, dx=dy=1mm, dz=2mm; the first level(L1=50mm), the second level(L2=10mm), the first branch tree begins at plane 2, and the distance from the top (first plane;surface plane) is dz*(2-1).

The smallest parallelepiped cylinder which is perfused(drained) by the single smallest arterial unit has a length of one node distance shorter than (L2). But from the linear perfusion point of view, both the starting point of the vessel and the end point of the vessel have blood going into tissues. Therefore, the actual perfused volume will be the same as the smallest parallelepiped cylinder.

1.For uniform perfusion (w=1):

For the smallest parallelepiped cylinder

Total mass flow rate $=(80/4)*(80/4)*10*0.001^3$

$=4.0\text{x}10^{-6}$ kg/s

velocity $v=5.093\text{x}10^{-3}$ m/s

let v6=velocity=v=vb

v5=2X(vb of v6)= $1.019\text{x}10^{-2}$ m/s

1,For uniform perfusion (w=1),

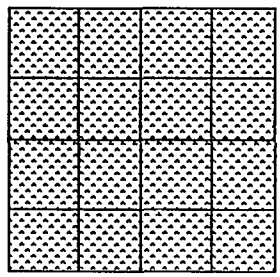

2.nonuniform perfusion(w1=1,w2=2)

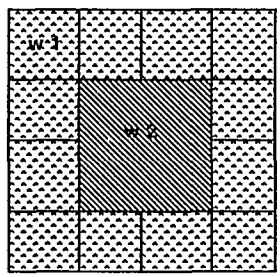

3.Change diameter ratio (ratio=0.9) ,L1=50mm, L2=10mm, Length=102mm

4.Change length (ratio=1.0) ,L1=40mm, L2=20mm, Length=82mm

Figure C.1 Four tested cases to calibrate the branch program which generates all vessels' information concerning locations, directions, lengths, velocities at the starting and end points.

v4(5)=4x5.093x10^{-3} =2.038x10^{-2} m/s

v4(4)=8*v=4.074x10^{-2} m/s

v4(3)=12*v=6.112x10^{-2} m/s

v4(2)=16*v=8.150x10^{-2} m/s

v4(1)=20*v=1.019x10^{-1} m/s

v3=v4(1)

v2=2*v3=2.038x10^{-1} m/s

v1(2)=0.1 m/s (This is a assumption)

v1(1)=0.1+2*v2=0.5076 m/s

2.For non-uniform perfusion(w1=1 outside;w2=2 center):

At the corner

For the smallest parallelepiped cylinder

Total mass flow rate =4.0x10^{-6} kg/s (if every node is perfusion 1)

but in the corner between perfusion 1 and perfusion 2 those nodes will be assigned perfusion (1+1+1+2)/4=1.25

extra perfusion will be 1.25-1=0.25

extra mass flow rate =0.25x1/4x1x1x10x$(10^{-3})^3$=6.25x10^{-10}

=0.000625x10^{-6} kg/s

Total mass flow rate =4.0x10^{-6}+0.000625x10^{-6}=4.000625x10^{-6} kg/s

But why does the program shows 4.0012146x10^{-6} kg/s ?

That is because the corner perfusion is assigned 1.5 not 1.25

Total mass flow rate =4.0012x10^{-6} kg/s

velocity =: 5.095×10^{-3} m/s

In region 2

Upper part of interface perfusion rate will be assigned (2+1)/2=1.5

extra perfusion rate =(1.5-1)=0.5 (for those interface nodes)

extra mass flow rate $=0.5 \times 20 \times 1 \times 1 \times 10 \times 0.5 \times (10^{-3})^3 = 0.05 \times 10^{-6}$ kg/s

total mass flow rate $=4 \times 10^{-6} + 0.05 \times 10^{-6} = 4.05 \times 10^{-6}$ kg/s

velocity $=5.157 \times 10^{-3}$ m/s

In region of perfusion 2:

each of two sides of interface perfusion is 1.5

short of mass flow rate= $(20+19.5) \times 10 \times 1 \times 1 \times 0.5 \times (10^{-3})^3 \times (-0.5) = -9.875 \times 10^{-8} = -0.09875 \times 10^{-6}$ kg/s

total mass flow rate $=8 \times 10^{-6}$ kg/s(if every node is perfusion 2)

Total mass flow rate $=8 \times 10^{-6} - 0.09875 \times 10^{-6} = 7.901 \times 10^{-6}$ kg/s

velocity= 1.006×10^{-2} m/s

v6 for non-uniform perfusion depends on its location from above. We know that there are three different v6's:

v5=2X(vb of v6) depends on what region it is.

v4(5)=(5.0945+5.1565+5.1565+10.06012)$X10^{-3}=2.5467X10^{-2}$

V4(4) ,V4(3) ,V4(2) ,V4(1) are calculated in the same way as uniform perfusion but depend on their location , and so are V3 ,V2, V1.

3.The case that changes diameter ratio(ratio=0.9,w=1) ,L1=50mm, L2=10mm ,Length=102mm has been tested successfully.

4.The case that changes length (ratio=1.0,w=1) ,L1=40mm, L2=20mm ,Length=82mm has been tested successfully.

APPENDIX D

THE VERIFICATION AND COMPARISON OF DIFFERENT SPACINGS (2mm & 1mm) FOR THE ENERGY BALANCE CACULATION OF THE CONVECTIVE THERMAL MODEL

The followings are the energy balance calculations of the entire model geometry for two cases.

1.Boundary information:

all boundaries are 37°C

2.Property information:

perfusion rate= 1.0

conductivity = 0.5

density= 1000.0

specific heat= 4000.0

3.Gridsize information:

(Dx=Dy=Dz,mm)=	2mm	1mm

4.Dimension information:

(X, Y, Z=(mm))=	80X80X42	80X80X41

5.Inflow information:		
inlet velocity(m/s)=	0.426	0.426
Inlet temperature(°c)=	37	37
energy convected in		
by main artery(w)=	49.512	49.512
6.Outflow information:		
outflow velocity(main)=	0.1	0.1
outlet temperature=	37.465	37.444
energy convected out		
by main artery=	11.770	11.763
7.External power Information:		
uniform power input		
per volume(w/m3)=	30000	30000
total power calculated		
node by node (w)=	7.299	7.498
8.Surface conduction information:		
a.heat loss from left=	0.617	0.645
b.heat loss from right=	0.617	0.645
c.heat loss from top=	0.588	0.618
d.heat loss from bottom=	0.588	0.618
e.heat loss from front=	0.984	1.081
f.heat loss from back=	1.431	1.520
total heat loss=	4.824	5.127

9.Highest temperature information:

highest temperature=	42.232	42.140
location=(nodes in x,y,z)	21,29,12	41,26,23
location=(in mm)	40,56,22	40,25,22

10.Perfusion information:

heat loss due to perfusion term $Wcb(T-T_{art})$ in BHTE=	0.321	0.297
heat loss due to linearly perfused by level 7 vessels=	39.920	39.808

11.Total energy information:

into the control volume(w)=	56.811	57.009
out of the control volume(w)=	56.835	56.996

12.Energy Balance Error information:

absolute error(%)=	0.043	0.023

APPENDIX E

THE FLOW CHART ILLUSTRATING THE PROCESS OF GENERATING VESSELS' INFORMATION OF THE BRANCH VESSEL SYSTEM AND OF SOLVING THE TEMPERATURE DISTRIBUTION.

The branch vessel data are obtained through the program (genseed1.for). The branch vessels' blood temperature in many vessels can be calculated from the given branch vessel data. The important data for calculating the blood vessel temperature would be the length, the direction, the location, the diameters, and the velocities of the vessels.

When the main artery first begins splitting, until the next splitting, the distance L1 is called one set of level 1 vessel between two splitting points along level 1 vessel. Also the distance L2 is called one set of level 4 vessel between two splitting points along level 4 vessel. If there are n1 sets of L1 and n2 sets of L2 then the total number of small parallelepipeds will be 16xn1xn2. That is, the whole region of tissue is perfused by 16xn1xn2 blood vessels.

Before generating data for the vascular system, the dimension of the geometry(whole control volume), gridsize of the temperature solver, the distances (L1,L2) of the branch set, the diameter of the first level, the diameter branching ratio(γ) and the uniform blood perfusion rate need to be input. Figure E.2 is a flow chart

illustrating the procedures for generating branch vessels' data. Notice that different gridsizes will effect the length of level 7 vessels as shown in Table E.1 There is one node difference between nodes in the z direction and nodes in the x or y direction because the first branching plane in level 1 vessel begins at node 2. Therefore, for the same pattern duplicated one more node will be in the z direction.

	gridsize 2 mm	gridsize 1 mm
number of nodes	n for even or odd	n*2 for even or odd
length of level 7	(n-1)*2mm	(n*2-1)*1mm

Table E.1 Comparison of different gridsizes

There are several data files that need to be read in solving the temperature field like perfusion data "blood.dat", conductivity data "conduct.dat", nodes and gridsize data "limit.dat", vessels data "seed.dat", contour data "contour.dat"(optional) and parameter data "parame.dat". Those properties like conductivity and blood perfusion rate are generated by "ctdigen program" and "grigen program". Figure E.1 shows the process of solving the temperature distribution and the data input of the branch program.

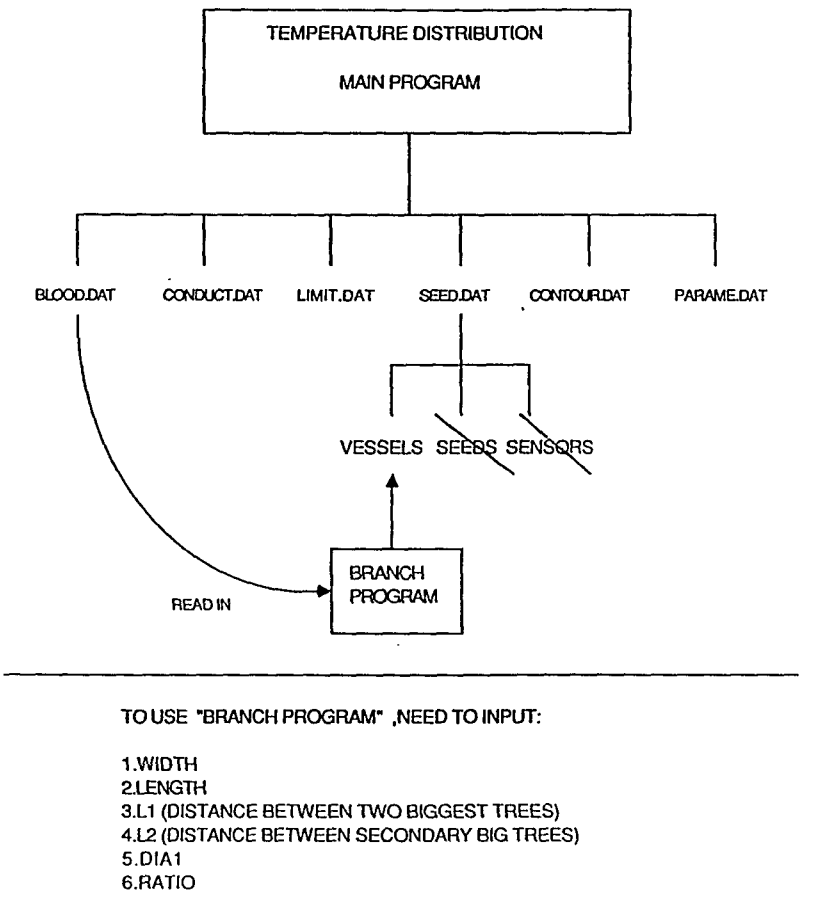

Figure E.1 Flow chart illustrating the process of solving for the temperature distribution and the input of the branch program.

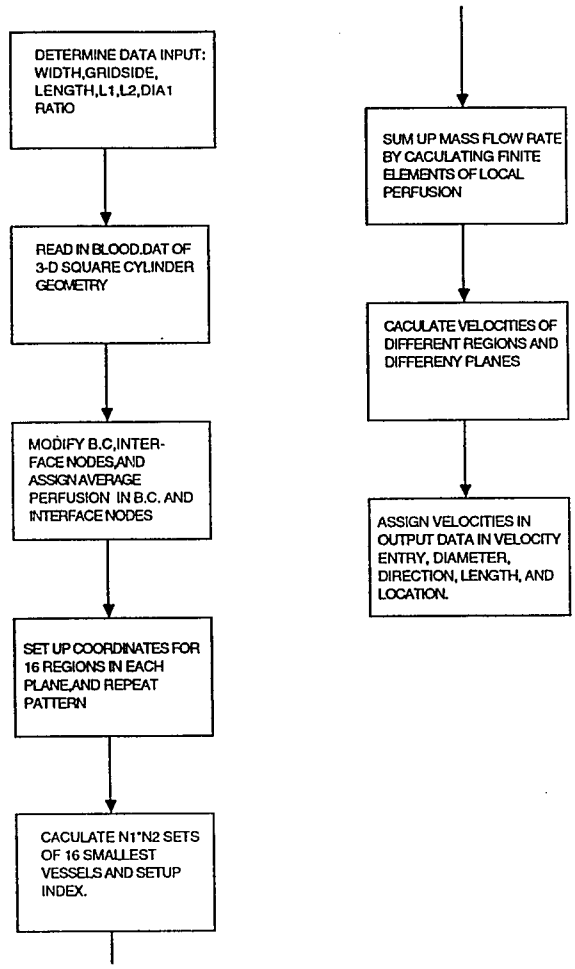

Figure E.2 Flow chart illustrating the process of generating vessels' information of the branch vessel system.

LIST OF REFERENCES

1. Roemer, R. B. (1988) "Heat transfer in hyperthermia treatment: basic principles and applications", in Biological ,Physical and Clinical Aspects of Hyperthermia (Paliwal, B. R., Hetzel, F. W., and Dewhirst, M. W. ed.), American Institute of Physics, New York, 210-242.

2. Roemer, R. B. (1990)"Equations for Describing Temperature Distributions: A Review of Alternative Formulations ,Derivation of a New Equation" (Accepted).

3. Roemer, R. B. (1991)"Optimal power deposition in hyperthermia. I. The treatment goal: the ideal temperature distribution: the role of large blood vessels" ,INT. J. HYPERTHERMIA ,vol. 7, No. 2, 317-341.

4. Chen, Z. P. (1989), Three dimensional hyperthermia cancer treatment simulation ,Ph.D. Dissertation, University of Arizona.

5. Charny, C. K. & Levin, R. L. (1989),"Bioheat Transfer in a Branching Countercurrent Network During Hyperthermia" ,Journal of Biomechanical Engineering , Vol.111/263 .

6. Charny, C. K. & Levin, R. L. (1988) ,"Heat Transfer Normal to Paired Arterioles and Venules Embedded in Perfused Tissue During Hyperthermia" ,Journal of Biomechanical Engineering , Vol.110/277.

7. Baish, J. W., Ayyaswamy, P. S. & Foster, K. R. (1986) ,"Heat Transport Mechanisms in Vascular Tissues: A Model Comparison" ,Transactions of the ASME., Vol.108.

8. Baish, J. W.(1990) ,"Heat Transport by Countercurrent Blood Vessels in the Presence of an Arbitrary Temperature Gradient" ,Journal of Biomechanical Engineering, Vol. 112/207 .

9. Baish, J. W. ,Foster, K. R. & Ayyaswamy, P. S. (1986),"Perfused Phantom Models of Microwave Irradiated Tissue" ,Journal of Biomechanical Engineering Vol.108/239.

10. Lagendijk, J.J.W. ,(1982)."The influence of blood flow in large vessels on the temperature distribution in hyperthermia" ,Phys.Med.Biol ,Vol. 27 No.1,17-23, Printed in Great Britain.

11. Crezee, J and Lagendijk, J.J.W. (1990)"Experimental verification of bioheat transfer theories: measurement of temperature profiles around large artificial vessels in perfused tissue" ,Phys. Med. Biol Vol.35.No.7.905-923, printed in the UK.

12. Torell, L. M. & Nilsson, S. K. (1978) ,"Temperature Gradients in Low-flow Vessels" , Phys. Med. Biol. ,Vol.23,No.1.

13. Chato, J. C. (1980)"Heat Transfer to Blood Vessels" ,Transactions of the ASME ,Vol.102 .

14. Chato, J. C. & Shitzer, A. (1975)"Analytical Prediction of the Heat Transfer From a Blood Vessel Near the Skin Surface Cooled by a Symmetrical Strip" by ,Journal of Engineering for Industry.

15. Weinbaum, S.& Jiji, L. M. (1989)"The Matching of Thermal Fields Surrounding Countercurrent Microvessels and the Closure Approximation in the Weinbaum-Jiji Equation" ,Journal of Biomechanical Engineering , ,Vol.111 .

16. Weinbaum, S. ,Jiji, L. M. & Lemons, D. E. (1984)"Theory and Experiment for the Effect of Vascular Microstructure on Surface Tissue Heat Transfer-Part I: Anatomical Foundation and Model Conceptualization", Journal of Biomechanical Engineering ,Vol.106.

17. Song, W. J. ,Weinbaum, S. & Jiji, L. M. (1987)"A Theoretical Model for Peripheral Tissue Heat Transfer Using the Bioheat Equation of Weinbaum and Jiji" ,Transactions of the ASME ,Vol.109.

18. Song, W. J. ,Weinbaum, S. ,Jiji, L. M. & Lemons, D. (1988)"A Combined Macro and Microvascular Model for Whole Limb Heat Transfer" ,Journal of Biomechanical Engineering ,Vol.110,Nov.1988

19. Zhu, M. ,Weinbaum, S. ,Jiji, L. M. & Lemons D. E.(1988)"On the Generalization of the Weinbaum-Jiji Bioheat Equation to Microvessels of Unequal Size; The Relation Between the Near Field and Local Average Tissue Temperatures" ,Transaction of the ASME ,Vol.110 .

20. Wissler, E. H. (1987)"Comments on the New Bioheat Equation Proposed by Weinbaum and Jiji" ,Transaction of the ASME ,Vol.109 .

21. Charny, C. K. ,Weinbaum, S. & Levin, R. L. (1989)"An Evaluation of the Weinbaum-Jiji Bioheat Transfer Model for Simulations of Hyperthermia" ASME.

22. Pennes, H. H.(1948), "Analysis of tissue and arterial blood temperatures in the resting human forearm", Journal of Applied Physiology, 1, 93-122.

23. Zhu, M., Weinbaum, S. and Jiji, L. M. (1990) "Heat exchange between unequal countercurrent vessels asymmetrically embedded

in a cylinder with surface convection", Int.J.Heat Mass Transfer. ,Vol.33.No.10.pp.2275-2284

24. Lagendijk,J.J.W. and Mooibroek, J.,(1986), "Hyperthermia Treatment Planning", in Recent Results in Cancer Reaserch ,Locoregional High-Frequency Hyperthermia and Temperature Measurement, Vol. 101 pp.119-131.

25. Lagendijk,J.J.W.,Schellekens, M.,Schipper, J. and Linden,P.M.van der. (1984), "A three-dimensional description of heating patterns in vascularised tissues during hyperthermic treatment",Phys.Med.Biol Vol.29,No.5,495-507.

26. Less, J.R.,Skalak,Thomas C.,Sevick,Eva M. and Jain,Rakesh K.(1991),"Microvascular Architecture in a Mammary Carcinoma:Branching Patterns and Vessel Dimensions",Cancer Research 51,265-273

27. Roemer, R. B. (1990),"The local tissue cooling coefficient: a unified approach to thermal washout and steady-state 'perfusion' calculations" ,Int. J. Hyperthermia. Vol 6,No.2,421-430.

28. Chen, Z. P., Miller, W.H., Roemer, R.B., Cetas, T.C., (1990) "Errors between two and three dimensional thermal model predictions of hyperthermia treatment", The International Journal of Hyperthermia,Vol.6, No.1 ,pp. 175-191.

29. Chen, Z. P. and Roemer, R.B. (1991),"Comparison of the effects of large blood vessel models on hyperthermia temperature distributions" submitted.

30. Jain, R. K. (1983),"Bioheat transfer: Mathematical models of thermal system. In Hyperthermia Cancer Therapy (storm, F.K.,ed), Hall Medical Publishers, Boston, Ma, P11.

31. Winifred Elizabeth Williams (1990),"A structural model of heat transfer due to blood vessels in living tissue", Phd dissertation.

32. Jaap Mooibroek and Jan J. W. Lagendijk (1991),"A fast and simple algorithm for the calculation of convective heat transfer by large vessels in three-dimensional inhomogeneous tissues" IEEE Transactions on Biomedical Engineering, Vol.38. NO.5.

33. G. S. Barozzi and A. Dumas (1991),"Convective heat transfer coefficients in the circulation", Transactions of the ASME, Vol.113.